

Instituto Tecnológico y de Estudios Superiores de Monterrey

Campus Monterrey

School of Engineering and Sciences



Pharmacokinetic-pharmacodynamic evaluation of a fraction with a
neuroprotective activity of *Tagetes lucida*

A dissertation presented by

Guadalupe Anislada Santibáñez García

Submitted to the
School of Engineering and Sciences
in partial fulfillment of the requirements for the degree of

Doctor

in

Biotechnology

Monterrey Nuevo León, December 5th, 2022

Declaration of Authorship

I, Guadalupe Anislada Santibáñez García, declare that this dissertation titled, Pharmacokinetic-pharmacodynamic evaluation of a fraction with the neuroprotective activity of *Tagetes lucida* and the work presented in it are my own. I confirm that:

- This work was done wholly or mainly while in candidature for a research degree at this University.
- Where any part of this thesis has previously been submitted for a degree or any other qualification at this University or any other institution, this has been clearly stated.
- Where I have consulted the published work of others, this is always clearly attributed.
- Where I have quoted from the work of others, the source is always given. With the exception of such quotations, this thesis is entirely my own work.
- I have acknowledged all main sources of help.
- Where the thesis is based on work done by myself jointly with others, I have made clear exactly what was done by others and what I have contributed myself.

Guadalupe Anislada Santibáñez García
Monterrey Nuevo León, December 5th, 2022

Dedication

My dear Mar, you know that you are part of each of my dreams and the goals achieved are also yours. This work like everything I do is dedicated to you. Te amo.

My beloved brother, I share with you the triumph of knowing that all dreams come true. Love you.

Anis, you deserve it, you did it. You know better than anyone how hard you've worked for what's here. Never give up. To you more than anyone I dedicate this. These lines are for you:

To all those who one day I went. Thanks.

To my forgotten parts that I left in places, I no longer remember. Thanks.

To my parts that were once broken and that I never found again. Thanks.

To my empty parts that I once tried to fill with distractions, attachments, and obsessions. Thanks.

To my frustrated and angry parts for the wishes never fulfilled. Thanks.

To my parts that no longer go with me. Thanks.

To my parts that I couldn't hug. Thanks.

To my parts that didn't believe in themselves. Thanks.

What is delayed is not denied. Dawn Staley.

Acknowledgments

I would like to begin by thanking Dr. Ashutosh Sharma, principal advisor, who was the main link to achieving a dream that I had tried to fulfill since I was very young, to be part of this prestigious institution that is the Tecnológico de Monterrey. I am very grateful for the trust he had in me on many occasions, from a distance, to achieve this goal.

To my thesis co-advisor, Dr. Enrique Jiménez-Ferrer, for taking me back down the path of wisdom and interest in continuing to innovate in different areas. For letting my imagination fly with my passion for scientific work and letting me know that curiosity is the best tool to achieve great discoveries.

I thank Dr. Maribel Herrera-Ruiz, who is not only an admirable person as a researcher but also as a woman. I have no way of thanking what she did for me a couple of years ago. It was a very difficult challenge to face, but she helped me realize that I would never be alone. You and Dr. Ferrer have all my gratitude and admiration.

I give special thanks to Dr. Manasés González and Dr. Pilar Nicasio. Doctor Manasés, the energy you put into life and science are worthy of being recognized, you are pure motivation. Dear Dr. Pilar, thank you for the pleasant reception I have had in your laboratory, I have my next goal: I want to be like you, independent and brave.

Rodrigo and Mari, thank you very much for giving me your friendship and for making this process much more bearable. Thank you because, although sometimes you didn't know it, sharing with you made me forget about the bad days. I love you.

I thank the people with whom I have shared a scientific, academic, or social space in the last four years. They are also part of this project.

Finally, I am extremely grateful to the Tecnológico de Monterrey for the academic scholarship, as I mentioned before, it was a dream to be part of its graduates, and today I am one step away from achieving it. Similarly, I thank CONACyT for the support for living with scholarship number 825903.

Pharmacokinetic-pharmacodynamic evaluation of a fraction with neuroprotective activity of *Tagetes lucida*

by

Guadalupe Anislada Santibáñez García

Abstract

Tagetes lucida has been widely used as a folk remedy in illnesses associated with the central nervous system (CNS) and inflammatory ailments. Among the compounds that stand out in the plant against these conditions are coumarins, such as 7-O-prenylscopoletin (PE), scoparone (SC), dimethylfraxetin (DF), herniarin (HR), and 7-O-prenylumbelliferone (PU). Therefore, the relationship between the therapeutic effect and the concentration can be evaluated through pharmacokinetic-pharmacodynamic (PK–PD) studies under a model of neuroinflammation induced by lipopolysaccharide (LPS).

In the present study, a bioanalytical method was established by HPLC-UV for the simultaneous quantification of the coumarins present in the active fraction of *T. lucida*, which was able to determine the temporal concentration profiles of each of the coumarins in the plasma, brain, kidney, and spleen samples of healthy and damaged mice. Coumarins showed an increase in plasma concentrations of up to three times in the neuroinflammation model, compared to healthy mice, so it was possible to quantify the therapeutic agents in the main target organ, the brain.

The ability of compounds to cross the blood-brain barrier is an advantage in the treatment of diseases associated with neuroinflammation processes. A pertinent assay that was proposed in the present investigation with *T. lucida*, is the measurement of the extravasation of the Evans blue dye in the brain of mice, with and without LPS, that causes neuroinflammation and an increase in the permeability of the blood-brain barrier. Future PK-PD assessments at different doses and longer test times are proposed to obtain parameters that determine the best possible effect without toxic responses.

Keywords: HPLC–UV; coumarins; *Tagetes lucida*; pharmacokinetics; blood-brain barrier

List of Figures

Figure 1. Acute and chronic neuroinflammation process by microglia and astrocytes activation.	5
Figure 2. Microglia pathway activation and its phenotypes.	7
Figure 3. TLR4 activation by MYD88 inducing NF- κ B signaling for inflammatory response.	9
Figure 4. <i>Tagetes lucida</i>	22
Figure 5. Drug discovery and development process from botanical sources.	27
Figure 6. Non-compartmental modeling and graphical representation.	33
Figure 7. Semilog plot demonstrating the estimation of λ_z	34
Figure 8. Chemical structures of the coumarins 7-O-prenylscopoletin (PE), scoparone (SC), dimethylfraxetin (DF), herniarin (HR), and 7-O-prenylumbelliferone (PU), and of the rutin (IS).	41
Figure 9. Chromatograms with retention time and specific UV spectra of (a) IS, (b) PE, (c) SC, (d) DF, (e) HR, and (f) PU at a concentration of 200 μ g/mL.	49
Figure 10. Representative chromatograms of (i) blank matrix, (ii) blank matrix spiked with LLOQ concentration, and processed samples collected at 15 min after oral administration of standardized fraction of <i>T. lucida</i> spiked with IS in plasma (iii), brain (iv), kidneys (v), and spleen (vi).	50
Figure 11. Evans blue dye and treatments administration and sacrifice schedule	63
Figure 12. Chromatogram of bioactive fraction of <i>T. lucida</i> at $\lambda = 330$ nm. PE = 7-O-prenylscopoletin, SC = scoparone, DF = dimethylfraxetin, HR = herniarin, and PU = 7-O-prenylumbelliferone.	65

Figure 13. Concentration–time profiles of coumarins: (a) PE, (b) SC, (c) DF, (d) HR, and (e) PU after a 10 mg/kg oral dose administration of hexanic extract of *T. lucida* in healthy (–□–) and LPS-damaged (–●–) ICR mice. Data are presented as mean ± SEM (n = 5 per time). 69

Figure 14. Distribution in the brain of (a) 7-O-prenylscopoletin (PE), (b)scoparone (SC), (c) dimethylfraxetin (DF), (d) herniarin (HR), (e) 7-O-prenylumbelliferone (PU) after an oral dose administration of hexanic extract of *T. lucida* in healthy and LPS-administered mice. Values are presented as mean SEM (n = 5). 72

Figure 15. Tissue distribution in kidneys and spleen of 7-O-prenylscopoletin (PE), scoparone (SC), dimethylfraxetin (DF), herniarin (HR), 7-O-prenylumbelliferone (PU) after an oral dose administration of hexanic extract of *T. lucida* in a neuroinflammation LPS-induced model. Values are presented as mean ± SEM (n = 5). 73

Figure 16. Standard curve for Evans blue dye concentration (µg/mL). OD: Optical density at 620 nm. 74

Figure 17. Kinetics of Evans blue dye extravasation observed in several tissues (brain, left and right kidneys, and spleen) after neuroinflammation LPS-induction. Each column represents the mean ± SEM (n = 5, per time. * p<0.05, ** p< 0.01 when compared to the vehicle with LPS (ANOVA post hoc Dunnett test). 76

Figure 18. Modulation of the inflammatory response by expression of cytokines TNF-α and IL-10 in brain after LPS-induced neuroinflammation. Each column represents the mean ± SEM (n = 5, per time. * p<0.05, ** p< 0.01 when compared to the vehicle with LPS (ANOVA post hoc Dunnett test). 77

List of Tables

Table 1. Elution gradient of the analytical method by HPLC-UV	44
Table 2. Linearity equations of calibration curves and LLOQ determined for coumarins in plasma and tissue matrices.....	51
Table 3. Data of accuracy and precision determined for coumarins in plasma and tissue matrices.....	53
Table 4. Data of extraction recovery and matrix effects determined for coumarins in plasma and tissue matrices.....	54
Table 5. Stability test of PE, ES, DF, HR, and PU in plasma and tissues matrices.....	55
Table 6. Identification parameters of coumarins by HPLC-UV	66
Table 7. Plasma concentrations of coumarins PE, SC, DF, HR, and PU in mice LPS-damaged.	67
Table 8. Plasma concentrations of coumarins PE, SC, DF, HR, and PU in healthy mice.	68
Table 9. Pharmacokinetic parameters of coumarins estimated by non-compartmental analysis in healthy ICR mice plasma.....	70
Table 10. Pharmacokinetic parameters of coumarins estimated by non-compartmental analysis in LPS-damaged ICR mice plasma.	71
Table 11. Evans blue dye concentrations and relative inhibition in neuroprotection assay.	75
Table 12. Abbreviations.....	85
Table 13. Variables and symbols.	87

Contents

Abstract	v
List of Figures	vi
List of Tables	vii
Introduction	1
1.1 Motivation.....	2
1.2 Research Question	2
1.3 Solution overview	3
1.4 Aims and objectives	3
1.4.1 Specific objectives	4
Theoretical Framework.....	5
2.1 Neuroinflammation	5
2.1.1 Microglial activation in neuroinflammation	6
2.1.2 Toll-like receptor (TLR) on microglia function	8
2.1.3 Molecular components in neuroinflammation	9
2.1.4 Neuroinflammation as a precursor of neurodegenerative diseases.....	11
2.1.5 Neuroprotector treatments.....	15
2.2 <i>Tagetes lucida</i>	21
2.2.1 Ethnopharmacological uses.....	22

2.2.2	Chemical profile	23
2.2.3	Pharmacological uses.....	23
2.3	Drug discovery and development from plant sources	26
2.3.1	Bioanalytical method validation in plant-based drug development	28
2.3.2	Relevance of preclinical PK in drug development.....	32
2.3.3	Preclinical neuroinflammation models	36
	Bioanalytical method validation for coumarins quantification	40
3.1.	Methods	40
	Chemicals and reagents	40
	Coumarins isolation from hexanic extract of <i>T. lucida</i>	40
	Preparation of standards	42
	Coumarin Extraction Process from Plasma and Tissue Samples	43
	HPLC-UV analysis conditions.....	43
	Validation of the HPLC-UV analytical method	44
3.2.	Results	48
	Optimization of chromatographic conditions	48
	Selectivity and specificity	50
	Linearity and sensitivity.....	50
	Accuracy and precision.....	51
	Extraction recovery and matrix effect.....	52

Stability	52
3.3. Discussion.....	56
Pharmacokinetic-pharmacodynamic study of bioactive fraction from <i>Tagetes lucida</i>	58
4.1 Methods	58
4.1.1 Chemicals.....	58
4.1.2 Hexanic extract preparation of <i>Tagetes lucida</i>	58
4.1.3 Bioactive fraction identification of hexanic extract	59
4.1.4 Preparation of administration solutions.....	59
4.1.5 Animals.....	59
4.1.6 Pharmacokinetic study and tissue distribution design	60
4.1.7 Samples collection and processing for PK study	60
4.1.8 Coumarins quantification by HPLC-UV.....	61
4.1.9 Pharmacokinetic and tissue distribution analysis.....	62
4.1.10 Vascular permeability evaluation with Evans blue dye	62
4.1.11 Cytokine quantification by ELISA's method	64
4.2 Results	65
4.2.1 Chemical composition determination of the bioactive fraction of <i>Tagetes lucida</i>	65
4.2.2 Pharmacokinetic study of coumarins in <i>Tagetes lucida</i>	66
4.2.3 Pharmacokinetic parameters estimation.....	70

4.2.4	Tissue distribution evaluation	71
4.2.5	Vascular permeability assay	74
4.2.6	Cytokine quantification.....	77
4.3	Discussion.....	78
	Conclusion and Perspectives	84
	Appendix A.....	85
	Abbreviations	85
	Appendix B.....	87
	Variables and Symbols	87
	Bibliography	88
	Published papers	105
	Curriculum Vitae.....	120

Chapter 1

Introduction

Neurodegenerative diseases are characterized by progressive dysfunction, as well as neuronal and functional loss of the CNS (Pringsheim et al., 2014). These include Alzheimer's disease (AD), Parkinson's disease (PaD), amyotrophic lateral sclerosis (ALS), and Huntington's disease (HD) (PAHO, 2021). Currently, they affect more than 50 million people around the world, but due to the increase in life expectancy, this number is expected to double approximately every twenty years. In addition, they represent the leading causes of disability and death among the elderly population (Liao et al., 2021).

The symptoms and pathological processes are varied in each disease, however, an optimal treatment has not been developed to delay, reverse, or even avoid the neurodegeneration process (Miller and Das, 2020). Among the new developments of pharmacological therapies, it has been determined that neuroinflammation is a common factor in the establishment and progression of neurodegeneration due to defects caused in the regulatory pathways of the CNS. Therefore, it has been explored as a target of the effects for the research and development of new drugs (Arbo et al., 2022; Gilhus and Deuschl, 2019). One of the main sources of new anti-inflammatory therapeutic agents is natural products derived from plants.

Tagetes lucida, a plant of the Asteraceae family, has well-documented ethnopharmacological reports that have been evaluated to test its activity in biological models, such as inflammatory inhibition (Monterrosas Brisson et al., 2020; Pérez-Ortega et al., 2016). At the same time, the chemical components associated with the effect have been determined, among which polyphenolic compounds, such as coumarins, stand out.

However, one of the limitations in obtaining herbal medicines and their subsequent transfer to clinical studies are the multiple compounds contained in the extracts or bioactive fractions derived from medicinal plants. These components cannot be correctly

evaluated due to the lack of standardization in the fraction and the poor quantification of the concentrations of the active agents that enter the system.

Therefore, in this thesis it was evaluated the time course concentrations of anti-inflammatory coumarins of *T. lucida* in different physiological sources, like plasma, brain, kidneys, and spleen, and their relationship with the neuroprotective effect based on an extravasation model in BBB by LPS-induced neuroinflammation. The quantification of the compounds could be carried out by the implementation of a quick, reliable, and validated bioanalytical method developed in here.

1.1 Motivation

Neurodegenerative diseases represent a public health problem worldwide, due to the increase in the population over 60 years of age. There are currently no effective treatments that stop or reverse neurodegeneration, so only the symptoms of the disease are treated. Neuroinflammation is a factor present at the beginning and during the development of this type of disease, which can worsen the conditions when it persists. Drugs used to treat CNS diseases commonly have low bioavailability in the brain due to selective exchange with the outside of the blood-brain barrier (BBB), which limits their effect. Therefore, the temporal evaluation of the concentration of standardized anti-inflammatory coumarins obtained from *T. lucida* and their effect on brain (target organ) associated with their plasma concentration, will determine their potential neuroprotective effect, through PK-PD studies.

1.2 Research Question

What is the relationship between the neuroprotective effect of a standardized fraction of *T. lucida* and the concentrations of anti-inflammatory coumarins evaluated in a PK study in an LPS-induced neuroinflammation model?

1.3 Solution overview

The active compounds in the *T. lucida* fraction can cross the BBB to exert an inhibitory effect on extravascular permeability, restoring the normal physiological process of the brain after LPS administration. Concentration profiles of coumarins in the brain are similar to kinetic behaviors in plasma, thus concentrations and effect were found to be linked.

1.4 Aims and objectives

The control of the inflammatory process induced by the systemic administration of LPS in murine models for preclinical biological evaluations allows to shed light on potential drugs against diseases associated with neuroinflammation. Therefore, a PK analysis of the components present in the drug must be carried out, comparing healthy and damaged animals. To adequately quantify the concentrations, a bioanalytical method must be established that can determine the detection and quantification of all the components included in the potential drug, in all the biological matrices used during the study. The effect should be evaluated in models that allow us to observe that the treatment can diminish the damage after neuroinflammation and, if applicable, that the system returns to normal physiological conditions. For this, the evaluation of vascular permeability with Evans blue dye will determine the integrity of the BBB by inhibiting the damage caused by LPS.

The main objective of this work is to establish the relationship of bioavailability, course-temporal concentration, and the effect of a neuroprotective fraction of *T. lucida*, standardized in its phytochemical content, on an LPS-induced neuroinflammation model.

1.4.1 Specific objectives

- 1) To standardize the active fraction with the potential neuroprotective effect that contains the coumarins of interest from the hexanic extract of *T. lucida*.
- 2) To develop and validate a method by high-performance liquid chromatography UV-coupled (HPLC-UV) to quantify coumarins of interest in biological matrices of plasma, brain, kidneys, and spleen.
- 3) To quantify the temporal plasma concentration in healthy and LPS-damaged mice of active coumarins after oral administration of the *T. lucida* fraction.
- 4) To determine the tissue distribution in the brain, kidneys, and spleen of the chemical components of the active fraction of *T. lucida* after oral administration in healthy models and with LPS-induced neuroinflammation.
- 5) To evaluate the active fraction's neuroprotective effect by inhibiting Evans blue dye's extravascular permeability in mice with LPS.

Chapter 0

Theoretical Framework

2.1 Neuroinflammation

Inflammation is a biological response activated by the presence of physical, chemical, or biological stimuli caused by damage or infection from exogenous or endogenous agents of the organism (Olajide and Sarker, 2020).

According to the immediacy and duration of the process, it is classified as acute or chronic (Figure 1). Acute inflammation is a rapid response where the first regulation and protection cells are activated, such as endothelial cells and macrophages, likewise, leukocytes are recruited, and antioxidants are released from phagocytic cells. On the other hand, chronic inflammation is produced by the continuous presence of inflammatory stimuli and the persistent production of proteins that regulate the immune system, such as proinflammatory cytokines, as well as highly reactive molecules capable of causing oxidative damage, known as reactive oxygen (ROS) or nitrogen (RNS) species (Olajide and Sarker, 2020).

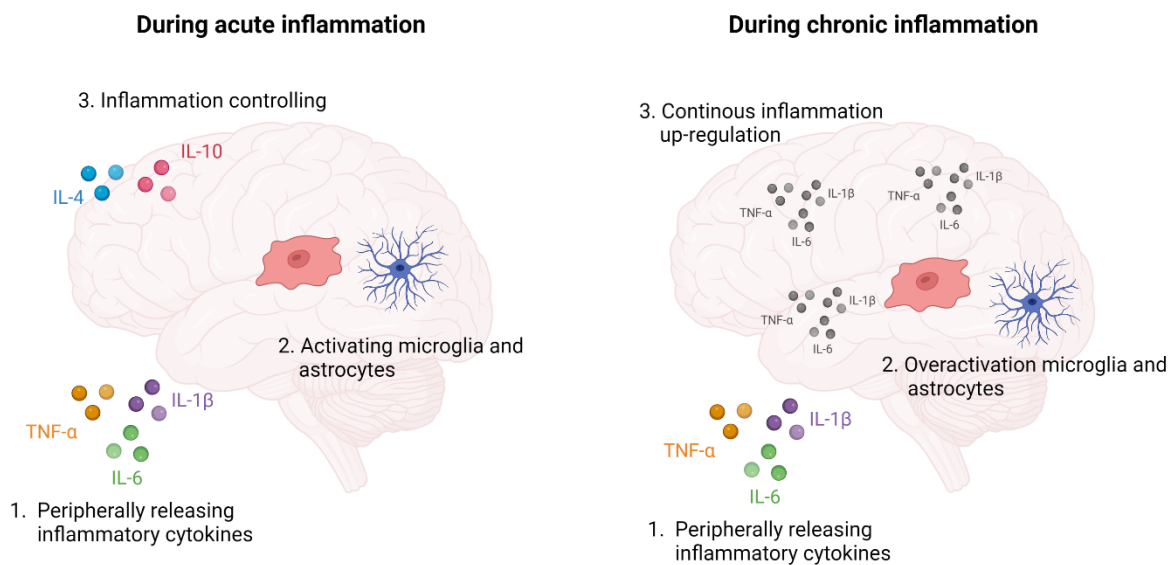


Figure 1. Acute and chronic neuroinflammation process by microglia and astrocytes activation.
Modified from (Rhie et al., 2020).

When inflammation affects the cells of the Central Nervous System (CNS), it generates a neuroinflammation process that refers to an innate immune response triggered by mechanisms such as glial reactions, oxidative stress, or damage to the local system that allows blocking infections and eliminating pathogens (Mishra et al., 2021; Olajide and Sarker, 2020).

As in any inflammatory process, in the acute phase of neuroinflammation, the response generated by specific CNS cells has a protective effect by maintaining optimal regulation within the brain (Mishra et al., 2021). For this, the CNS microenvironment is monitored by microglia, which are resident cells of the local immune system that maintain neuronal homeostasis by controlling neuron growth, modulating synapses, preventing the formation of protein aggregates, and eliminating pathogens (Gilhus and Deuschl, 2019; Mishra et al., 2021).

Therefore, the main task of the microglia is to maintain a healthy state in the CNS, since when conditions that threaten the integrity of the system occur, the microglia can produce anti-inflammatory agents, as well as neurotrophic factors that help restore normal function. Unfortunately, the imbalance caused by harmful factors at the same time activates a process where the microglia trigger cascades of proinflammatory components that can initiate and even exacerbate pathological conditions within the CNS such as neurodegenerative diseases (Subhramanyam et al., 2019).

2.1.1 Microglial activation in neuroinflammation

Under normal conditions, microglia maintain an adequate state of operation, however, under certain pathological conditions or harmful stimuli against the CNS, these cells are activated, giving rise to the presence of two phenotypes commonly characterized by its neurotoxic (M1) or neuroprotective (M2) effects, which also modify the ramified structure in the resting state of the microglia to pass to an amoebic morphology when activated (Liu et al., 2021).

Activation of microglia is the main pathway for inducing neuroinflammation. The M1 phenotype is related to the production of harmful mediators, where ROS and RNS stand out, as well as proinflammatory cytokines such as tumor necrosis factor-alpha (TNF- α), interferon-gamma (IFN- γ), and interleukins-6 (IL-6) and -1 β (IL-1 β) mainly. While its M2 counterpart exerts an anti-inflammatory effect by releasing cytokines such as IL-4, and IL-10, and transforming growth factor-beta (TGF- β) (Liu et al., 2021; Mishra et al., 2021).

When the CNS cells remain activated for long periods contribute to the development of diseases associated with neurodegeneration (Figure 2). The expression of M1 and M2, together with the pro- and anti-inflammatory mediators released in response to microglia activation, are used as markers of neurodegenerative diseases (Liu et al., 2021; Shabab et al., 2017).

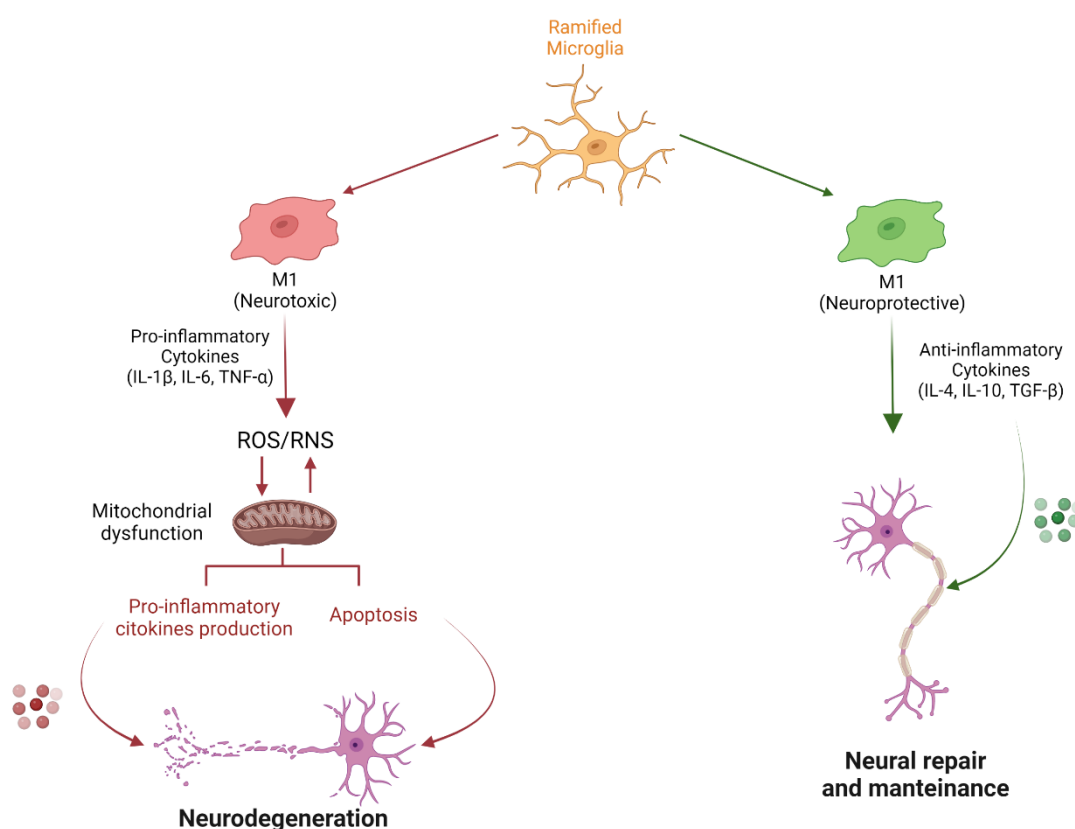


Figure 2. Microglia pathway activation and its phenotypes.

Modified from (Shabab et al., 2017).

Therefore, the inhibition of damaging mediators would be an effective therapeutic approach to avoid, reverse or alleviate the establishment of neurodegenerative diseases (Kaur et al., 2020; Mishra et al., 2021; Shabab et al., 2017).

2.1.2 Toll-like receptor (TLR) on microglia function

Neuroinflammation mediated by microglia activation is associated with different environmental, genetic, and aging factors, among others. Toll-like receptors (TLRs) are membrane proteins that function as the first line of defense when activated by the recognition of exogenous bacterial agents. Its activation triggers signaling cascades of inflammatory response that lead to the elimination or death of the pathogen (Kaur et al., 2020; Liu et al., 2021; Shabab et al., 2017).

Through their binding sites, they recognize specific ligands that initiate the inflammatory response, by activating molecules such as nuclear factor kappa B (NF- κ B), which stimulates the adaptive immune response through microglial phagocytosis, as well as the release of cytokines. The neuroinflammatory response is initiated by the binding of a signaling ligand known as myeloid differentiation factor 88 (MyD88) to TLRs expressed by microglia. Through the Toll/IL-1 (TIR) domains, this complex activates different signal transduction pathways that cause NF- κ B activation and ultimately neuroinflammation (Shabab et al., 2017).

Except TLR3, all TLRs are activated by MyD88, and their role in the initiation of CNS infections is well known, which subsequently activates astrocytes and microglia for long-lasting periods, developing important neuroinflammatory disorders (Kaur et al., 2020). Specifically, TLR4 is activated by the presence of lipopolysaccharide (LPS), an endotoxin found in the outer membrane of gram-negative bacteria (Figure 3).

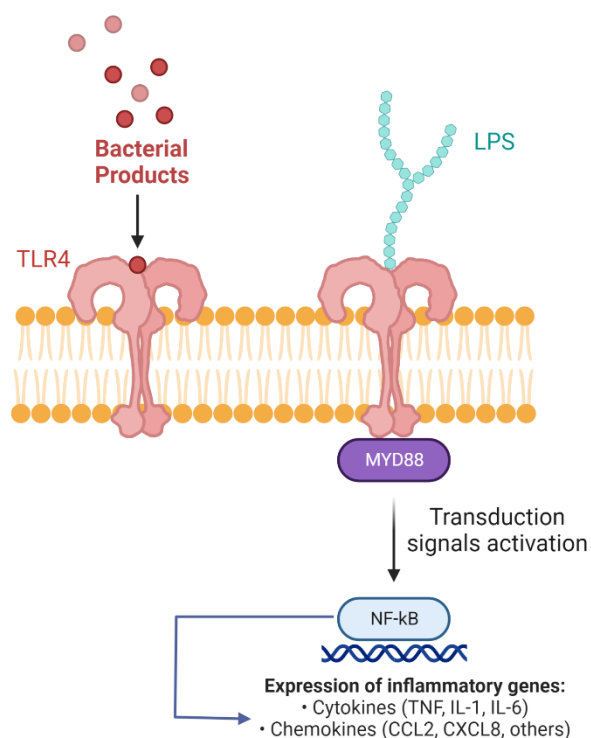


Figure 3. TLR4 activation by MYD88 inducing NF- κ B signaling for inflammatory response.

LPS activates signaling cascades such as phosphoinositide 3-kinase/protein kinase B (PI3K/AKT) and mitogen-activated protein kinase (MAPK), which ultimately activate NF- κ B, so that its activation releases proinflammatory cytokines such as TNF- α and IL-1 β , ROS, inducible enzymes such as iNOS and chemokines such as COX-2, to end in neuroinflammation (Kaur et al., 2020; Lyman et al., 2014). Therefore, interventions aimed at the downregulation of signaling pathways associated with TLR4 represent potential therapeutic candidates to reduce the molecular components released, avoiding neuroinflammation and the diseases derived from it. (Liu et al., 2021; Shabab et al., 2017).

2.1.3 Molecular components in neuroinflammation

The blood-brain barrier (BBB) is an endothelial layer that allows the regulation of the entry of molecules from the bloodstream into the brain tissue through selective transporters.

Through some of the active transport systems of the BBB, it has been determined that cell signaling proteins such as cytokines, proteins with functions on cell proliferation, survival, and death, are capable of crossing the BBB from the periphery to reach the brain, especially under detrimental conditions of inflammation that increase the permeability of the BBB (Lyman et al., 2014).

Although some of these cytokines, such as TNF- α and IL-1 β , are important in the formation and intensity of synaptic connections under normal physiological levels, when their presence is exacerbated they trigger processes of inflammation and apoptosis, due to the proinflammatory nature that characterizes these cytokines (Seo et al., 2019). Entry of TNF- α and IL-1 β into the BBB itself damages the tight integrity of the BBB, leading to increased levels of inflammatory cytokines that ultimately lead to CNS disease states (Jeon and Kim, 2018; Lyman et al., 2014).

TNF- α is a highly inflammatory cytokine able of binding to two types of tumor necrosis receptors (TNFR). When it binds to the extracellular receptor TNFR1, it induces proapoptotic proteins by activating NF- κ B, which plays an essential role in inflammation, immunity, and cell survival. Although, on the other hand, by binding to TNFR2 and activating NF- κ B, it manages to mediate the transcription of anti-apoptotic and anti-inflammatory genes that regulate CNS activities (Kaur et al., 2020; Lyman et al., 2014). In their case, when interleukin IL-1 β binds to the IL-1 receptor, it initiates signal transduction cascades, such as mitogen-activated protein kinase (MAPK) pathways, which activate other inflammatory responses and the production of pro-inflammatory cytokines, such as IL-6, a mediator of inflammation in brain pathologies (Lyman et al., 2014).

Other molecules involved in the inflammation process of brain tissue are ROS, these molecules are produced by the mitochondria and under normal conditions regulate cell metabolism. However, the excessive production of ROS causes mitochondrial dysfunction that activates the transcription of several genes that regulate the expression of proinflammatory molecules such as the previously mentioned cytokines, causing cycled signaling of inflammatory processes in the brain (Seo et al., 2019).

On the other hand, within the neuroinflammatory process, there are also anti-inflammatory molecules with immunomodulatory functions against the inflammatory response, such is the case of IL-10, IL-4, and TGF- β . For example, IL-10 has a key role in the resolution of inflammation, this cytokine is produced by monocytes and granulocytes, as well as by microglia and astrocytes derived from the presence of inflammatory cytokines such as TNF- α and IL-6 (Burmeister and Marriott, 2018).

Expression levels of IL-10 gradually increase when there is damage to the CNS, to preserve neuronal integrity after the activation of signaling pathways of factors that inhibit the synthesis of proinflammatory proteins. IL-10 can exert its effect on the CNS because the receptor for this cytokine is expressed in microglia to produce its activity locally. This receptor is composed of two IL-10 receptor subunits (IL-10R) 1 and IL-10R2 (Burmeister and Marriott, 2018). In addition, IL-10 inhibits the activation of harmful cytokine receptors, dampening or terminating the chain of inflammatory response (Garcia et al., 2017).

Molecular components previously described are part of the neuroinflammatory cascade that is involved as a potential etiopathogenic agent of copious neurological and neurodegenerative diseases, such as Alzheimer's disease, Parkinson's disease, epilepsy, multiple sclerosis, depression, among others. Therefore, the understanding of the control of the agents involved in the inflammation processes within the CNS offers valuable tools for the development of drugs capable of preventing, stopping or reversing the damage generated by neurodegenerative diseases, by ending the chronic inflammation process associated with neuronal damage that leads to these diseases (Kaur et al., 2020; Mishra et al., 2021).

2.1.4 Neuroinflammation as a precursor of neurodegenerative diseases

Neuronal degeneration or neurodegeneration is the functional and structural alteration of CNS cells, which causes a chronic and progressive loss of neuronal cells (Amor et al., 2014). This set of detrimental processes determine the appearance of neurological alterations such as: Alzheimer's disease (AD), Parkinson's disease (PaD), amyotrophic lateral sclerosis (ALS), Huntington's disease (HD), among others (Subhramanyam et al.,

2019). Each of these pathologies is characterized by devastating symptoms that affect both cognitive functions and motor and sensory areas, limiting the ability to perform basic actions of the body such as moving, speaking and even breathing (Gitler et al., 2017; Nieoullon, 2011).

The innate immune response plays a central role in the establishment, evolution and prognosis of neurodegenerative diseases, especially what has to do with the activation of microglia, which lead to the neuroinflammatory process despite the heterogeneity in the pathological mechanisms involved in CNS disorders (Chitnis and Weiner, 2017; Christensen et al., 2013). Some of the basic mechanisms that generate neuronal loss are triggered by proinflammatory mediators such as IL-1 β , TNF- α and ROS at different stages of the neurodegenerative process (Shi et al., 2006). At the beginning of neuroinflammation, these components help eliminate the debris of damaged neurons, however, the chronic activation of microglia that release inflammatory molecules exacerbates the pathology of neurological conditions, triggering a cycle of factors that are harmful to the CNS. (Subhramanyam et al., 2019).

2.1.4.1 Neuroinflammation in Alzheimer's disease (AD)

Alzheimer's disease (AD) is one of the most common forms of dementia, affecting approximately 150 million people worldwide (Kwon and Koh, 2020; Subhramanyam et al., 2019). AD is characterized by the deposition of β -amyloid peptides (A β) that form senile plaques and neurofibrillary tangles, causing memory loss and deterioration of cognitive functions. A β plaques, within individuals affected by this disease, are commonly found in proximal areas of reactive microglia, which can be activated through TLRs which release neuroinflammatory mediators (Kwon and Koh, 2020; Subhramanyam et al., 2019).

Initially, the microglia exert a neuroprotective role due to the degradation of these peptide assemblies, although the constant interaction with A β and tau proteins exceeds the clarification capacity of the microglia, increasing the size of the plaques and tangles present in the disease (Kwon and Koh, 2020; Rauf et al., 2022). Another process of microglia activation may be due to prolonged oxidative stress or increased levels of

proinflammatory mediators such as TNF- α and IL-1 β causing a constant neuroinflammatory response (Jung et al., 2019; Kwon and Koh, 2020). The chronic inflammatory state initiates a process of neurodegeneration due to the fact that the high production of these agents in the microglia transforms it into its M1 phenotype, which triggers the formation of tau fibrillary tangles in addition to activating various parts of the amyloid pathway until AD is finally developed (Jung et al., 2019; Rauf et al., 2022; Subhramanyam et al., 2019).

2.1.4.2 Neuroinflammation in Parkinson's disease (PaD)

Parkinson's disease (PaD) is the second most common neurodegenerative disease. The most relevant clinical involvement is on motor skills, which includes tremors, muscle rigidity and bradykinesia (Jung et al., 2019; Subhramanyam et al., 2019). Its etiology focuses on the deterioration and death of dopaminergic neurons in the *substantia nigra pars compacta*, accompanied by microglial and astrocytic activation, where some of the main inflammatory mediators are produced that lead to continuous and prolonged neuronal death (Kwon and Koh, 2020).

Different chemicals and neurotoxins selectively target dopaminergic neurons such as α -synuclein aggregates and LPS. Both cause copious death of dopaminergic neurons by activating microglia, by the production of proinflammatory cytokines such as IL-1 β by binding to TLR (Subhramanyam et al., 2019).

In addition, the presence of exacerbated levels of proinflammatory factors such as TNF- α , IL-6 and IL-1 β has been observed in the brains of patients with PaD, obtained from post-mortem autopsies, which may be related to the disruption of the BBB caused by the same factors and the high sensitivity of dopaminergic neurons to these cytokines and to oxidative stress, which in turn promotes α -synuclein aggregation (Jung et al., 2019; Rauf et al., 2022; Scudamore and Ciossek, 2018).

Thus, the overexpression of α -synuclein promotes the presence of reactive microglia by releasing TNF- α , NO, ROS and IL-1 β , unleashing a cycle of neuroinflammation due to microglial stimulation and neurodegeneration in PaD (Rauf et al., 2022).

2.1.4.3 *Neuroinflammation in other neurodegenerative diseases*

Little is known about the role of microglia in the development of neurodegeneration in diseases such as Huntington's Disease (HD), Multiple Sclerosis (MS) and Amyotrophic Lateral Sclerosis (ALS), but in both cases the specific polarity of microglia phenotypes during neuroinflammation has been described.

In HD, characterized by cognitive, motor, and emotional dysfunction, microglia lead to increased levels of IL-1 β within the brain, as well as the presence of plasma TNF- α , IL-6, and clusterin responsible for clearance of cellular debris, which constitutes the pathological cascade of neuroinflammation (Rauf et al., 2022). Further, the neuroprotective effect of microglia is established in the early stages of the disease by maintaining the migratory capacity and cell mobility that allow neuronal survival by regulating the expression of abnormal fragments of the huntingtin protein, responsible for the development of HD (Rauf et al., 2022; Subhramanyam et al., 2019). Likewise, microglia maintain the iron levels necessary to protect neuronal cells, due to the increase in ferritin in patients with this disease (Subhramanyam et al., 2019).

Another condition where the duality of microglia phenotypes occurs is in MS, which causes demyelination of axons due to the infiltration of immune cells from the periphery to the CNS. In it, the M2 microglia act in the initial stages of the disease, by reducing the production of TNF- α , the main cytokine involved in the progression of MS. However, the prolonged activation of microglia leads to an exacerbated release of inflammatory cytokines that increase the recruitment levels of peripheral immune cells that later cause demyelination (Jung et al., 2019).

Finally, ALS has the basis of its pathological mechanism based on the selective affectation of motor neurons by mutations of the enzyme superoxide dismutase 1 (SOD-

1), responsible for the elimination of free radicals. During the early stage of ALS, it expresses low levels of proinflammatory cytokines initially associated with the M2 phenotype. Nonetheless, in this disease, microglia are activated by TLR receptors, producing high levels of IL-1 β and TNF- α that inhibit the neuroprotective function of microglia and, in turn, continue to increase the proportion of proinflammatory cytokines, exacerbating neuronal damage (Kwon and Koh, 2020; Subhramanyam et al., 2019).

Therefore, the modulation or inhibition of neuroinflammatory components that mediate microglia activation show an effective therapeutic intervention capable of exerting a neuroprotective effect to attenuate or prevent previously described neurodegenerative pathologies.

2.1.5 Neuroprotector treatments

Neurons are one of the main structural and functional components of the CNS, unfortunately, as previously described, neurodegenerative diseases together with some pathological and physiological factors such as brain trauma, aging, among others, lead to premature neuronal death known as neurotoxicity, this is driven by different pathways such as oxidative stress, glial destruction and neuroinflammation (Mendel Nzogang and Boris Donkeng, 2020). Neuroprotective elements are sought in order to avoid the triggering of these dangerous mechanisms.

Neuroprotection encompasses all the pharmacological and physical resources that help prevent or avoid the biochemical processes that cause neurotoxicity for the rescue, recovery or regeneration of the CNS and its cells (Mendel Nzogang and Boris Donkeng, 2020). Many of the neuroprotective strategies are directed at CNS inflammation (Mishra et al., 2021). Some of them have proven their effectiveness in preclinical models associated with neurological diseases, although once extrapolated to clinical studies, their effects in preventing the onset or arrest of the development of neurodegenerative diseases have not been conclusive (Mendel Nzogang and Boris Donkeng, 2020).

One of these cases is the evaluation of hypnotic drugs such as thiopental, midazolam, or propofol that have immunomodulatory effects by inhibiting the release of free radicals and

proinflammatory cytokines such as IL-1 β and TNF- α in preclinical models (Mendel Nzogang and Boris Donkeng, 2020). Medications such as thalidomide have shown a positive impact on the attenuation of neuroinflammation in PaD models, delaying or preventing the onset of the disease by blocking neurotoxin-induced loss of dopaminergic neurons due to their TNF- α inhibitory capacity (Jung et al., 2019).

Other molecules such as sitagliptin, used in the treatment of type 2 diabetes, showed that its administration in patients with AD manages to reduce the cognitive impairment score in a mental state examination test, this is associated with the inhibition of the synthesis of proinflammatory cytokines and increased anti-inflammatory cytokines (Wiciński et al., 2018). In the line of blood cholesterol-lowering drugs, statins such as simvastatin and atorvastatin show a decrease in the production and infiltration of proinflammatory cytokines in the CNS and reduced microglia count in AD mouse models. However, when pharmacological evaluations have been conducted in humans, they offer limited benefit in inhibiting the risk of dementia progression. (Rauf et al., 2022).

Various evaluations of non-steroidal anti-inflammatory drugs (NSAIDs) as a treatment for neurodegenerative diseases show inconsistencies regarding their protective effects. Some drugs with selective and non-selective COX2 inhibitors do not show notable effects on cognitive dysfunction in AD, although they do exhibit neuroprotective effects in PaD patients, such as ibuprofen (Mishra et al., 2021). Nimesulide and indomethacin have shown neuroprotective effects by inhibiting transfer of peripheral inflammatory cells by the BBB to the CNS in brain-injured neonatal mice (Mendel Nzogang and Boris Donkeng, 2020). Although other anti-inflammatories such as acetylsalicylic acid, prednisone, naproxen, and diclofenac did not show improvements in the reversal of the establishment of AD compared to the placebo group and even the adverse effects were potentiated (Aisen et al., 2000, 2003; Bentham et al., 2008; Scharf et al., 1999).

It has been established that among the main reasons for the limited capacity of potential drugs to exert their neuroprotective effect is that neuroinflammation is a trigger of pathologies rather than a factor of neurodegeneration itself. In turn, the function of microglia activation beyond its potential harmful process against CNS cells, if this is

avoided, interferes with its initial neuroprotective function that will ultimately result in neuronal damage. Other explanations frame the severity of the treated condition, the lack of direction to the target site and one of the most relevant is the limited entry of the drug from the peripheral circulation to the CNS through the BBB (Mishra et al., 2021).

Therefore, it is suggested that a potential neuroprotective strategy against the mechanisms of neurotoxic inflammation is that the drugs can be directed to the adjustment of the transfer between the peripheral components and the CNS. As well as the modulation of the inhibition between proinflammatory cytokines (TNF- α and IL- β) and their intracerebral targets, always taking into account that they are capable of reaching their site of action (Mendel Nzogang and Boris Donkeng, 2020; Mishra et al., 2021).

For several years, the use of medicinal plants to treat and prevent different diseases has been the pillar of traditional medicine, an important source of pharmacological agents and synthetic derivatives inspired by these natural resources. Plant-derived drugs, unlike some synthetic anti-inflammatory agents, such as COX inhibitors that cause renal and gastrointestinal complications, have reported fewer adverse effects, thus contributing to the (re)discovery of potential remedies. Furthermore, most of these plant resources are readily available, cheap, and contain large amounts of polyphenols, making them an appropriate alternative for research into health-promoting compounds (Hano and Tungmunnithum, 2020).

2.1.5.1 *Phytochemical neuroprotector treatments*

Phytochemicals are biologically active compounds that usually correspond to secondary metabolites derived from plants and can offer various therapeutic effects in cardiovascular, oncological, and degenerative diseases, mainly (Kaur et al., 2020). Some of the potential alternative anti-inflammatory therapeutic agents obtained from plants are polyphenolic compounds, which correspond to chemical compounds characterized by the presence of phenolic hydroxyl groups in their structure, such as phenolic acids, coumarins, flavonoids, stilbenes and lignans (Singh et al., 2020).

Polyphenolic compounds have been studied for their anti-inflammatory and antioxidant properties that can help prevent and alleviate the onset of neurodegenerative diseases (Nuzzo, 2021). Regarding inflammation, polyphenols are capable of modulating various cell signaling pathways that prevent the synthesis and release of proteins and proinflammatory enzymes regulated by NF- κ B (Singh et al., 2020). For its part, the processes of oxidative damage induced by the excess of ROS and RNS, formed mainly within the mitochondria, can also be controlled by the antioxidant effects exhibited by phenolic compounds (Hano and Tungmunnithum, 2020).

Some of the most notable secondary metabolites with anti-inflammatory and antioxidant activity are curcumin, resveratrol, and chlorogenic acid. The latter compound exerts its effect by down-regulating the expression of proinflammatory agents such as TNF- α , IL-1 β , and iNOS, as well as reducing glial cell activation (Singh et al., 2018). Curcumin has been evaluated in models of neurotoxicity induced by LPS and by α -synuclein aggregation, where it was determined that it was capable of modulating microglial activation to direct it to the neuroprotective phenotype together with the reduction of the expression of COX-2 and iNOS enzymes, and different proinflammatory cytokines (Tripanichkul and Jaroensuppaperch, 2012). Finally, resveratrol, widely known for its neuroprotective activity, is capable of scavenging free radicals, promoting polarization of microglia to the M2 phenotype, inhibiting NF- κ B activity, and even enhancing the release of anti-inflammatory cytokines such as IL-10 (Yang et al., 2017).

A notable group of polyphenols with a potential contribution to the prevention and treatment of diseases are coumarins. These compounds are derivatives of benzopyrones widely distributed in plant species (Hano and Tungmunnithum, 2020). Due to their chemical nature, they are capable of binding to various active sites in the body, showing a wide range of biological activities, such as anticoagulant, antimicrobial, anticarcinogenic, antioxidant and anti-inflammatory. In addition to their strong pharmacological activity, coumarins as therapeutic candidates show high bioavailability in the body, low toxicity, diverse medicinal effects and practically no adverse effects (Peng et al., 2013).

Among the most notable examples of its activity on neuroinflammation systems associated with neurodegeneration we find scoparone, which suppresses the increase in the neuroinflammatory response induced by LPS in microglial cells, while inhibiting the production of proinflammatory cytokines (Cho et al., 2016). Also, MC13, identified as a new coumarin isolated from the *Murraya* plant, exerts neuroprotective effects by inhibiting several inflammatory mediators such as NO, TNF- α and IL-6, by inactivating NF- κ B and its interference in the binding of LPS to the surface of the cell membrane (Zeng et al., 2015). Likewise, hydrangenol attenuates iNOS and NO expression by inhibiting the translocation of NF- κ B subunits in microglial cells affected by LPS (Kim et al., 2016).

Esculetin, for its part, partially inhibits the progression of mutant huntingtin proteins, preventing cell death and oxidative stress promoted by the mutation of the proteins that cause MS (Pruccoli et al., 2021). Simpler coumarins such as 4-hydroxycoumarins have an important effect on the elimination of ROS, exerting an antioxidant effect by preventing damage due to the release of free radicals (Kostova et al., 2012). These studies demonstrate the ability of coumarins to treat or prevent brain diseases associated with neuroinflammation, especially in LPS-induced damage systems, so they can potentially influence or modulate the inflammatory response associated with different neurodegenerative diseases (An et al., 2020).

In addition, due to its lipophilic nature, it allows infiltration through the BBB even of those O-methylated derivatives (Singh et al., 2020). This allows its uniform bioavailability in the brain after intravenous and oral administrations of this type of polyphenolic compounds, further contributing to its therapeutic relevance in CNS diseases thanks to its availability at the target site (Singh et al., 2020).

In vitro and *in vivo* models have shown the relevant beneficial effects of polyphenols in general as mediators of neuroinflammation (Ahmad, 2020). However, it is necessary to carry out a comprehensive discovery and development analysis on the way in which they exert their effect and establish their effectiveness associated with the concentration of phenolic compounds, for a potential useful anti-neuroinflammatory treatment for the

prevention of neurodegenerative diseases and its interpretation in subsequent clinical trials.

2.1.5.1.1 Phytochemical drug discovery and development in preclinical use

Traditional medicine commonly uses complex mixtures of compounds obtained from the extracts of plant species to which it is attributed, by popular knowledge, the relief of symptoms of an illness. Therefore, it is crucial to carry out scientific validations that support the discovery, development and large-scale production of potential drugs (Hano and Tungmunnithum, 2020; SSA, 2012). However, there are several preliminary considerations about the rationalized attribution of biological activity and the future development of an herbal medicine for its pharmaceutical application.

The first of these considerations is the authentication of the source to obtain the compounds, since some plants are popularly known by different names and even the same name can refer to another plant, this depends largely on the region or country where it is obtained. Next, environmental or genetic factors influence the variation of the phytochemical profile of the extracts obtained and even the extraction processes and conditions themselves affect their chemical composition and therefore their therapeutic activity (Ahmad, 2020).

Therefore, it is necessary to establish systems for the phytochemical characterization of the extracts through analytical methods such as gas chromatography (GC), high-resolution liquid chromatography (HPLC) or ultra-resolution (UPLC), among others. In turn, they can be coupled to other tools such as ultraviolet-visible absorption (UV-VIS) or mass spectrometry, depending on the type or types of bioactive compounds to be identified (Siddiqui et al., 2017). Among the final stages of the discovery and development of herbal medicines are the biological evaluations, which in the end will give an answer to the therapeutic activity of the extracts or isolated compounds obtained from the plant material, as well as an approach to the results of the complex synergism that they can offer (Hano and Tungmunnithum, 2020).

It is important to consider that there is increasing evidence that neuroinflammation associated with the establishment of CNS diseases takes different biochemical pathways, which is why various molecular targets are involved. Therefore, the canons that a single drug should solve a single disease have revealed the failures of new drugs against multifactorial disorders such as neurodegenerative diseases. This shows an advantage of plant-derived extracts to exert their effects on different inflammatory mechanisms of action, which is expected to improve clinical outcomes associated with neuroinflammation through their interaction with different biochemical events, biological receptors, proinflammatory mediators and immune modulation systems in which they are involved (Rauf et al., 2022).

Finally, and before going to clinical trials, the compound or compounds with a potential therapeutic effect must comply with studies that guarantee their efficacy and safety in preclinical models, such as toxicity evaluations and pharmacokinetic and pharmacodynamic studies. This with the intention of determining the appropriate doses, determining the bioavailability of the compounds, ensuring that they reach the sites of action and that they exert their effect adequately (Egbuna et al., 2019).

2.2 *Tagetes lucida*

As previously described, the selection of the plant source of chemical compounds is the first step for the discovery and development of novel drugs with potential curative activity on diseases that involve neuroinflammation processes. Based on the popular knowledge of the Mexican population, *T. lucida* offers a valuable tool for obtaining phytochemicals capable of functioning as therapeutic agents on different CNS diseases.

Tagetes lucida, also known as “pericón”, belongs to the Asteraceae family and is an erect herb with sizes between 30 to 100 cm tall. Its yellow flowers in the form of tabs are grouped in heads arranged in corymbs (Figure 4). Both the flowers and their green leaves with jagged edges release anise scents, another of the characteristic synonyms with

which it is associated, "hierba anís". It grows in places with a warm and temperate climate up to 4000 meters above sea level and is native to Mexico, Guatemala and Honduras. (Biblioteca Digital de la Medicina Tradicional Mexicana, 2009; Perdomo-Roldán, Francisco, Mondragón-Pichardo, Juana, 2009).



Figure 4. *Tagetes lucida*.

Picture taken by: Pedro Tenorio Lezama (Perdomo-Roldán, Francisco, Mondragón-Pichardo, Juana, 2009).

2.2.1 Ethnopharmacological uses

In addition to being used as a ceremonial plant to "drive away evil" in some states of central Mexico, in traditional medicine it is frequently used to treat digestive and respiratory disorders such as diarrhea, indigestion, vomiting, asthma, colds and typhoid. (Biblioteca Digital de la Medicina Tradicional Mexicana, 2009; Perdomo-Roldán, Francisco, Mondragón-Pichardo, Juana, 2009). Its use is also recommended to treat stress and diseases associated with the CNS such as "fright" and "nerves", as well as irritability, anxiety and depression (Linares et al., 1995; Linares and Bye, 1987; Pérez-Ortega et al., 2016).

2.2.2 Chemical profile

The essential oil has been extensively analyzed, in which a high content of methyl chavicol has been found as the main component. Although other compounds such as linalool, β -myrcene, trans- β -ocimene, limonene, β -caryophyllene, geranyl acetate, and geraniol have been identified (Bandeira Reidel et al., 2018; Caballero-Gallardo et al., 2011; Hernandez-Leon et al., 2020; Vera et al., 2014).

Phenolic acids such as protocatechuic acid, chlorogenic acid, 3-(2-O- β -D-glucopyranosyl-4-methoxyphenyl) propanoic acid and its methylester have been identified in the methanolic extract of aerial parts of *T. lucida*; flavonoids, mainly quercetin, patuletin, quercetagenin, and apigenin; flavonols such as quercetagenin 3,4'-dimethyl ether 7-O- β -D-glucopyranoside, as well as coumarins such as 7-methoxycoumarin, 7,8-dihydroxycoumarin, umbelliferone, scoparone, esculetin, 6-hydroxy-7-methoxycoumarin, herniarin, and scopoletin, which were also isolated from the dichloromethane extract (Aquino et al., 2002; Castañeda et al., 2013; Céspedes et al., 2006).

Other polar extracts of aerial parts, such as ethanolic and aqueous, contain coumarins such as 6,7,8-trimethoxycoumarin, 6,7-dimethoxycoumarin, and 7-methoxycoumarin, herniarin, and umbelliferone, which have already been identified in other extracts (Estrada-Soto et al., 2021; González-Trujano et al., 2019; Ventura-Martinez et al., 2020). Due to the high concentration of coumarins in *T. lucida* in hexane and acetone extracts, the following coumarins have been characterized: 7-isoprenyloxy coumarin, herniarin, 6-methoxy-7-isoprenyloxycoumarin, 6,7,8-trimethoxycoumarin, and scoparone (Monterrosas Brisson et al., 2020).

2.2.3 Pharmacological uses

Antidepressant effects can be found among the widely studied pharmacological properties in *T. lucida*. Various studies have evaluated this property with the aqueous extract at doses between 5 and 200 mg/kg. In a forced swimming test in rats, it was shown

that the daily oral administration of the aqueous extract at doses of 10, 50 and 100 mg/kg for 14 days managed to reduce the time of immobility without affecting their motor activity (Guadarrama-Cruz et al., 2008).

Other similar studies involving the serotonergic system determined that the 50 mg/kg dose was able to promote antidepressant activity at 7 days without adverse effects on the gastrointestinal system. Although administrations between 1 and 72 hours prior to the trial were also evaluated, which also had an antidepressant effect at doses of 100 and 200 mg/kg (Bonilla-Jaime et al., 2015; Guadarrama-Cruz et al., 2012).

In addition to its antifungal and insecticidal properties, the essential oil of *T. lucida* shows an antinociceptive and anti-inflammatory effect in a formalin test, which confirms the analgesic effect, as well as the participation of opioid, serotonergic and benzodiazepine receptors of the components (Bandeira Reidel et al., 2018; Caballero-Gallardo et al., 2011; Hernandez-Leon et al., 2020; Vera et al., 2014). Under the same conditions, the ethanolic extract was analyzed, which, in addition to establishing a significant antinociceptive response, was able to prevent gastric damage when combined with analgesic agents such as ketorolac (González-Trujano et al., 2019).

One of the studies that supports its traditional use of *T. lucida* is the antispasmodic evaluation in precontracted pig ileum segments, as well as its antidiarrheal activity in a mouse charcoal meal test evaluated with the aqueous extract and its components umbelliferone and herniarin (Ventura-Martinez et al., 2020).

Other constituents, among which phenolic acids, flavonoids and their glycosylated derivatives obtained from methanolic extracts of aerial parts, exert a free radical scavenging effect according to antioxidant evaluations by the DPPH test (Aquino et al., 2002; Castañeda et al., 2013).

Several hydroxylated coumarins such as 7,8-dihydroxycoumarin, scoparone, 6,7-dimethoxy-4-methylcoumarin, 7,8-dihydroxy-6-methoxycoumarin, among others, had important antibacterial activities against Gram-positive and -negative bacteria, such as

Bacillus subtilis, *Escherichia coli*, *Proteus mirabilis*, *Klebsiella pneumoniae*, *Salmonella* sp., *Shigella boydii*, *Sarcina lutea*, *Staphylococcus epidermidis*, *Staphylococcus aureus*, and *Vibrio cholerae* (Céspedes et al., 2006; Hernández et al., 2006).

The ethanolic and aqueous extracts, where dimethylfraxetine (DF) was identified as its main component, showed its anxiolytic and sedative effect in open field tests, plus maze and barbiturate-induced potentiation of hypnosis. They were also inhibited in the presence of 5-HT_{1A} and GABA/BDZ receptor antagonists, so it was determined that they were involved in serotonergic and GABAergic neurotransmission (Pérez-Ortega et al., 2016).

Another evaluation of the ethanolic extract, with a high content of coumarins, showed antihypertensive and vasorelaxant activity in an *in vivo* test carried out in SHR rats, decreasing systolic and diastolic pressure and its subsequent evaluation in aortic rings contracted with norepinephrine (Estrada-Soto et al., 2021).

One of the recently targeted activities of drugs in development to treat CNS conditions is the modulation of inflammation. The coumarins present in the hexane and acetone extracts were able to inhibit the formation of atrial edema TPA-induced by up to 81%, so this type of compound represents potential therapeutic agents in the treatment of neuroinflammation (Monterrosas Brisson et al., 2020).

Antioxidant and anti-inflammatory activities determined in *T. lucida*, as well as the compounds linked to them, are highly relevant in the search for alternative treatments for CNS disorders associated with oxidative stress and neuroinflammation, mainly. However, its mechanism of action, direction to target sites, as well as bioavailability evaluation in systems as complex as the brain have not been evaluated. Having said the above, it is crucial to search for transcendental tools for the discovery of molecules and the development of herbal medicines under the evaluation of models and concentrations that can specify the correct combination to obtain the desired response.

2.3 Drug discovery and development from plant sources

The development of new drugs, whether synthetic or natural, is a process that requires large amounts of time and money. For a drug to reach advanced clinical stages it can take up to 12 years with costs that exceed a billion dollars (Katiyar et al., 2012).

Plants are one of the main natural resources for the discovery of new chemical entities with pharmacological properties (Katiyar et al., 2012). These sources of potentially active compounds have been used throughout history to treat different ailments, acting as immunomodulators, antioxidants, anticarcinogenic, antidiabetic, anti-inflammatory, etc. (Newman et al., 2003).

In addition to having diverse and complex chemical structures, these secondary metabolites have shown a more affable biological affinity, largely avoiding the adverse effects caused by synthetic drugs (Mathur and Hoskins, 2017; Parasuraman, 2018). However, the biggest problem related to the success rate of compounds obtained from plants is related to the process for obtaining herbal medicines. Therefore, any plant species that suggests a pharmacological resource must follow a well-designed strategy for drug discovery and development (Najmi et al., 2022).

Based on the literature, there are ten main stages within the process of discovery and development of an herbal medicine, defined by the Ministry of Health of Mexico as the pharmaceutical presentation of those products made with parts or extracts of some plant material whose therapeutic efficacy and safety have been scientifically confirmed (SSA, 2012). These stages are listed below and summarized in Figure 5 (Amit Koparde et al., 2019; Katiyar et al., 2012; Mathur and Hoskins, 2017; Najmi et al., 2022; Parasuraman, 2018):

- 1) Selection of plant material based on ethnopharmacological use or chemical compounds previously identified in similar plants.
- 2) Collection and identification of the plant by taxonomic, macroscopic, chromatographic, or genomic authentication.

- 3) Extraction and preparation of extracts with solvents of different polarities (nonpolar to polar) that contain compounds with different chemical and biological properties.
- 4) Fractionation guided by biological activity (bioguided study) by the evaluation of the extracts and fractions with different methods of biological tests.
- 5) Screening of compounds using chromatographic analysis techniques.
- 6) Isolation and structural elucidation of the isolated bioactive compound(s) with subsequent activity evaluations.
- 7) Pharmacokinetic (PK) and pharmacodynamic (PD) studies with *in vitro* and *in vivo* pharmacological tests to determine the potency and selectivity of the extracts and their isolated components.
- 8) Toxicological studies that determine the safety of active compounds.
- 9) Chemical improvement with molecular modeling studies and preparation, if necessary, of derivatives of the active compounds.
- 10) Clinical Trials (Phase I-III).

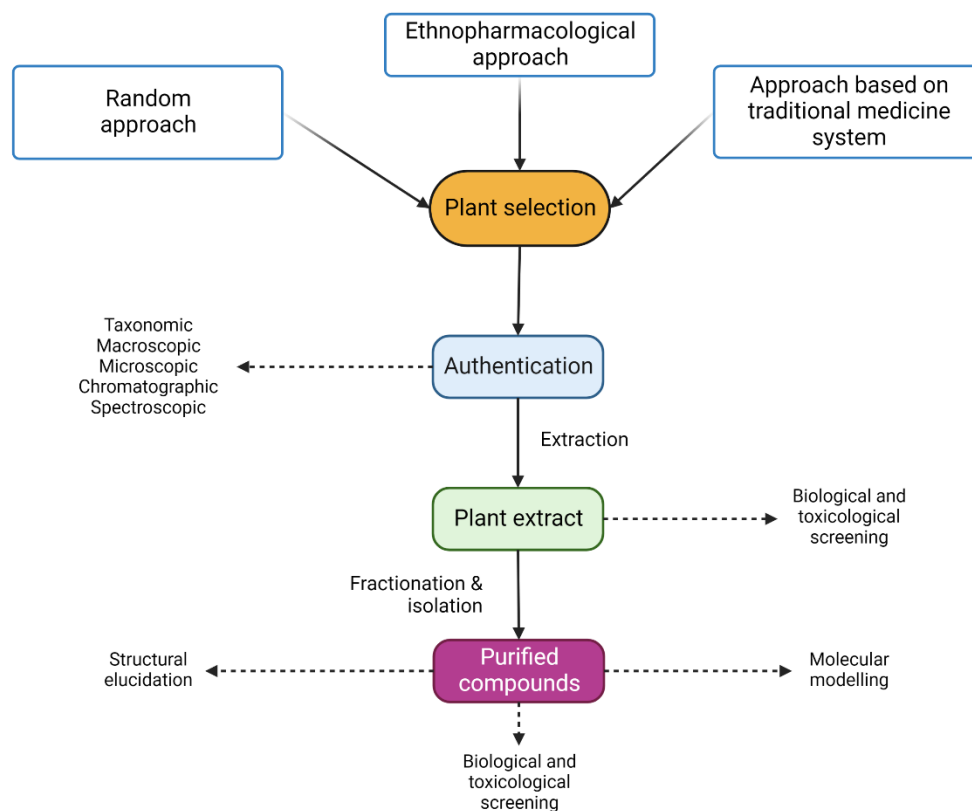


Figure 5. Drug discovery and development process from botanical sources.
Modified from (Najmi et al., 2022)

For phytochemical compounds to be classified as potential medicines, it is necessary that they affect the target in a tolerable and therapeutically useful way. Therefore, although each of the stages indicated above represents pillars in drug development, once the biological activities have been determined through bio-guided studies, special attention must be paid in the subsequent phases (Amit Koparde et al., 2019; Mohs and Greig, 2017).

Therefore, identification analysis methods using validated chromatographic techniques, as well as PK and PD studies, become essential to provide information on the prediction of the behavior between the dose and the exposure of the molecules at the site of action to evaluate the properties and therapeutic efficacy that it has with the binding to the target, as well as the distribution, metabolism and excretion of the chemical participants (Amit Koparde et al., 2019; Katiyar et al., 2012; Mohs and Greig, 2017). It should be noted that these studies are particularly complex in targets of CNS diseases, essentially due to the presence of the BBB, one of the main limitations in getting bioactive compounds to reach the site of action (Mohs and Greig, 2017).

2.3.1 Bioanalytical method validation in plant-based drug development

Bioanalytical analysis methods are an essential part in the development of PK studies to obtain and develop new herbal medicines. (Moein et al., 2017). Due to the complex mixture of chemical compounds present in the extracts or fractions with biological activity, the validation of these methods ensures the quality in the quantification of different types of analytes contained in biological matrices such as blood, plasma, urine, feces and organs that are of interest for evaluations of therapeutic activity (Indrayanto et al., 2021; Moein et al., 2017; Thomford et al., 2018). The development of bioanalytical methods is composed of different stages that range from the collection of samples to the reporting of data from the analyzed samples, divided into two main sections: preparation and detection of the sample (Moein et al., 2017).

The preparation of the sample is the most important process in the development of the bioanalytical method, since it aims to obtain a clean extract of the therapeutic molecules contained in the biological matrices with a high extraction efficiency, considering the properties of the analytes such as polarity and stability. The most common sample preparation methods are protein precipitation (PPT), liquid-liquid extraction (LLE) and solid phase extraction (SPE) (Moein et al., 2017; Tijare et al., 2016).

PPT is a type of simple extraction commonly used in the recovery of compounds in blood and plasma samples, through the addition of organic solvents such as acetonitrile, acetone, or methanol. In some cases, it is accompanied by other extraction methods such as SPE or LLE to obtain better efficiency. LLE uses immiscible organic solvents that are mixed for the subsequent separation of the analyte in the organic phase, which allows optimal recovery of a clean sample for injection into the analysis instrument (Moein et al., 2017).

One of the most powerful analytical instruments for the separation and detection of analytes is high performance liquid chromatography (HPLC). In HPLC, compounds suspended in solvents are separated according to their shape, size, or charge when they pass through a solid phase, analytical column, which allows obtaining a type of characteristic chromatographic fingerprints of the different components of the extract. Separation of phytochemicals can be done through the use of isocratic systems, with a single mobile phase, or through elution gradients, where the composition of the mobile phase is gradually modified from an organic solvent to water (Moein et al., 2017). After elution, the identification of bioactive compounds is carried out by a detector, such as UV detectors, highly sensitive, cost effective, and popularly used with HPLC (Thomford et al., 2018; Tijare et al., 2016).

Validation of bioanalytical quantification methods, such as HPLC coupled to a UV detector (HPLC-UV), is part of good laboratory practices in the data management and report from clinical and preclinical studies for the development of new herbal medicines. In addition to ensuring the reliability, reproducibility and quality of the method, it supports

the veracity and regulation of the pharmacological use indicated for the potential herbal medicine (Moein et al., 2017).

Different guides such as the American Food and Drug Administration (FDA) Bioanalytical Method Validation Guide for industry describe the experiments necessary to carry out the complete validation of newly developed bioanalytical methods (FDA, 2018). Validation of analytical methods, based on FDA guidelines, includes parameters such as linearity, sensitivity, selectivity, specificity, accuracy, precision (repeatability and reproducibility), and stability, which will be described in subsequent sections (FDA, 2018).

In addition, aspects such as extraction recovery and matrix effect can be analyzed using internal standard (IS) methods. An IS, is a substance other than the components of the extract that may have characteristics or structures similar to the analytes of interest. This is added in known and constant proportions to all samples to be analyzed to compensate for matrix effects and ensure accurate results (Moein et al., 2017).

2.3.1.1 Linearity and sensitivity

Linearity is the ability of an analytical method to show that the response of the instrument is proportional to the concentration of the analyte in the study sample. The linear range is prepared in the study matrices and must contain at least five points of standard concentrations spiked with the single concentration of the IS. The range must include the lower limit of quantification (LLOQ), that is, the lowest concentration of the analyte that can be precisely and accurately quantified and that defines the sensitivity of the method. Three separate runs should be made on the same day (intra-day) and on different days (inter-day) for the full range.

Additionally, at least six repetitions of quality control (QC) samples should be considered, corresponding to three levels of known concentrations, within the linearity range, added to blank matrices: high QC (QCH), medium (QCM), and low (QCL).

The FDA's proposed acceptance criteria for matrix linearity suggest that the coefficient of determination should be greater than 0.995 ($r^2 > 0.995$), the LLOQ should be 5-fold

compared to the matrix blank response. The relative standard error (%RSD) with respect to the nominal concentration must be equal to or less than 15% for all standard concentrations and QC levels, except for the LLOQ which must be $\leq 20\%$.

2.3.1.2 Selectivity

The FDA indicates that the analyst must verify that the method can distinguish the desired analytes from potential interfering substances in the biological matrix that include endogenous components of the matrix, such as metabolites or breakdown products, as well as other impurities. The selectivity of the method is demonstrated by testing at least six individual sources of target biological matrices compared to IS spiked matrices, as well as QCL and QCH levels. The analyst must confirm that the matrix blanks are free from interfering analyte and IS retention times to define that the method is selective.

2.3.1.3 Accuracy and precision

The accuracy of the method describes the closeness of the concentration value obtained by the method to the expected concentration, while the precision indicates the similarity of individual measurements between samples of the same concentration. Precision is divided into repeatability, evaluated with tests within the same day, and reproducibility, when they are carried out on different days. Both precision and accuracy are calculated with five determinations of each QC level in intra- and inter-day assays, with three sets of samples per day, on at least three different days. The variation in precision, expressed in %RSD, should not exceed 15% for QC, and 20% for LLOQ. Similarly, the accuracy must be within $\pm 15\%$ of the true value and $\pm 20\%$ for the LLOQ.

2.3.1.4 Stability

The analytes can undergo modifications by the different storage conditions to which they are subjected during the studies, for which the evaluation of the stability of the samples represents a critical factor in the validation of the method. The stability of the analytes in the biological samples must estimate the storage time without important modifications or losses, for this at least three aliquots of QCL, QCM, and QCH must be analyzed under

short-term storage conditions (up to 24 hours), at long term (more than one day), and in cycles of freezing-thawing (three cycles). The nominal concentration must be $\pm 15\%$ (%RE) and $\leq 15\%$ (%RSD).

2.3.1.5 *Extraction recovery and matrix effect*

Extraction recovery is the difference in response of analytes when added post-extraction compared to the response from a normal extraction procedure. On the other hand, the effect of the matrix identifies the affectation that the endogenous components of the matrix have in the quantification of the analytes extracted from biological samples compared to concentrations added directly in the solvent used for the injection. In both cases, parameters are determined using five replicates of each QC of extracted samples compared to post-extraction spiked samples (recovery) or against spiked solvent blanks (matrix effect). Accuracy and precision shall be $\pm 15\%$ and $\leq 15\%$, respectively.

2.3.2 Relevance of preclinical PK in drug development

Pharmacokinetics (PK) is defined as the study and temporal characterization of drugs and their metabolites in the body, through the kinetic analysis of concentration-time curves obtained from samples of organic fluids (Doménech Berrozpe et al., 1997). From the concentration-time curves, parameters associated with the processes of absorption, distribution, metabolism, and excretion (ADME) of said compounds can be established.

Absorption stage occurs in the administration of compounds by the extravascular route, through which the drug is transferred from the site of administration to the general or systemic circulation. Once it reaches the systemic circulation, it is distributed throughout the body, where it is reversibly transferred from the general circulation to the tissues as blood concentrations increase, until a steady state in distribution is achieved. Simultaneously, elimination takes place, which involves metabolism, whereby the drug molecule is changed into a different molecule, or excretion, where the drug molecule is

excreted in the liquid, solid, or gaseous "waste" of the body (Doménech Berrozpe et al., 1997; Waller et al., 2021).

To establish an adequate description of the temporal evolution of drug levels, models are used in which the speeds of the ADME processes are expressed mathematically, developing equations that allow describing and predicting the amounts or concentrations of the drug in the body time function.

Non-compartmental analyzes (NCA) are an important tool in determining the PK of a drug. Once the drug is ingested, the concentration-time profiles are recorded from biological fluids such as plasma, from these data inferences can be made about the ADME processes of the drug components, as shown in Figure 6 (Bulitta and Holford, 2014).

Unlike compartmental models, which show the test organism as a composite of a few compartments, noncompartmental models estimate pharmacokinetic parameters in a single system with drug components available in continuous cycles through the circulatory system (Bulitta and Holford, 2014). Due to the above, the modeling of the differential equations that describe the NCA becomes simpler and much more realistic estimates are made physiologically speaking (Gillespie, 1991).

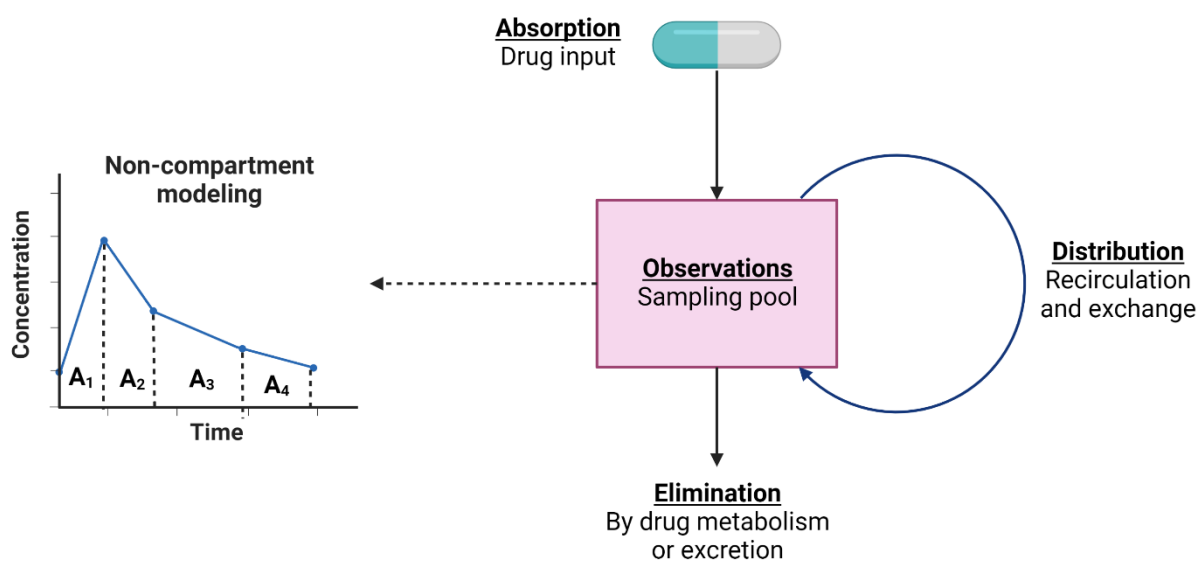


Figure 6. Non-compartmental modeling and graphical representation.

Pharmacokinetic parameters can be categorized as descriptive and quantitative (Foster, 2007). The first ones are observational and include the maximum concentration (C_{\max}) and the maximum time (T_{\max}). The quantitative parameters, obtained through mathematical calculations, are the area under the curve from the initial time to an assigned time (AUC_{0-t}), the AUC from zero to infinity ($AUC_{0-\infty}$), the mean residence time (MRT), the apparent clearance rate (CL/F), terminal slope (λ_z), and half-life ($t_{1/2z}$). The equations to calculate them will be presented later (Bulitta and Holford, 2014; Foster, 2007; Gabrielsson and Weiner, 2012; Noe, 2020).

The C_{\max} estimates the maximum concentration achieved after the oral dose presented graphically by the quantification of concentrations along the PK. In turn, T_{\max} is the time at which C_{\max} occurs. If more than one C_{\max} is identified, the first one will correspond to T_{\max} . The accuracy to identify both parameters will depend on the sampling frequency and the more continuous the sampling, the closer the values will be to the real PK behavior (Noe, 2020).

The terminal phase disposition rate constant corresponds to λ_z and is calculated by linear regression on a semi-log scale of the concentrations-time (Figure 7), followed by calculation of the half-life in the terminal phase, $t_{1/2z}$, using (1).

$$t_{1/2} = \frac{\ln(2)}{\lambda_z} \quad (1)$$

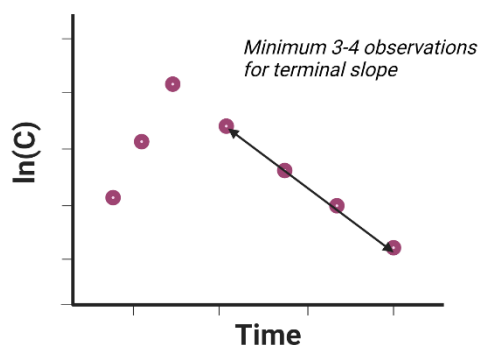


Figure 7. Semilog plot demonstrating the estimation of λ_z .
Modified from(Gabrielsson and Weiner, 2012)

Since the NCA assumes that there are no specifically defined compartments, measurements of the area under the plasma concentration-time curve are calculated by interpolation with the linear trapezoidal rule (2) or log-linear trapezoidal rule (3):

Linear interpolation:

$$AUC_0^t = \sum_{i=1}^n \frac{C_i + C_{i+1}}{2} \cdot \Delta t \quad (2)$$

Logarithmic interpolation:

$$AUC_0^t = \sum_{i=1}^n \frac{C_{i+1} - C_i}{\ln\left(\frac{C_{i+1}}{C_i}\right)} \cdot \Delta t \quad (3)$$

To calculate the $AUC_{0-\infty}$, we must consider the AUC_{0-t} and obtain the AUC of the last measured concentration (C_{last}) at the concentration in infinite time (AUC_{t-last}), the latter is calculated by extrapolation in the terminal phase of the decrease in concentration in a log-linear manner, with (4):

$$AUC_{last-\infty} = \frac{C_{last}}{\lambda_z} \quad (4)$$

Finally, $AUC_{0-\infty}$, is calculated by (5) as:

$$AUC_{0-\infty} = AUC_{0-last} + AUC_{last-\infty} \quad (5)$$

Another parameter of great importance in the elimination process is the systemic clearance, which translates as the rate of removal proportional to the concentration of the drug (bioavailability=F). In extravascular administration it is known as apparent clearance and is calculated as follows (6):

$$CL/F = \frac{\text{Dose}}{AUC_{0-\infty}} \quad (6)$$

Finally, there are some parameters that can be determined in an apparent way, using specialized PK software, such as *PK Solver* (Zhang et al., 2010). This add-on suggests that the drug is available at a constant rate over a period to calculate the MRT (7), the time a drug molecule remains in the body.

$$MRT = \frac{AUMC_{0-\infty}}{AUC_{0-\infty}} \quad (7)$$

To do this, the value of the area under the curve of the first moment of the curve from 0 to infinite time ($AUMC_{0-\infty}$) is obtained, defined as the AUC of the product of concentration and time against time, as shown below (8):

$$AUMC_{0-\infty} = AUMC_{0-last} + \frac{C_{last} \cdot t_{last}}{\lambda_z} + \frac{C_{last}}{\lambda_z^2} \quad (8)$$

As has already been explained, PK models offer information on the behavior of the organism regarding the drug, which determines the success rate that it may have on specific diseases, especially when the diseases have a complex mechanism of development and access to the target organ to be treated, such as CNS diseases. For this, in combination with the evaluation of the pharmacokinetic profile in a healthy organism, the implementation of damaged models is suggested to study the efficacy and safety of a drug, integrating PK and PD evaluations, which allows accelerating the development of new therapeutic entities (Chien et al., 2005; Katzung and Vanderah, 2018; Schentag et al., 2001).

2.3.3 Preclinical neuroinflammation models

Several CNS diseases, such as neurodegenerative diseases, have associated neuroinflammation as one of the key factors in their triggering. Therefore, the evaluation stages, specifically PK and PD, that are included in the development of potential pharmacological agents against these pathologies should be tested in models associated with inflammation at CNS level as a therapeutic target.

In order to verify the ability to reach the site of action, but above all to maintain the protection entities of the brain, such as the BBB. To this end, models such as LPS-induced neuroinflammation and its subsequent evaluation of vascular permeability with Evans blue dye offer important tools for the above objective (Batista et al., 2019; Nidavani et al., 2014).

2.3.3.1 *Lipopolysaccharide-induced neuroinflammation model*

Local or peripheral administration of LPS, an endotoxin purified from the cell wall of gram-negative bacteria, activates immune cells that trigger a systemic and peripheral inflammatory response. LPS interacts with glial cells through the TLR4 receptor, which activates microglia and astrocytes, as well as immune cells in different organs. By binding to the TLR4 complex, it polarizes microglia to the M1 phenotype that triggers its inflammatory effects (Hernandez-Baltazar et al., 2020).

Among the main damages caused by LPS, neuronal alterations, cellular stress in peripheral organs and the release of proinflammatory cytokines by microglia stand out. Although it has been determined that cytokines cannot cross the BBB, they are capable of transferring signals from the inflammatory process to the brain (Banks et al., 2015; Peng et al., 2021). In addition, it has been shown that LPS is capable of inducing the production of proinflammatory molecules from the periphery (Nava Catorce and Gevorkian, 2016). Therefore, it is one of the most widely used models of neuroinflammation, especially in diseases where microglia play a central role in triggering pathological pathways (Batista et al., 2019; Hernandez-Baltazar et al., 2020).

LPS-induced inflammation models have been carried out mainly by administration routes: intracerebroventricular, intraperitoneal and intravenous, with dose ranges from 0.02 mg/kg to 5 mg/kg, where through one or several administrations, increased expression of IL-1 β , IL-6 and TNF- α has been observed (Banks et al., 2015; Batista et al., 2019; Jangula and Murphy, 2013; Nava Catorce and Gevorkian, 2016).

The effects of LPS between the different studies show variations in the responses that depend on the mouse strain used, the form of administration, the concentrations of LPS and the time of analysis of the biological samples after administration. Although it has been generally established that the peripheral administration of LPS in adult and old mice at high doses produces an exacerbated neuroinflammatory response, it therefore offers an ideal model for the evaluation of herbal medicines in development (Banks et al., 2015; Nava Catorce and Gevorkian, 2016).

2.3.3.2 *Cerebrovascular permeability with blue Evans dye*

BBB is a selective interface that functions as a regulator of substances and communication between the CNS and the peripheral system. Its main function is to protect the brain from exposure to neurotoxic agents or immune cells activated by endogenous or exogenous molecules that threaten cerebral homeostasis (Goldim et al., 2019; Petronilho et al., 2019).

For optimal maintenance of BBB cohesion and selectivity, brain endothelial cells are closely aligned with specific structures, known as adherens junctions and tight junctions. Adherens junctions are responsible for maintaining the structure, while the tight junctions correspond to a complex of cytoplasmic and transmembrane proteins that regulate the passage of those substances necessary in the brain (Goldim et al., 2019).

However, damaging processes such as inflammation, oxidative stress, stimuli related to the immune system, as well as some traumas, can alter the permeability of the BBB by breaking down the structures that maintain its integrity (Goldim et al., 2019; Petronilho et al., 2019). Therefore, the BBB plays a fundamental role in preventing the development of CNS pathologies, mainly those induced in response to inflammation (Saunders et al., 2015)

The acute inflammatory response suddenly produces three important events: 1) vasodilation and increased blood flow, 2) increased vascular permeability, and 3) the presence of immunomodulatory molecules in the affected tissues (Nidavani et al., 2014).

The permeability of the BBB can be determined by dye injection such as Evans blue (EB), based on that compounds above 180 Da cannot cross a healthy BBB. Because the molecular weight of EB is 961 Da, it is used as a marker of permeability in the BBB. (Goldim et al., 2019; Nidavani et al., 2014; Petronilho et al., 2019).

To this end, the evaluation of this assay is based on the fact that, after injection of EB intravenously (femoral or caudal), it binds rapidly, strongly and exclusively to the plasmatic protein albumin (Saunders et al., 2015). Under normal physiological conditions, albumin is unable to cross the BBB, but when the structures of this barrier are degraded, the EB-albumin complex, with a weight of 68,500 Da, will give colorations within the tissue that will show if there are leaks to the brain by the damage done to the BBB (Goldim et al., 2019; Radu and Chernoff, 2013).

The EB-albumin conjugate can be identified macroscopically by the color change in the tissue, but it can also be evaluated and quantified from biological fluids such as serum and homogenized tissue samples (Nidavani et al., 2014). Although it is a simple method, the correct administration of the dye by injecting it through the lateral caudal vein is essential to obtain ideal results (Radu and Chernoff, 2013).

Chapter 3

Bioanalytical method validation for coumarins quantification

3.1. Methods

Chemicals and reagents

Rutin (internal standard, IS) and trifluoroacetic acid (TFA), were purchased from Sigma-Aldrich (St. Louis, MO, USA). HPLC-grade solvents: acetonitrile, methanol, and water, were acquired from Tecsiquim (Mexico, Mexico), and reagent-grade hexane and ethyl acetate were purchased from Merck (Darmstadt, Germany). Coumarins 6-methoxy-7-isoprenyloxy coumarin or 7-*O*-prenylscopoletin (PE); 6,7-dimethoxycoumarin or scoparone (SC); 6,7,8-trimethoxycoumarin or dimethylfraxetin (DF); 7-methoxycoumarin or herniarin (HR), and isoprenyloxy coumarin or 7-*O*-prenylumbelliferone (PU) were isolated and purified in the laboratory from a hexanic extract from *T. lucida* further described.

Coumarins isolation from hexanic extract of *T. lucida*

Coumarins 7-*O*-prenylscopoletin (PE); scoparone (SC); dimethylfraxetin (DF); herniarin (HR), and 7-*O*-prenylumbelliferone (PU) were isolated from hexanic extract of *T. lucida* following the methodology described by Monterrosas Brisson et al. (2020), therefore, the purification process carried out by the authors is briefly described (Monterrosas Brisson et al., 2020).

Twenty-five grams of hexanic extract of *T. lucida* were subjected to separation by open column chromatography packed with normal phase silica gel (200 g, 70-230 mesh, Merck) and a solvent system composed of hexane/ethyl acetate was used. to elute the column, yielding 55 fractions. Subsequently, the fractions: F7, F11, F15, F17 and F18, which contained the coumarins of interest, were individually subjected to open column separations with silica gel reversed phase (RP-18, 40-63 µm, Merck) under systems of water/acetonitrile. Finally, the identity of the coumarins PE, SC, DF, HR, and PU were

verified by UV coupled high performance liquid chromatography (HPLC-UV) compared with the standards of those obtained previously. The chemical structures of the five coumarins and the IS are shown in Figure 8.

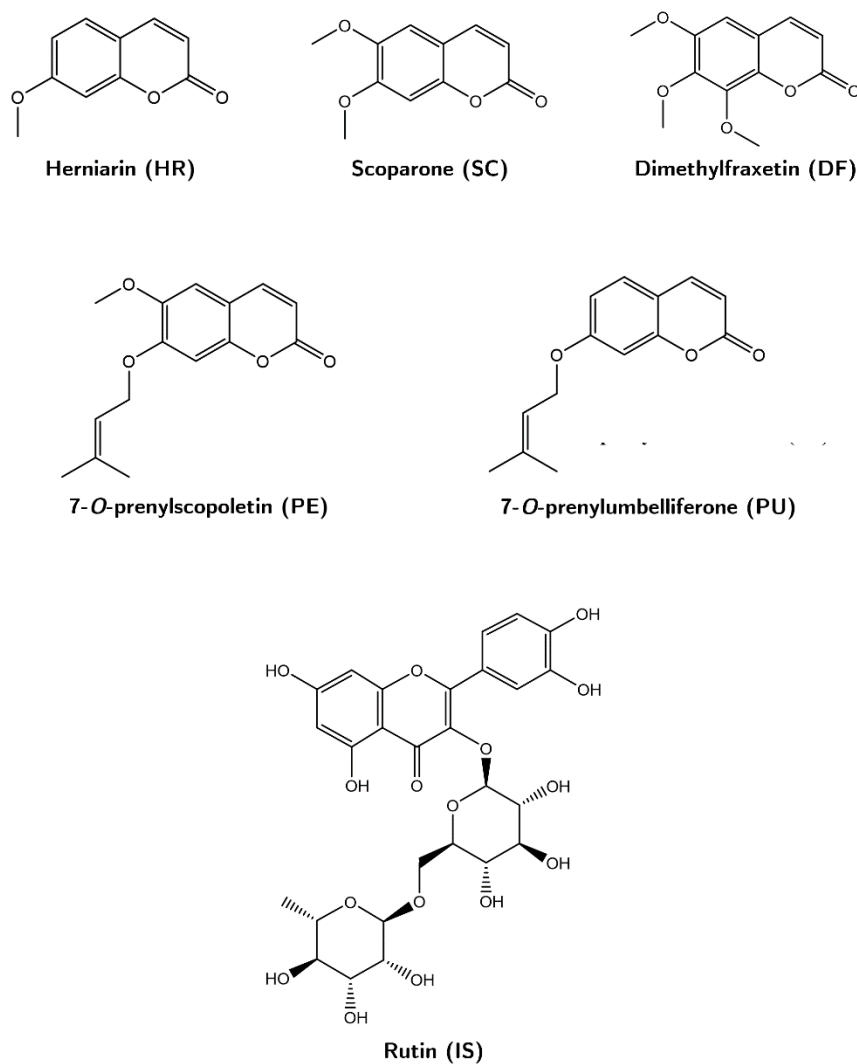


Figure 8. Chemical structures of the coumarins 7-O-prenylscopoletin (PE), scoparone (SC), dimethylfraxetin (DF), herniarin (HR), and 7-O-prenylumbelliferone (PU), and of the rutin (IS).

Preparation of standards

The batch of reference standards used in the validation of the analytical method for the determination and quantification of the compounds of interest was obtained in accordance with the guide published by the FDA (2015): Analytical Procedures and Methods Validation for Drugs and Biologics (FDA, 2015).

This guide states that all standards and reference materials used for validation must ensure proper preparation, storage, and use to avoid interfering or contaminating, in order to perform an adequate analysis.

3.1.1.1. Preparation of working solution, calibration curve, and quality control samples

Ten mg of each coumarin: PE, SC, DF, HR, and PU obtained previously were weighed to prepare individual stock solutions of each of the compounds at concentrations of 1.0 mg/mL, dissolved in methanol. Solutions were stored at -4°C until use.

From the stock solutions, each coumarin was added to prepare a working solution containing the mixture of the five coumarins at concentrations of 200 µg/mL for each compound. With the working solution, serial dilutions were made, ranging from 200 µg/mL to 0.781 µg/mL of each coumarin. The dilutions were also stored until use under previously established conditions.

Subsequently, the calibration curve was prepared, for which 20 µL of the points of the serial dilutions were individually spiked, under three conditions. The first condition was the preparation directly in the injection system, methanol, for a final volume of 100 µL. For the other conditions, the same quantities of the calibration curves were evaluated, but in the biological study matrices corresponding to fluids (plasma) and tissues (brain, kidneys, and spleen). These samples were subjected to an extraction process described below. In each condition, final concentrations were obtained at 40, 20, 10, 5, 2.5, 1.25, 0.625, 0.312, and 0.156 µg/mL.

Finally, quality control (QC) samples were prepared at three concentration levels: high (30.0 µg/mL), medium (3.0 µg/mL), and low (0.3 µg/mL), included in the range of the calibration curve.

3.1.1.2. Internal standard preparation

Rutin (10 mg), used as internal standard (IS), was dissolved in methanol to reach a final concentration of 1.0 mg/mL. The IS working solution was prepared by diluting 1.0 mL of the solution in 99.0 mL of acetonitrile to reach a final concentration of 10 µg/mL.

Coumarin Extraction Process from Plasma and Tissue Samples

Plasma samples and tissue homogenates were subjected to a protein precipitation method followed by liquid-liquid extraction.

Three hundred µL of acetonitrile containing the IS were added to 100 µL of spiked matrices with the concentrations defined in the calibration curve and the QC samples, for protein precipitation. Subsequently, they were mixed in a vortex for 3 min, 200 µL of dichloromethane were added, to continue with the liquid-liquid extraction, vortex for 5 min and centrifuged at 14,000 rpm for 10 min. The organic phase was placed in new tubes and the solvents were completely evaporated at room temperature.

Finally, for quantitative analysis, the recovered samples were resuspended in 100 µL of methanol, filtered, transferred to sampling microvials and injected into the validated chromatographic system described below.

HPLC-UV analysis conditions

Biological and standards samples analysis was carried out using a Waters 2695 series high-performance liquid chromatography (HPLC) method. With a separation module (Waters 2695) consisting of a quaternary pump, degasser, autosampler, and a

thermostatted column, additionally connected to a photodiode array UV-VIS detector (Waters 2696).

Chromatographic separation and method validation were performed using a C18 column (250 x 4.6 mm, 5 μ m, SUPELCO Discovery®, Merck). The method of detection and quantification of the compounds has a duration of 30 minutes, the injection volume is 10 μ L per sample at a flow of 0.9 mL/min of the mobile phase composed of an aqueous solution of trifluoroacetic acid at 0.5% (A) and acetonitrile (B). The elution gradient used is shown in Table 1.

Table 1. Elution gradient of the analytical method by HPLC-UV

Time (min)	% A	% B
0.00	100.00	0.00
1.00	100.00	0.00
2.00	95.00	5.00
3.00	95.00	5.00
4.00	70.00	30.00
20.00	70.00	30.00
21.00	50.00	50.00
23.00	50.00	50.00
24.00	20.00	80.00
25.00	20.00	80.00
26.00	0.00	100.00
27.00	0.00	100.00
28.00	100.00	0.00
30.00	100.00	0.00

The samples were read at a wavelength (λ) of 330 nm and were processed with Empower Pro 3.0 software (Waters, MA, USA).

Validation of the HPLC-UV analytical method

Validation of the HPLC-UV analytical method for the determination and quantification of the coumarins of interest present in the extract of *T. lucida* was carried out in accordance

with that described in the FDA Bioanalytical Method Validation: Guidance for Industry (FDA, 2018).

3.1.1.3. *Selectivity and specificity*

The selectivity must demonstrate no interferences in the system or the biological matrices under study at the retention times (RT) established for the compounds analyzed and the IS. The specificity determines that there are no endogenous or exogenous interferences in the matrices. For this, six units obtained from diverse sources of each of the following samples were evaluated:

- a) Blank system
- b) Blank matrices
- c) LLOQ spiked in system
- d) LLOQ spiked in matrices

For the method to be considered selective and specific, the blank samples must be free of agents that intervene in the correct quantification of the compounds and IS at the previously established TR. Additionally, spiked samples must maintain a margin of $\pm 20\%$ from the lower limit of quantitation (LLOQ).

3.1.1.4. *Linearity*

The linearity of the compounds was determined using five calibration curves prepared and analyzed on different days, both in the injection system and in the biological matrices under study, as indicated in the section *Preparation of working solution, calibration curves, and quality control samples*. The calibration curves prepared on the matrices were subjected to the extraction process indicated in *Coumarin Extraction Process from Plasma and Tissue Samples* before being injected into the HPLC-UV quantification method.

In both cases, a blank of reagents was included, corresponding to samples not added, and a blank spiked only with IS.

The ratio of the area under the curve (AUC) of each compound over the IS signal, compared against the nominal concentration of the analytes, was plotted. Linearity was determined by linear regression of the graphical representation of the calibration curves. Linearity acceptance parameters suggest a coefficient of determination (r^2) greater than 0.995.

3.1.1.5. Sensitivity

The lowest non-zero concentration that can be present on the calibration curve defines the sensitivity of the system, also known as LLOQ.

Sensitivity was qualitatively determined using the parameter that establishes that the LLOQ value corresponds to ≥ 5 times the signal/noise with respect to the response of the analyte in a sample blank. Subsequently, the value of the LLOQ was adjusted by its numerical determination as part of the precision and accuracy analyzes through six replicates in nine different runs of the lowest concentration of the curve where the relative standard deviation (RSD) and the relative error (RE) must be less than 20%.

3.1.1.6. Accuracy and Precision

Intra- and inter-day accuracy and precision were established by analyzing sample sets composed of six replicates of the high, medium, and low concentration levels of the QCs and the LLOQ (24 samples) for repeatability. Each set was injected into the method on three independent days to meet reproducibility evaluations.

Therefore, the concentration obtained in the accuracy evaluation must comply with a variation of RE $\pm 15\%$ for the QC and $\pm 20\%$ for the LLOQ according to its nominal concentration. The RSD for precision should be $\leq 15\%$ or $\leq 20\%$ on QC or LLOQ samples, respectively.

3.1.1.7. Extraction recovery and matrix effects

The effect of each biological matrix on the compounds was obtained by comparing five QC samples extracted from plasma against five samples prepared directly in methanol.

The matrix effect of each compound had to be between 80 to 120% to be approved. It was calculated by averaging the ratio of the AUCs of samples drawn from plasma and those prepared in methanol and the IS response signal for each. The equation for its calculation is shown below:

$$\text{Matrix effect} = \frac{AUC_{AM}/AUC_{SM}}{AUC_{AS}/AUC_{SS}} \cdot 100\% \quad (9)$$

Where:

AUC_{AM} = AUC of analyte extracted from matrix

AUC_{SM} = AUC of IS extracted from matrix

AUC_{AS} = AUC of analyte prepared in system

AUC_{SS} = AUC of IS prepared in system

Five replicates of QC samples, extracted from biological matrices were analyzed for extraction recovery compared to concentrations obtained from spiked samples post-extraction of matrix blanks at the same QC concentrations. The nominal concentration obtained in the processed matrices must range between $\pm 15\%$, evaluated by RE and $\leq 15\%$ for RSD.

3.1.1.8. Stability

Five replicates evaluated the responses of the analytes to the designated concentrations in the QCs. The stability studies covered the conditions of temperature and time of storage and processing of the samples. In all cases, the concentrations obtained from the stability studies were compared with freshly prepared samples and the RE and RSD of the concentration was calculated. The analytes were considered stable in plasma and tissues

when the concentration difference between the fresh samples and the test samples was less than 15%.

Short-term stability at room temperature (24 hours)

For short-term stability, the QCs were evaluated in the processed biological matrices maintained in the chromatograph's autosampler at room temperature for 24 hours and the concentrations obtained were compared against the nominal concentration.

Long-term stability at freezing temperature (-70°C)

Samples were prepared and subsequently evaluated at 30 days. The samples were stored at -70°C for the established period and the validation acceptance criteria were evaluated.

Freeze and thaw stability

The stability of the analytes was determined after three freeze-thaw cycles. The samples with the three levels of different concentrations were stored at -70°C for 24 h, then proceeded to thaw them at room temperature; Once thawed, they were frozen again under the same conditions. The freeze-thaw cycle was repeated until the third cycle was completed, when the samples were analyzed.

3.2. Results

Optimization of chromatographic conditions

The five coumarins 7-O-prenylscopoletin (PE); scoparone (SC); dimethylfraxetin (DF); herniarin (HR), and 7-O-prenylumbelliferone (PU) contained in the hexanic extract of *T. lucida* were injected under the conditions of the HPLC-UV system for their identification. The analytical method allowed an adequate separation of the compounds useful for their subsequent quantification in the system validation. Considering that the maximum absorption wavelengths (λ) of the analyzed compounds are between 320 and 350 nm, a

single λ at 330 nm was taken to identify and quantify of all the analytes in a single reading. Using the system, it was possible to determine the retention time (RT) and the specific UV spectrum for each compound, including the internal standard (rutin, IS), shown in Figure 9.

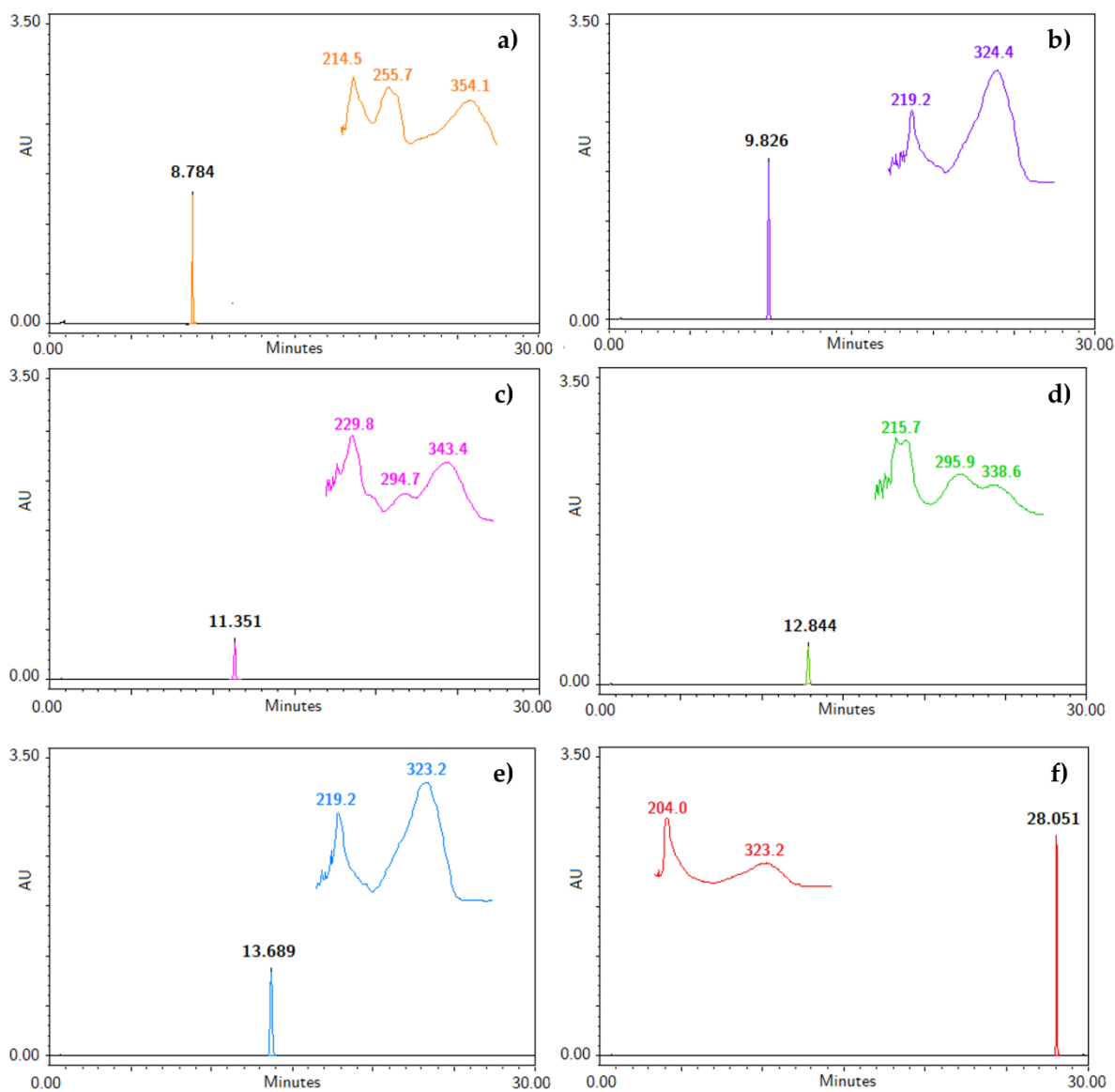


Figure 9. Chromatograms with retention time and specific UV spectra of (a) IS, (b) PE, (c) SC, (d) DF, (e) HR, and (f) PU at a concentration of 200 $\mu\text{g/mL}$.

Selectivity and specificity

Selectivity and specificity were evaluated by comparing the chromatograms of a representative matrix blank of the five matrices used (plasma and organs), a representative matrix blanks spiked with the concentrations corresponding to the LLOQs. The plasma and tissue samples extracted that were collected from mice 15 min after oral administration of a standardized fraction of bioactive coumarins from *T. lucida* (Figure 10).

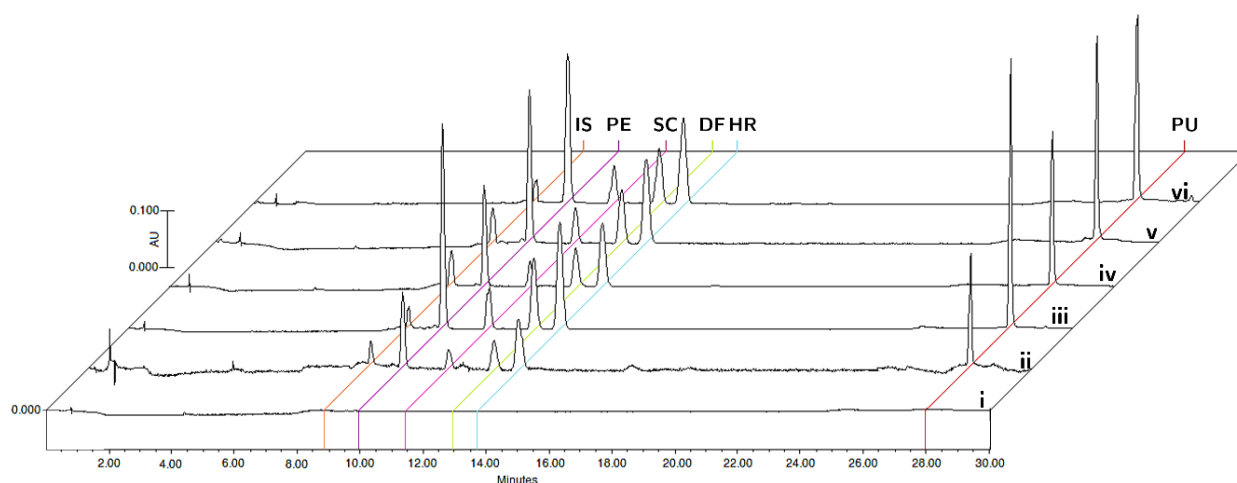


Figure 10. Representative chromatograms of (i) blank matrix, (ii) blank matrix spiked with LLOQ concentration, and processed samples collected at 15 min after oral administration of standardized fraction of *T. lucida* spiked with IS in plasma (iii), brain (iv), kidneys (v), and spleen (vi).

Figure 10(i) shows that the method is specific since there are no endogenous or exogenous agents present in the analysis matrices. In addition to this, Figure 10(ii) shows the selectivity of the method with the lowest concentration values of the compounds included in the calibration curve, delimited by LLOQ. Since there are no interferences in the TR for the detection of PE (9.8 min), SC (11.4 min), DF (12.8 min), HR (13.7 min), PU (28.0 min), and IS (8.8 min) and the blank response does not exceed 5% of IS response.

Linearity and sensitivity

The graphical representation of the calibration curve constructed with the ratio of the peak areas of the 9 standard concentrations of each coumarin in relation to the IS area was fitted to the least squares linear regression that gave the best fit to the data. The coefficient of determination (r^2) for all the calibration curves was greater than 0.9965.

Table 2 summarizes the equations that describe the linear regression models, the r^2 , and the specific LLOQs of each compound in the different biological matrices. The LLOQs presented in Table 2 were the values obtained from the visual determination of signal/noise ≥ 5 with respect to the sample blank. Therefore, through the accuracy and precision evaluations, a single value was determined for the LLOQs corresponding to 156 ng/mL, the minimum value of the calibration curves.

Table 2. Linearity equations of calibration curves and LLOQ determined for coumarins in plasma and tissue matrices.

Matrix	Analytes	Linearity equation	r^2	LLOQ ($\mu\text{g/mL}$)
Plasma	PE	$y = 0.2278x + 0.0246$	0.9996	0.18
	SC	$y = 0.0743x - 0.0126$	0.9987	0.05
	DF	$y = 0.1260x - 0.0322$	0.9965	0.15
	HR	$y = 0.2082x + 0.0294$	0.9997	0.17
	PU	$y = 0.2705x + 0.0916$	0.9976	0.10
Brain	PE	$y = 0.1607x + 0.0046$	0.9995	0.13
	SC	$y = 0.0510x - 0.0094$	0.9991	0.10
	DF	$y = 0.0841x - 0.0037$	0.9997	0.08
	HR	$y = 0.1455x - 0.0043$	0.9969	0.10
	PU	$y = 0.1886x + 0.0275$	0.9997	0.02
Kidney	PE	$y = 0.2394x + 0.024$	0.9998	0.07
	SC	$y = 0.0746x - 0.0054$	0.9995	0.18
	DF	$y = 0.1273x - 0.0119$	0.9994	0.03
	HR	$y = 0.2104x - 0.0376$	0.9986	0.16
	PU	$y = 0.2794x - 0.0397$	0.9993	0.02
Spleen	PE	$y = 0.3918x + 0.0278$	0.9996	0.12
	SC	$y = 0.1238x - 0.0284$	0.9986	0.02
	DF	$y = 0.2090x - 0.0218$	0.9991	0.05
	HR	$y = 0.3603x + 0.0271$	0.9989	0.11
	PU	$y = 0.4728x - 0.1095$	0.9989	0.02

PE = 7-O-prenylscopoletin, SC = scoparone, DF = dimethylfraxetin, HR = herniarin, and PU = 7-O-prenylumbelliferone. LLOQ = Lower limit of quantification. Values obtained from the calibration curves ($n=5$).

Accuracy and precision

The precision and accuracy estimated at the intra- and inter-day levels were evaluated in the five biological matrices by analyte mixed with the concentrations established for the low, medium, and high levels of the QC samples. The accuracy and precision results are presented in Table 3. The intra- and inter-day accuracy values range from 86-108%, and

87-105%, respectively, according to the error percentages shown in Table 3, with the lowest values in the plasma matrices.

On the other hand, the repeatability precision has an RSD between 0.90–10.71%, both limits found at the intermediate QC concentration. The reproducibility of the analytical method ranges from 0.75–11.05%. All values are included in the approval limits.

Extraction recovery and matrix effect

Plasma and tissue matrices, spiked after the extraction process with QC levels, were compared to the previously spiked samples to determine the extraction recovery of both, coumarins and IS. The lowest extraction value was 87.15% for PE in plasma (Table 4).

Likewise, the percentage differences from the observed concentrations in biological matrices compared with the QC samples prepared in the injection system were recorded for matrix effect evaluation. The accuracy of the values was between 85.09% and 107.77%, with RSD < 12.6%, for the different coumarins, while the IS varied up to 7.59%, in a range of 92.24–109.67%, as shown in Table 4.

Stability

In general, all the evaluations of the compounds in the matrices adequately met the three test conditions for stability, presented in Table 5. After 24 hours in the autosampler at room temperature, all the compounds showed variations below 10 % of the theoretical concentration and differences between -10.42–14.32% compared to fresh samples. Samples kept frozen for one month exhibited the highest RSD in spleen samples, up to 14.11%, and the lowest recoveries of 85.7% in the plasma matrix. QC samples subjected to freeze-thaw cycles showed the lowest variation values, below 10%.

Table 3. Data of accuracy and precision determined for coumarins in plasma and tissue matrices.

Nominal Concentrations (µg/mL)		30.0				3.0				0.3			
Matrix	Analytes	Repeatability		Reproducibility		Repeatability		Reproducibility		Repeatability		Reproducibility	
		RE (%)	RSD (%)	RE (%)	RSD (%)	RE (%)	RSD (%)	RE (%)	RSD (%)	RE (%)	RSD (%)	RE (%)	RSD (%)
Plasma	PE	1.30	1.73	1.05	1.49	1.44	1.79	1.71	1.34	8.66	1.49	4.59	4.83
	SC	-5.28	2.41	-4.94	1.73	-9.61	3.74	-8.25	3.04	-6.67	3.55	-12.71	6.69
	DF	-11.95	1.45	-7.80	5.19	-7.85	1.08	-5.39	2.93	-14.01	6.30	-10.64	5.7
	HR	-6.69	1.51	-2.56	4.74	1.31	1.03	1.84	1.02	-2.18	2.83	0.06	3.07
	PU	1.96	1.66	1.94	1.27	-0.17	0.90	0.06	0.75	-5.66	2.11	-4.36	2.02
Brain	PE	0.99	4.14	-0.12	3.10	5.34	1.58	2.96	2.76	2.09	1.28	2.37	1.94
	SC	-0.64	1.82	-1.81	2.19	3.97	0.61	1.96	2.39	-6.41	5.35	-7.98	5.41
	DF	1.97	3.71	1.54	2.46	7.81	2.78	3.17	7.07	-4.03	2.36	-2.68	3.77
	HR	1.77	3.74	1.17	3.47	-1.79	3.70	-5.53	5.10	2.78	1.35	3.69	1.62
	PU	3.47	1.98	1.49	2.75	4.32	0.92	-0.98	6.28	-5.11	6.81	-7.60	5.42
Kidney	PE	-3.59	2.30	-2.08	2.35	0.94	0.23	0.51	1.06	-2.02	1.21	-1.46	1.06
	SC	-0.65	2.03	-0.90	1.45	2.39	1.04	1.35	1.51	0.07	1.27	0.20	0.86
	DF	-0.27	1.23	-0.20	0.90	-2.18	6.29	-1.81	4.08	-0.07	3.08	-1.08	4.33
	HR	3.58	3.12	2.10	2.99	-4.14	2.43	-0.26	5.07	-6.52	3.33	-7.12	2.66
	PU	-0.21	2.02	-0.15	1.90	-4.41	6.51	-1.66	5.24	-5.93	6.14	-4.70	5.71
Spleen	PE	1.64	1.30	1.90	3.04	-10.29	6.93	-4.80	8.00	-4.52	2.50	-8.01	9.87
	SC	-0.43	7.32	-2.54	11.05	-12.42	3.32	-11.73	6.25	-6.69	8.82	-7.46	8.03
	DF	-9.08	7.89	-10.04	5.33	-4.93	10.71	-5.10	8.77	-3.77	9.44	-4.16	7.76
	HR	2.34	2.65	1.47	2.95	-3.52	9.67	-2.20	6.82	-2.38	5.45	-5.44	6.58
	PU	-7.17	4.30	-6.18	3.39	-10.72	2.70	-8.36	7.00	-8.99	2.94	-4.00	6.55

PE = 7-O-prenylscopoletin, SC = scoparone, DF = dimethylfraxetin, HR = herniarin, and PU = 7-O-prenylumbelliferone. RE = Relative error; RSD = Relative standard deviation. Values for repeatability were calculated by one set of QC samples ($n=6$, per level). Values for reproducibility by three sets of QC samples ($n=18$, per level).

Table 4. Data of extraction recovery and matrix effects determined for coumarins in plasma and tissue matrices.

Spiked Concentrations ($\mu\text{g/mL}$)		30.0				3.0				0.3			
Matrix	Analytes	Extraction Recovery		Matrix Effect		Extraction Recovery		Matrix Effect		Extraction Recovery		Matrix Effect	
		ACC (%)	RSD (%)	ACC (%)	RSD (%)	ACC (%)	RSD (%)	ACC (%)	RSD (%)	ACC (%)	RSD (%)	ACC (%)	RSD (%)
Plasma	PE	99.04	7.11	94.60	7.78	87.15	8.25	89.72	9.55	88.00	10.41	86.27	10.43
	SC	98.30	2.38	98.55	7.53	91.67	8.16	92.52	9.53	94.13	5.78	89.59	9.33
	DF	102.04	3.91	101.23	5.45	100.88	10.35	94.83	11.26	97.58	7.33	102.99	4.70
	HR	99.67	6.21	94.79	6.08	87.83	7.20	92.93	8.53	93.82	3.83	99.70	6.13
	PU	102.17	8.05	94.66	7.11	94.77	1.27	85.09	3.10	101.67	9.42	108.91	10.23
	IS	99.42	4.66	99.61	7.59	94.22	2.43	92.24	2.38	99.71	3.77	100.59	3.66
Brain	PE	91.64	4.80	106.08	6.48	88.01	0.54	102.28	2.64	92.19	1.21	98.72	3.11
	SC	99.44	1.23	104.99	7.68	94.65	1.06	100.94	4.21	89.70	6.03	94.89	4.67
	DF	90.13	1.60	107.26	5.22	96.44	5.16	105.50	7.29	93.08	3.45	94.55	5.75
	HR	91.81	3.22	105.11	4.90	94.27	3.10	104.20	5.42	112.29	1.54	100.92	3.04
	PU	93.49	5.98	107.77	7.35	99.56	3.95	101.16	9.57	95.23	5.72	96.32	9.37
	IS	95.11	2.75	95.32	6.31	98.97	2.28	99.01	2.81	99.84	2.65	94.71	3.90
Kidney	PE	97.95	2.29	96.77	2.67	99.28	0.93	96.08	6.18	91.30	1.16	100.34	4.79
	SC	99.99	2.80	98.86	1.70	105.72	0.97	95.55	5.96	94.28	9.05	100.39	12.60
	DF	99.40	2.30	97.20	2.81	104.84	4.78	98.51	7.05	87.24	2.72	96.97	9.83
	HR	103.06	6.55	100.89	4.06	91.38	2.42	95.68	6.09	90.39	1.25	99.26	5.03
	PU	100.87	8.68	98.52	5.28	103.27	5.16	97.70	10.57	93.11	3.89	97.25	6.83
	IS	101.26	1.25	101.28	1.63	103.72	3.20	103.89	5.66	99.94	2.75	109.67	4.86
Spleen	PE	98.33	11.85	99.87	6.05	100.55	1.93	100.36	2.92	90.36	1.02	100.04	4.43
	SC	100.16	3.04	101.09	5.38	109.71	1.28	99.54	1.78	88.30	7.77	103.43	9.26
	DF	100.77	6.28	101.70	5.41	104.20	2.71	98.98	5.98	92.01	6.31	105.13	7.23
	HR	100.99	10.13	101.12	6.77	92.58	2.45	98.66	3.54	88.74	1.56	101.12	3.64
	PU	99.31	14.67	98.83	3.34	105.05	4.03	102.63	6.70	91.89	4.61	99.32	4.65
	IS	98.87	3.19	98.96	4.87	99.98	0.94	100.00	1.73	99.02	2.74	97.02	2.78

PE = 7-O-prenylscopoletin, SC = scoparone, DF = dimethylfraxetin, HR = herniarin, PU = 7-O-prenylumbelliferone, and IS = internal standard (rutin). ACC = Accuracy (100% - Relative error); RSD = Relative standard deviation. Values were calculated by QC samples evaluation ($n=5$, per level).

Table 5. Stability test of PE, ES, DF, HR, and PU in plasma and tissues matrices.

Nominal concentrations (µg/mL)		30.0						3.0						0.3					
Matrix	Analytes	Autosampler		Long-Term		Freeze-Thaw		Autosampler		Long-Term		Freeze-Thaw		Autosampler		Long-Term		Freeze-Thaw	
		RE (%)	RSD (%)	RE (%)	RSD (%)	RE (%)	RSD (%)	RE (%)	RSD (%)	RE (%)	RSD (%)	RE (%)	RSD (%)	RE (%)	RSD (%)	RE (%)	RSD (%)	RE (%)	RSD (%)
Plasma	PE	8.22	3.33	-5.20	4.14	-5.55	3.19	11.12	1.75	-4.44	0.14	-2.01	0.02	-4.00	7.11	-6.86	2.04	2.80	3.14
	SC	4.74	3.06	-8.41	0.4	-0.10	4.63	8.27	4.44	-14.30	3.23	2.70	1.75	10.18	3.67	-3.50	3.42	-14.02	2.78
	DF	4.21	1.83	-3.40	1.51	0.49	4.29	-1.38	3.34	-3.13	1.20	2.47	0.56	2.59	3.62	-6.74	3.52	-12.33	3.60
	HR	14.32	3.84	3.55	0.85	-5.47	3.27	12.83	2.62	3.99	1.26	-7.90	0.12	8.34	3.82	9.39	2.22	0.67	2.99
	PU	-9.86	0.32	-4.81	0.79	-5.10	3.30	-11.68	2.19	-10.56	3.79	-9.78	0.06	-6.02	6.04	-8.22	3.78	-9.54	2.90
Brain	PE	4.05	2.41	-3.82	7.36	-1.25	1.84	-0.34	0.42	-3.44	2.93	-2.34	0.81	-2.37	2.25	-0.63	2.20	-1.15	2.22
	SC	4.78	0.82	-4.75	5.16	-2.00	2.06	0.37	0.55	-0.94	3.18	-3.09	1.05	-2.15	6.74	-0.19	7.54	-1.98	3.52
	DF	3.21	1.84	-4.35	4.84	-0.35	2.71	3.73	4.47	0.46	7.28	-6.72	6.02	-4.07	3.93	-0.62	4.73	0.03	6.75
	HR	3.86	4.66	-4.72	7.56	-1.02	2.32	2.31	3.40	-0.98	4.02	-5.14	2.86	-3.47	2.28	-0.21	4.32	-0.69	3.43
	PU	4.57	1.36	-4.61	4.89	-1.74	3.57	1.80	6.54	-5.42	7.69	-4.49	1.81	2.13	7.31	3.45	5.33	-6.54	1.62
Kidney	PE	1.61	4.83	7.34	2.86	1.12	0.67	3.99	3.25	2.69	2.61	0.91	1.11	7.06	3.54	3.02	4.06	2.26	1.48
	SC	-0.35	3.02	4.36	0.96	0.49	1.25	5.72	4.22	2.63	4.94	1.51	1.10	7.01	2.06	3.92	2.74	2.62	1.16
	DF	0.66	2.66	5.67	1.09	0.47	2.83	4.79	3.43	8.12	6.10	0.82	2.74	5.83	0.91	5.19	0.61	-0.65	4.96
	HR	1.35	3.92	3.32	3.31	2.25	0.33	2.81	4.89	3.06	2.88	-0.62	2.98	8.17	0.69	5.12	4.41	2.03	0.52
	PU	1.66	5.07	6.46	2.54	-1.02	1.16	5.21	2.66	8.68	4.53	2.01	7.60	7.10	3.77	5.54	2.78	3.61	6.04
Spleen	PE	-1.02	3.87	2.78	1.68	2.38	1.95	-10.42	4.70	3.67	5.55	4.42	9.54	-5.98	4.42	1.51	14.11	2.50	9.85
	SC	-0.99	1.97	-2.12	9.82	-4.22	1.60	-6.71	2.83	2.22	9.10	-2.65	5.26	-7.70	5.57	-9.67	2.35	-9.57	5.92
	DF	1.50	6.07	7.60	7.81	-1.06	3.27	-1.66	9.62	7.09	4.06	0.49	2.05	6.88	8.79	5.43	6.32	-0.67	7.82
	HR	1.18	4.27	2.92	3.61	0.49	2.02	-0.16	11.83	7.44	2.80	4.87	3.30	5.46	6.29	0.22	5.85	-0.63	3.77
	PU	-2.63	5.87	4.26	1.51	2.27	5.02	-4.98	5.34	7.56	4.95	2.88	4.42	-0.09	1.99	-6.92	3.30	-8.53	6.45

PE = 7-O-prenylscopoletin, SC = scoparone, DF = dimethylfraxetin, HR = herniarin, and PU = 7-O-prenylumbelliferone. RE = Relative error; RSD = Relative standard deviation. Values were calculated by QC samples evaluation ($n=5$, per level).

3.3. Discussion

The HPLC-UV analytical method described in this thesis is capable of quantifying concentrations of five anti-inflammatory coumarins, with potential neuroprotective effects, in a precise and exact way in minimum volumes (100 μ L) extracted from mouse plasma and tissues. Although other research has established methods capable of measuring the concentrations of different coumarins in similar volumes, the organisms used to obtain biological samples, such as rats, are bigger, so they require different space conditions and care. Therefore, it represents an increase in the costs of maintenance and management of the animals (Zhao et al., 2013, 2016).

One of the important advantages of the method is the simultaneous quantification at low concentrations of the compounds of interest in the study, especially since medicines from natural sources commonly contain more than one active compound and are administered orally, which implies a loss in the bioavailability of the compounds limited by the absorption process carried out by the intestine. This method was able to determine concentrations of up to 20 ng/mL in the case of SC and PU in the spleen, kidneys, and brain (Table 2). Those concentrations above 156 ng/mL (LLOQ) were appropriately quantified under the parameters established by the FDA in its validation guide. Therefore, it was possible to maximize the collection of multiple data on the concentrations of the components, without the need to assign study animals for each compound, even at very low concentrations.

The extraction process is essential to achieve any of the stages of method validation and quantification of compounds in biological matrices. Due to its ease and speed, some studies use liquid-liquid extraction (LLE). Unfortunately, many times based on the type of biological material from which the compounds are extracted, such as tissues, it is necessary to carry out a protein precipitation process, although this does not ensure optimal recovery (Cárdenas et al., 2017; Zhao et al., 2016). The extraction process carried out in this study by PP with acetonitrile followed by LLE with dichloromethane ensured that more than 87% of the concentration of the compounds was recovered. For its part, the effects of the matrix were negligible because in all cases they were within the

allowed limits. Regardless of the biological source or the coumarin to be analyzed, they will be correctly quantified by the analytical method with variations of less than 12.6%.

During the development of drugs, the analysis times of the samples derived from preclinical studies can be prolonged for long times, even for months. In this way, the stability tests allow the evaluation of the modifications that the compounds may undergo or, where appropriate, to observe if they maintain their composition until the time of their analysis. One study performed stability tests on a series of coumarins and their derivatives in aqueous conditions at different pHs (Dragojević et al., 2011). This evaluation determined that, in general, coumarins maintain their stability, which was verified here under three test conditions that represented the temperature changes and handling times to which the samples were subjected throughout the validation.

An analytical method capable of simultaneously quantifying coumarins: 7-O-prenylscopoletin, scoparone, dimethylfraxetin, herniarin, and 7-O-prenylumbelliferone in mouse plasma and organs was successfully developed. The assay was validated according to its specificity, selectivity, linearity, sensitivity, accuracy, precision, recovery, and stability. This simple and highly specific method can be applied in preclinical pharmacokinetic studies such as the one described in the next chapter for the evaluation of coumarin concentrations contained in a biologically active fraction of *T. lucida* after its administration in murine models.

Chapter 4

Pharmacokinetic-pharmacodynamic study of bioactive fraction from

Tagetes lucida

4.1 Methods

4.1.1 Chemicals

Rutin (internal standard, IS), trifluoroacetic acid (TFA), lipopolysaccharide (LPS), blue Evans dye, sodium chloride (NaCl), sodium dihydrogen phosphate (Na_2HPO_4), were purchased from Sigma-Aldrich (St. Louis, MO, USA). HPLC-grade solvents: acetonitrile, methanol, and water, were acquired from Tecsiquim (Mexico, Mexico), Tween 20, potassium chloride (KCl), potassium dihydrogen phosphate (KH_2PO_4), and reagent-grade hexane and ethyl acetate were purchased from Merck (Darmstadt, Germany).

4.1.2 Hexanic extract preparation of *Tagetes lucida*

The aerial parts of the *T. lucida* species were collected in Xochitepec, Morelos, Mexico. A specimen was deposited in the Botanical Garden and Museum of Traditional and Herbal Medicine of the National Institute of Anthropology and History of Morelos, and was identified by biologists Margarita Aviles and Macrina Fuentes Mata, with folio number 2081.

The aerial parts of *T. lucida* were dried and pulverized (4-6 mm) in a mill (PULVEX-PLASTIC®). Subsequently, the dried plant material (1 Kg) was subjected to a maceration process with hexane (3 L), said system was left to stand for 24 hours, then it was filtered with Whatman No. 4 paper. The extract was concentrated through a process of distillation at reduced pressure in a rotary evaporator (Heidolp Laborota G3, Germany) at 50°C. This process was carried out in triplicate and subjected to a lyophilization process (LABCONCO®) until completely dry.

4.1.3 Bioactive fraction identification of hexanic extract

A column (280 x 85 mm) was packed with 200 g of silica gel (70-230 mesh, Merck) through which 25 g of previously adsorbed hexanic extract were passed. Five elution gradient systems (hexane/ethyl acetate) each of 250 mL were used, varying their proportions with 5% increases in polarity, starting at 100% hexane. The pool of systems was concentrated on a rotary evaporator under reduced pressure at 50°C. Finally, the concentrate, identified as the bioactive fraction, was injected into a HPLC-UV system, described later, at a concentration of 1 mg/mL.

4.1.4 Preparation of administration solutions

A 200 µg/mL solution of lipopolysaccharide (LPS) and another of 0.5% Evans blue dye were prepared independently, contained in sterile phosphate-buffered saline (PBS) with 1% Tween-20. PBS contained NaCl (8.06g/L), KCl (0.22g/L), Na₂HPO₄ (1.15g/L), and KH₂PO₄ (0.20g/L), adjusted to pH 7.4.

Likewise, the active fraction with a high coumarin content of interest was used for an aqueous preparation with 1% Tween-20. The concentration of the solution was 1 mg/mL.

4.1.5 Animals

Male mice ($n = 70$) of the ICR strain weighing between (35 ± 5 g), provided by the Century XXI Medical Center animal facility, were used throughout the experiments. Six mice per cage were placed and kept under the conditions of the vivarium with cycles of 12 hours of light/darkness (07:00 to 19:00 h) at 25 °C. Access to food (Rodent Laboratory Diet pellets, Harlan) and water was allowed ad libitum up to 12 h before the start of the evaluations. The mice were adapted to the laboratory environment three weeks prior to their use in the experiments.

The studies were carried out in accordance with the Official Mexican Standard NOM-062-ZOO-1999: Technical specifications for the production, care, and use of laboratory

animals (SEMARNAT, 2011). This project was approved by the Local Health and Ethics Research Committee of the Instituto Mexicano del Seguro Social (IMSS) on August 16, 2021, under registration number R 2021-1702-009.

4.1.6 Pharmacokinetic study and tissue distribution design

A pharmacokinetic and tissue distribution study of coumarins PE, SC, DF, HR and PU was performed in seventy mice equally divided into two groups. Mice according to group were identified as healthy and LPS-damaged. Each group was divided into seven subgroups corresponding to the times of sample collection.

Ten minutes before starting the study, the mice corresponding to the LPS-damaged group underwent an acute neuroinflammation process caused by the intraperitoneal (i.p.) administration of the LPS solution at 2 mg/kg. Once the time had elapsed, the mice were administered with a dose of 10 mg/kg of the active fraction, previously prepared. Blood and tissue samples were obtained and processed at 0, 0.25, 0.75, 1.5, 2, 4, and 6 h post-dosing, as indicated in the following section.

4.1.7 Samples collection and processing for PK study

Blood samples were obtained, at the established times, from the retro-orbital sinus of the mice and 500 μ L of blood were collected in heparinized Eppendorf tubes of 1.5 mL capacity. The plasma was separated, as soon as possible, by centrifugation at 3500 rpm for 5 minutes and the plasma was separated into new tubes stored at -70 °C until use.

Immediately after obtaining the blood samples, the mice were sacrificed by an overdose of anesthesia in a chloroform chamber, to remove the brain, kidneys, and spleen. The organs were rinsed with saline solution, to avoid exogenous contaminants or interfering in the quantification, and immediately placed on ice. The fresh weight of the organs was recorded, they were subjected to a freeze-drying process (LABCONCO ®), they were grounded and finally dry weighed.

Each of the grounded organs were suspended in methanol in 1:1 dry weight:volume ratios for 24 h and centrifugated at 14,000 rpm for 7 min. Finally, the supernatants were collected in clean tubes and stored at -70 °C until use.

To 100 µL of the plasma or tissue homogenate samples obtained in the PK study, 300 µL of acetonitrile with IS (10 µg/mL) were added and placed in a vortex for 3 min. Subsequently, 200 µL of dichloromethane were added and mixed for 5 min. The aggregate was centrifuged at 14,000 rpm for 10 min and the organic layer was separated and filtered into new tubes to be brought to dryness. For HPLC-UV analysis, samples were resuspended in methanol and 10 µL of sample was injected into the system.

4.1.8 Coumarins quantification by HPLC-UV

Biological samples analysis was carried out by a high-performance liquid chromatography Waters 2695 series. The Waters 2995 series HPLC separation module consisted of a quaternary pump, degasser, autosampler, and thermostatted column. Additionally, it was connected to a photodiode array UV–VIS detector, Waters 2996 series. A Supelco Discovery® C18 column (250 x 4.6 mm, 5 µm, Merck) was used for chromatographic separation.

A mobile phase flow set at 0.9 mL/min, consisting of a 0.5% trifluoroacetic acid aqueous solution (A) and acetonitrile (B) was used. The final run time of the samples was established at 30 min, with a gradient solution as follows: 0–2 min, 100–95% (A); 2–4 min, 95–70% (A); 4–21 min, 70–50% (A); 21–24 min, 50–20% (A); 24–27 min, 20–0% (A); and 27–30 min, 0–100% (A). The readings were carried out at a wavelength of 330 nm and processed with the Empower Pro 3.0 software (Waters, MA, USA). The ratio of the AUC of each peak of the coumarins against the IS was evaluated in the linearity equations obtained in Table 2 of the previous chapter.

4.1.9 Pharmacokinetic and tissue distribution analysis

Pharmacokinetic parameters of PE, SC, DF, HR, and PU in plasma from healthy and LPS-damaged mice were calculated by PKSolver software (Zhang et al., 2010). The maximum plasma concentration (C_{max}), time to reach the maximal concentration (T_{max}), half-life time ($t_{1/2}$), area under the concentration–time curve to 6 h (AUC_{0-6}) and to infinity ($AUC_{0-\infty}$), mean residence time (MRT), and the observed oral clearance (CL/F) were obtained using a non-compartmental model, expressed as mean \pm SEM.

To evaluate the distribution in the tissues, bioactive coumarins were quantified in the lyophilized organs, and concentrations were adjusted to the volumes of liquid obtained by the difference between the dry and fresh weights of each tissue to simulate a distribution approximation of the compounds by tissue system.

4.1.10 Vascular permeability evaluation with Evans blue dye

A study to evaluate the integrity of the BBB after LPS administration was performed in ICR mice ($n = 45$). For this, the animals were distributed, as listed below:

1. Basal Group ($n = 5$ for each time point)
 - a) B45: 0.75 h post-vehicle
 - b) B120: 2 h post-vehicle
 - c) B240: 4 h post-vehicle

2. Vehicle Group ($n = 5$ for each time point)
 - a) Veh45: 0.75 h post-vehicle
 - b) Veh120: 2 h post-vehicle
 - c) Veh240: 4 h post-vehicle

3. Treatment Group ($n = 5$ for each time point)
 - a) Tx45: 0.75 h post-treatment

- b) Tx120: 2 h post-treatment
- c) Tx240: 4 h post-treatment

Mice in the Vehicle (Veh) and Treatment (Tx) groups underwent an acute inflammation process induced by the intraperitoneal (i.p.) administration of LPS at 2 mg/kg. After 10 minutes of damage induction, the Basal and Veh groups were administered orally with an aqueous solution containing 1% Tween-20, with which the bioactive fraction identified as the treatment (Tx) was prepared. The remaining mice were administered with the coumarin Tx at 10 mg/kg. After 15 minutes of Veh or Tx administration, 200 μ L of a PBS solution added with 0.5% Evans blue were perfused through the lateral tail vein.

The mice were sacrificed by anesthetic overdose in a chloroform chamber at 0.75, 2 and 4 h after the administration of Tx or Veh, as appropriate. The process of administration and sacrifice according to the groups is shown in Figure 11:

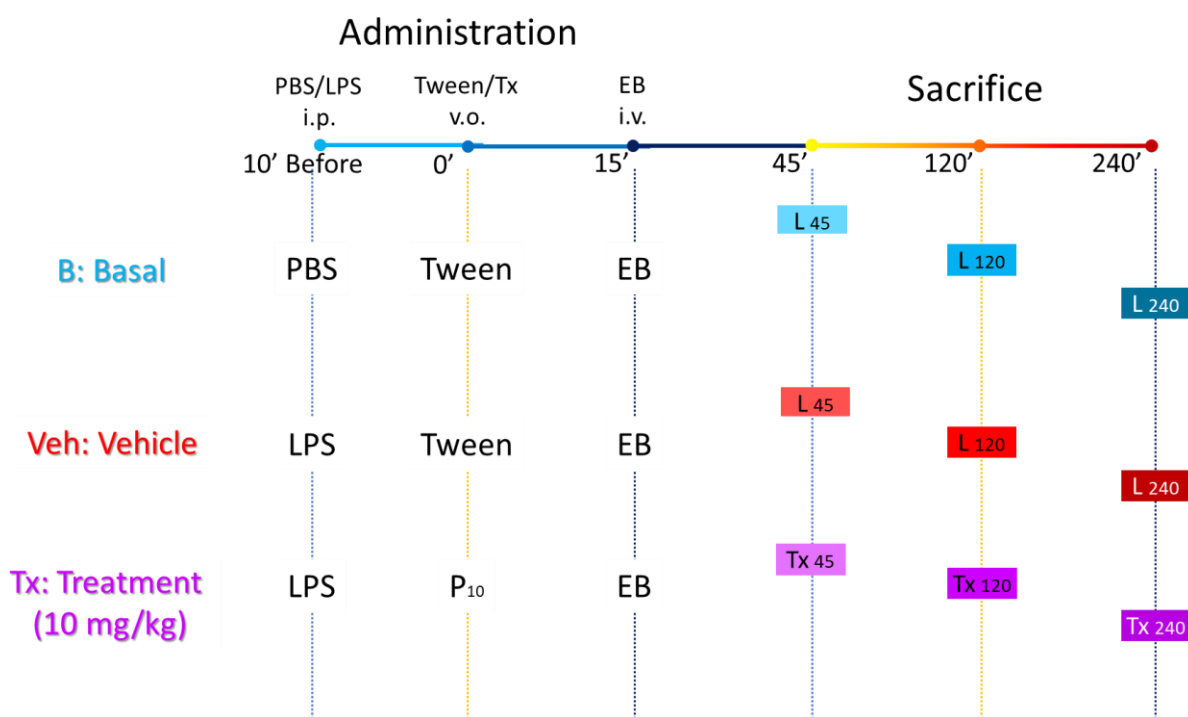


Figure 11. Evans blue dye and treatments administration and sacrifice schedule

The brain, kidneys, and spleens of mice were immediately dissected, rinsed with saline, weighted, and incubated in a 55°C water bath in Eppendorf tubes containing 500 µL of formamide for 24 hours. Once the time had elapsed, they were centrifuged at 14,000 rpm for 7 minutes and 300 µL of the supernatant were recovered in 96-well microplates for analysis in the spectrophotometer at $\lambda = 620$ nm, using formamide as blank. A quantitative analysis of the content of BE in the tissues was carried out with a calibration curve based on external standard method, in formamide.

4.1.11 Cytokine quantification by ELISA's method

The organs were individually homogenized at a 5:1 weight:volume ratio with a PBS solution at pH 7.4 with 1% phenyl methyl sulfonyl fluoride (PMSF), using an ULTRA-TURRAX T25 basic polytron at 6500 rpm. After homogenization, the samples were centrifuged at 14,000 rpm for 7 min, the supernatant was recovered for cytokine quantification by the ELISA method, according to the manufacturer's instructions for IL-10 and TNF- α : Mouse IL-10 ELISA Set (Cat. No. 555252) and Mouse TNF Mono/Mono ELISA Set (Cat. No. 555268), respectively.

4.2 Results

4.2.1 Chemical composition determination of the bioactive fraction of *Tagetes lucida*

The administration fraction, with a high content of anti-inflammatory coumarins, obtained from the hexane extract of *T. lucida* was analyzed at $\lambda=330$ nm by HPLC-UV (Figure 12).

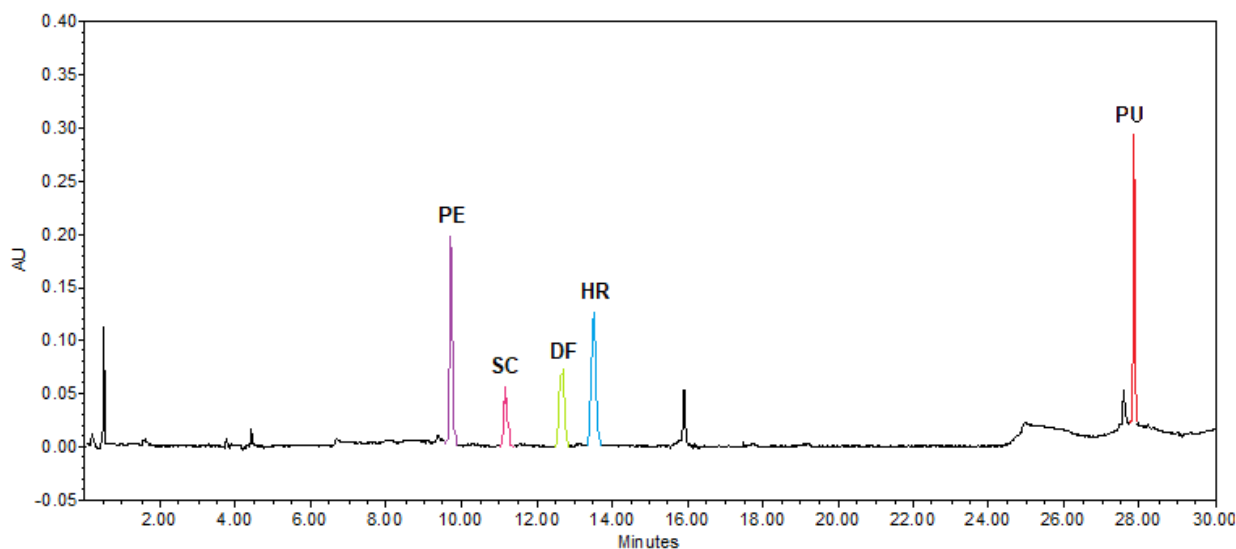


Figure 12. Chromatogram of bioactive fraction of *T. lucida* at $\lambda = 330$ nm. PE = 7-O-prenylscopoletin, SC = scoparone, DF = dimethylfraxetin, HR = herniarin, and PU = 7-O-prenylumbelliferone.

The RT and UV spectra were compared with the PE, SC, DF, HR, and PU standards obtained by prior purification in the laboratory to determine which corresponded to the coumarins of interest. The RT values, maximum absorbance (λ_{\max}), and the concentrations of each coumarin quantified in the fraction are shown in Table 6.

Table 6. Identification parameters of coumarins by HPLC-UV

Analyte	Concentration ($\mu\text{g/mL}$)	TR (min)	$\lambda_{\text{max}1}$ (nm)	$\lambda_{\text{max}2}$ (nm)	$\lambda_{\text{max}3}$ (nm)
PE	165.9	9.826	219.2	324.4	---
SC	225.9	11.351	229.8	294.7	343.4
DF	234.6	12.844	215.7	295.9	338.6
HR	203.0	13.689	219.2	323.2	---
PU	103.8	28.051	204.0	323.2	---

PE = 7-O-prenylscopoletin, SC = scoparone, DF = dimethylfraxetin, HR = herniarin, and PU = 7-O-prenylumbelliferone.

4.2.2 Pharmacokinetic study of coumarins in *Tagetes lucida*

Using the validated HPLC-UV method, the temporal profiles of plasma concentration of coumarins PE, SC, DF, HR, and PU were evaluated after the administration of a fraction obtained from the hexanic extract of *T. lucida* at a dose of 10 mg/kg. In all cases, coumarins were not detected at time zero. Tables 7 and 8 detail the results of the 6-hour PK study performed in healthy and LPS-induced neuroinflammation animals, respectively. SC and PU were not quantified or detected (below LLOQ) at 6 hours after oral administration in the neuroinflammation model. On the other hand, in healthy mice, all coumarins were only detected at the last time point, except for SC, which could be quantified.

Table 7. Plasma concentrations of coumarins PE, SC, DF, HR, and PU in mice LPS-damaged.

Analyte	Time (h)	Sample repetition					Concentration ($\mu\text{g/mL}$)
		R1	R2	R3	R4	R5	
PE	0.25	0.52	0.70	2.10	2.79	0.14	1.25 \pm 0.51
	0.75	1.37	0.29	0.59	0.51	0.33	0.62 \pm 0.20
	1.50	0.67	1.03	0.56	0.88	1.54	0.93 \pm 0.17
	2.00	0.80	0.48	0.33	0.53	0.60	0.55 \pm 0.08
	4.00	0.41	0.67	0.42	0.31	0.72	0.50 \pm 0.08
	6.00	0.42	0.54	0.42	0.30	0.27	0.39 \pm 0.05
SC	0.25	0.17	0.18	1.60	1.35	1.03	0.87 \pm 0.30
	0.75	1.38	0.30	0.64	0.69	0.33	0.67 \pm 0.20
	1.50	0.29	0.50	0.64	0.58	0.62	0.52 \pm 0.06
	2.00	0.84	1.04	0.39	0.25	0.19	0.54 \pm 0.17
	4.00	0.55	0.69	0.36	0.33	0.63	0.51 \pm 0.07
	6.00	ND	ND	ND	ND	ND	N/A
DF	0.25	1.32	1.12	2.39	2.53	0.69	1.61 \pm 0.36
	0.75	D	0.24	0.63	0.90	1.68	0.72 \pm 0.28
	1.50	0.93	1.20	0.43	0.27	0.27	0.62 \pm 0.19
	2.00	0.81	0.68	0.61	0.31	0.75	0.63 \pm 0.09
	4.00	0.59	0.56	0.02	1.00	D	0.44 \pm 0.19
	6.00	D	D	0.26	0.21	0.16	0.14 \pm 0.05
HR	0.25	2.07	1.73	1.16	1.38	1.02	1.48 \pm 0.19
	0.75	0.16	0.27	0.62	0.51	0.34	0.38 \pm 0.08
	1.50	0.65	1.07	0.73	0.89	0.34	0.74 \pm 0.12
	2.00	0.54	0.80	0.46	0.35	0.26	0.48 \pm 0.09
	4.00	0.44	0.68	0.27	0.36	0.77	0.50 \pm 0.10
	6.00	ND	0.21	D	D	ND	0.09 \pm 0.04
PU	0.25	0.96	0.33	D	0.43	D	0.35 \pm 0.17
	0.75	0.13	0.23	0.54	0.69	0.31	0.38 \pm 0.10
	1.50	0.29	0.32	0.43	0.37	0.58	0.40 \pm 0.05
	2.00	0.75	0.70	0.29	0.27	0.22	0.44 \pm 0.11
	4.00	0.76	0.59	0.53	0.25	0.46	0.52 \pm 0.08
	6.00	ND	ND	ND	ND	ND	N/A

PE = 7-O-prenylscopoletin, SC = scoparone, DF = dimethylfraxetin, HR = herniarin, and PU = 7-O-prenylumbelliferone. Concentration values are presented as mean \pm SEM ($n=5$, per time). ND = Not detected; D = detected (below LLOQ); N/A = Not applicable (if three or more values cannot be quantified).

Table 8. Plasma concentrations of coumarins PE, SC, DF, HR, and PU in healthy mice.

Analyte	Time (h)	Sample repetition					Concentration ($\mu\text{g/mL}$)
		R1	R2	R3	R4	R5	
PE	0.25	0.22	0.72	0.14	0.12	0.41	0.32 ± 0.11
	0.75	0.07	0.06	0.10	0.09	0.18	0.10 ± 0.02
	1.50	0.33	0.47	0.21	0.12	0.30	0.29 ± 0.06
	2.00	0.06	0.11	1.94	1.16	0.48	0.75 ± 0.36
	4.00	0.20	0.08	0.05	0.08	0.12	0.11 ± 0.02
	6.00	D	D	D	D	D	N/A
SC	0.25	0.84	0.94	0.57	0.35	0.77	0.69 ± 0.10
	0.75	0.32	0.65	0.56	0.32	0.21	0.41 ± 0.08
	1.50	1.23	0.57	0.81	0.72	1.14	0.89 ± 0.13
	2.00	0.59	0.69	0.53	0.56	0.61	0.59 ± 0.03
	4.00	0.40	0.38	0.39	0.65	0.22	0.41 ± 0.07
	*6.00	D	0.16	0.16	0.38	0.33	0.23 ± 0.05
DF	0.25	0.36	0.49	0.23	0.54	0.62	0.45 ± 0.07
	0.75	0.32	0.23	0.47	0.60	0.28	0.38 ± 0.07
	1.50	0.53	0.59	0.23	0.25	0.19	0.36 ± 0.08
	2.00	0.31	0.44	0.54	0.18	0.59	0.41 ± 0.07
	4.00	0.23	0.22	0.38	0.02	0.30	0.23 ± 0.06
	6.00	D	ND	ND	ND	D	N/A
HR	0.25	0.30	0.25	0.28	0.08	1.97	0.57 ± 0.35
	0.75	0.32	0.19	0.18	0.17	0.09	0.19 ± 0.04
	1.50	0.30	0.28	0.19	0.14	0.10	0.20 ± 0.04
	2.00	0.16	0.18	0.16	0.23	0.13	0.17 ± 0.02
	4.00	0.07	0.16	0.07	0.08	0.15	0.11 ± 0.02
	6.00	D	ND	D	ND	D	N/A
PU	0.25	0.43	0.44	0.33	0.31	0.40	0.38 ± 0.03
	0.75	0.33	0.21	0.51	0.28	0.30	0.33 ± 0.05
	1.50	0.45	0.22	0.29	0.50	0.33	0.36 ± 0.05
	2.00	0.40	0.56	0.44	0.22	0.76	0.48 ± 0.09
	4.00	0.24	0.02	0.15	0.21	0.13	0.15 ± 0.04
	6.00	D	D	D	D	D	N/A

PE = 7-O-prenylscopoletin, SC = scoparone, DF = dimethylfraxetin, HR = herniarin, and PU = 7-O-prenylumbelliferone. Concentration values are presented as mean \pm SEM ($n=5$, per time). ND =Not detected; D = detected (below LLOQ); N/A = Not applicable (if three or more values cannot be quantified).

Figure 13 graphically shows the comparison, between the healthy and damaged models with LPS, of the behavior of the concentrations of each coumarin over time.

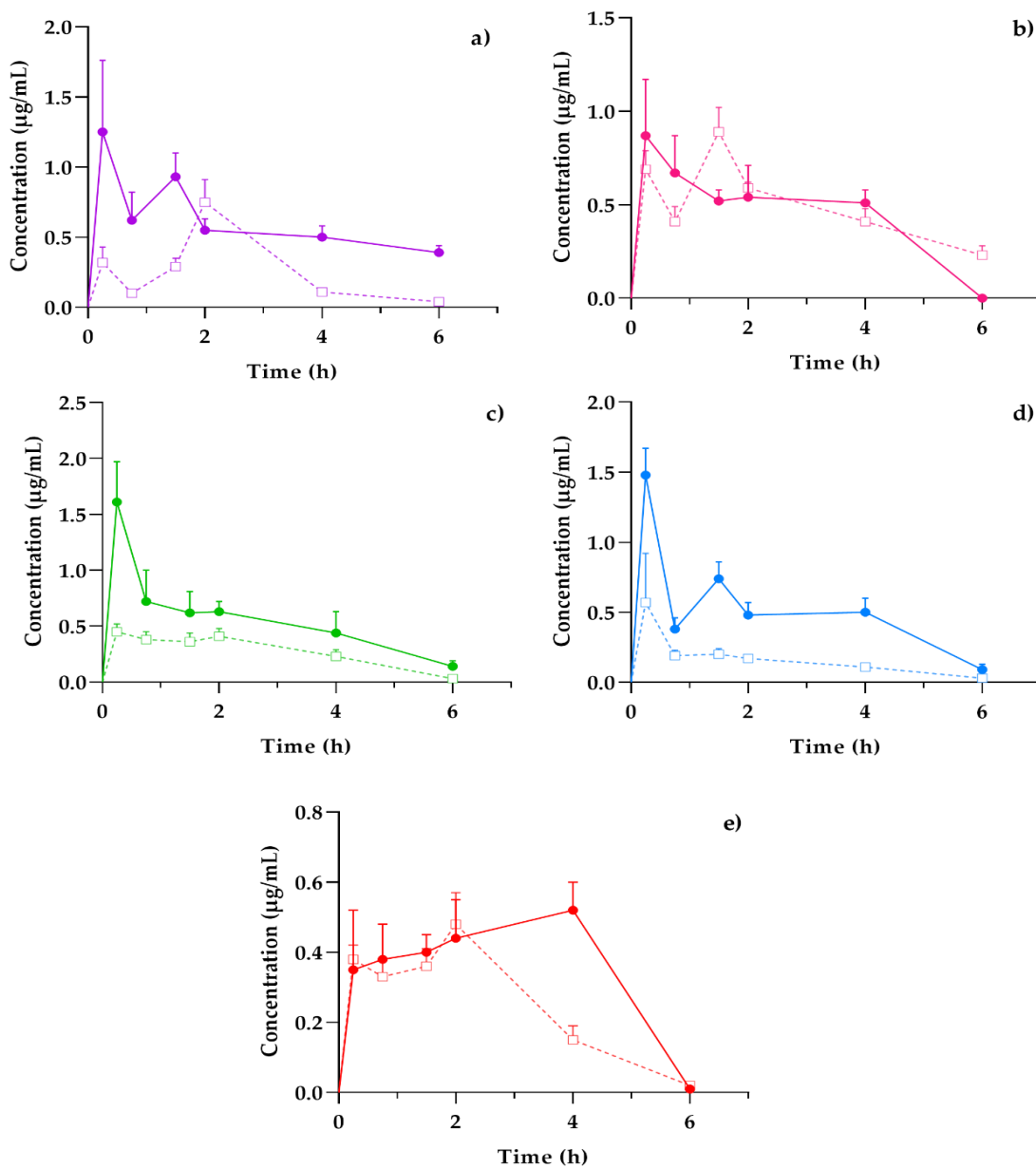


Figure 13. Concentration–time profiles of coumarins: (a) PE, (b) SC, (c) DF, (d) HR, and (e) PU after a 10 mg/kg oral dose administration of hexanic extract of *T. lucida* in healthy (□-) and LPS-damaged (●-) ICR mice. Data are presented as mean ± SEM (n = 5 per time).

Most of the coumarins, regardless of being subjected to a damage condition, reach their C_{max} 15 min after the administration of the evaluation fraction, which indicates a rapid absorption of the compounds by the digestive tract. PU maintains a sustained absorption process for up to 2 and 4 hours in normal and damaged systems, respectively.

In general, all coumarins showed a broad distribution process, thus they were fully quantified up to 4 hours. After this time, the elimination slopes were more pronounced, indicating that coumarins are less available in the plasma.

4.2.3 Pharmacokinetic parameters estimation

A noncompartmental model was used to evaluate PK parameters based on temporal evaluations of a 10 mg/kg dose of the bioactive fraction in the healthy and impaired groups. Tables 9 and 10 summarize the main PK parameters obtained from plasma concentrations in healthy mice, and previously administered with LPS.

The C_{max} , AUC, and MRT have higher values in the neuroinflammation models, except for the SC which adequately contrasts with the graphic profiles previously exposed (Figure 13). The opposite case for the T_{max} and $t_{1/2}$, which determine the high behavior of the CL/F values in healthy systems.

Table 9. Pharmacokinetic parameters of coumarins estimated by non-compartmental analysis in healthy ICR mice plasma.

Parameter	Unit	PE	SC	DF	HR	PU
C_{max}	µg/mL	0.93 ± 0.29	0.97 ± 0.10	0.58 ± 0.02	0.62 ± 0.34	0.56 ± 0.05
T_{max}	h	1.55 ± 0.34	1.25 ± 0.25	1.20 ± 0.31	0.95 ± 0.35	1.55 ± 0.23
$t_{1/2}$	h	1.86 ± 0.55	2.88 ± 0.83	0.98 ± 0.27	1.66 ± 0.46	0.92 ± 0.06
AUC_{0-t}	µg·h/mL	1.56 ± 0.35	2.87 ± 0.09	1.64 ± 0.17	0.92 ± 0.12	1.49 ± 0.11
$AUC_{0-∞}$	µg·h/mL	1.70 ± 0.31	4.03 ± 0.63	1.71 ± 0.19	1.03 ± 0.14	1.52 ± 0.12
MRT	h	3.04 ± 0.45	4.68 ± 1.16	2.35 ± 0.33	2.77 ± 0.35	2.15 ± 0.11
CL/F	*	65.83 ± 10.18	26.64 ± 3.00	62.45 ± 9.38	103.7 ± 13.0	67.37 ± 5.33

Concentration quantification after oral administration D = 10 mg/kg. Values represent mean ± SEM (n = 5). PE = 7-O-prenylscopoletin, SC = scoparone, DF = dimethylfraxetin, HR = herniarin, and PU = 7-O-prenylumbelliferone. * (mg/kg)/(µg/ml)/h.

Table 10. Pharmacokinetic parameters of coumarins estimated by non-compartmental analysis in LPS-damaged ICR mice plasma.

Parameter	Unit	PE	SC	DF	HR	PU
C_{max}	µg/mL	1.77 ± 0.31	1.28 ± 0.11	1.82 ± 0.27	1.48 ± 0.19	0.69 ± 0.07
T_{max}	h	0.85 ± 0.28	0.70 ± 0.34	0.60 ± 0.24	0.25 ± 0.00	1.05 ± 0.31
t_{1/2}	h	4.48 ± 1.31	0.65 ± 0.06	1.50 ± 0.37	1.49 ± 0.35	0.95 ± 0.10
AUC_{0-t}	µg·h/mL	3.52 ± 0.10	2.77 ± 0.21	3.25 ± 0.31	2.95 ± 0.28	2.22 ± 0.26
AUC_{0-∞}	µg·h/mL	6.37 ± 1.20	2.78 ± 0.21	3.61 ± 0.40	3.21 ± 0.38	2.24 ± 0.26
MRT	h	6.96 ± 1.92	2.26 ± 0.17	2.72 ± 0.30	2.77 ± 0.25	2.68 ± 0.14
CL/F	*	17.38 ± 2.25	36.52 ± 2.68	28.81 ± 2.51	32.50 ± 2.91	46.95 ± 5.03

Concentration quantification after oral administration D = 10 mg/kg Values represent mean ± SEM (n = 5). PE = 7-O-prenylscopoletin, SC = scoparone, DF = dimethylfraxetin, HR = herniarin, and PU = 7-O-prenylumbelliferone. * (mg/kg)/(µg/ml)/h.

4.2.4 Tissue distribution evaluation

The brain is the main target organ identified in neuroinflammation processes, for which the distribution behaviors of each of the study coumarins in brain tissue were independently contrasted under conditions of normal functioning and inflammation. The coumarins PE, DF and HR maintain lower contents under normal physiological conditions, and even reach tissue concentrations up to 5 times higher when exposed to LPS (Figure 14).

In the ADME processes, as well as in the inflammatory events, different organs that fulfill specific functions are involved, especially in the elimination of drugs and the defense of the organism against harmful agents. Figure 15 shows the time variations of coumarins in both kidneys and the spleen of mice induced to neuroinflammation with LPS, where it is observed that coumarins are capable of penetrating said organs, including the brain as previously shown (Figure 14).

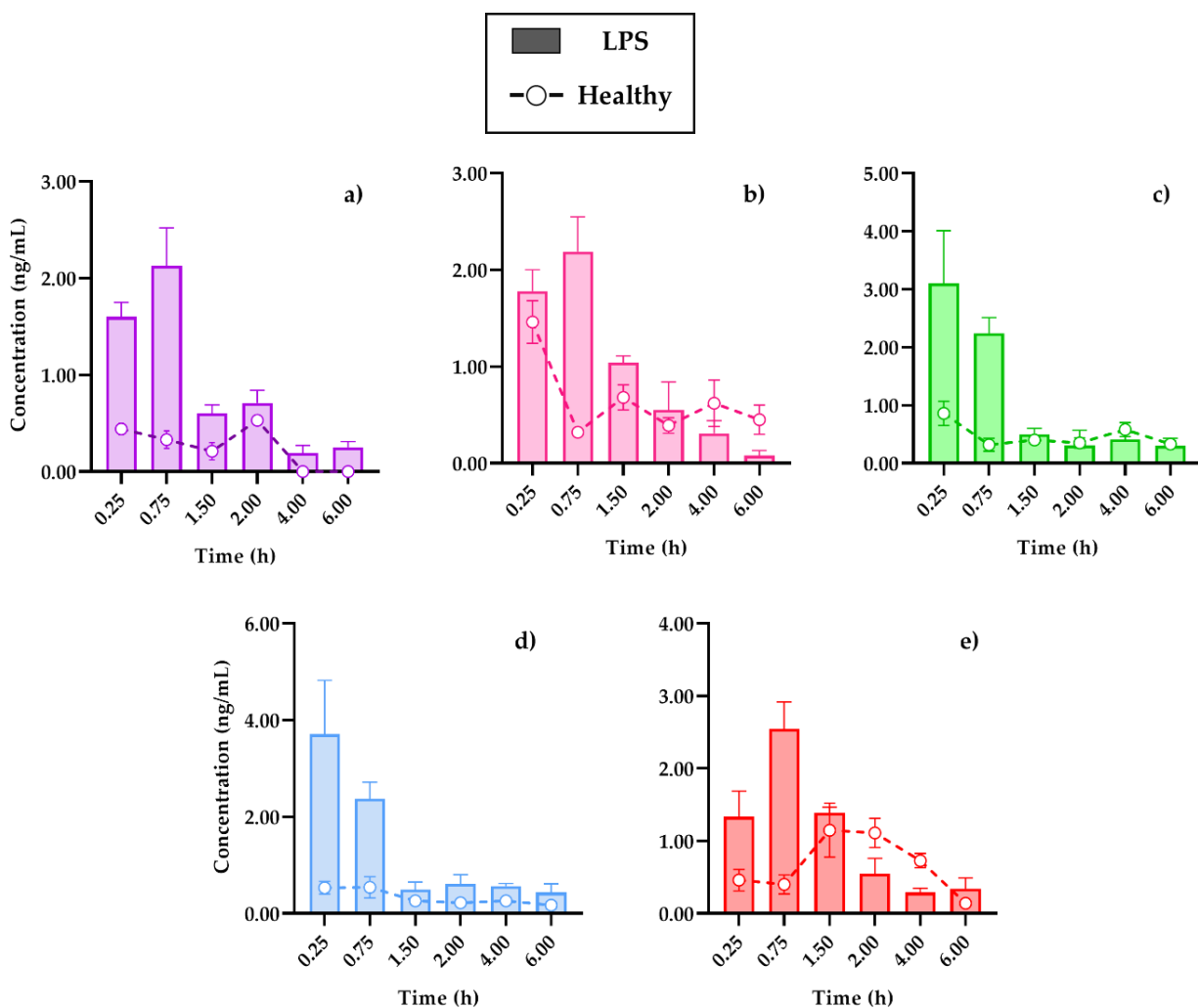


Figure 14. Distribution in the brain of (a) 7-O-prenylscopoletin (PE), (b) scoparone (SC), (c) dimethylfraxetin (DF), (d) herniarin (HR), (e) 7-O-prenylumbelliferone (PU) after an oral dose administration of hexanic extract of *T. lucida* in healthy and LPS-administered mice. Values are presented as mean SEM (n = 5).

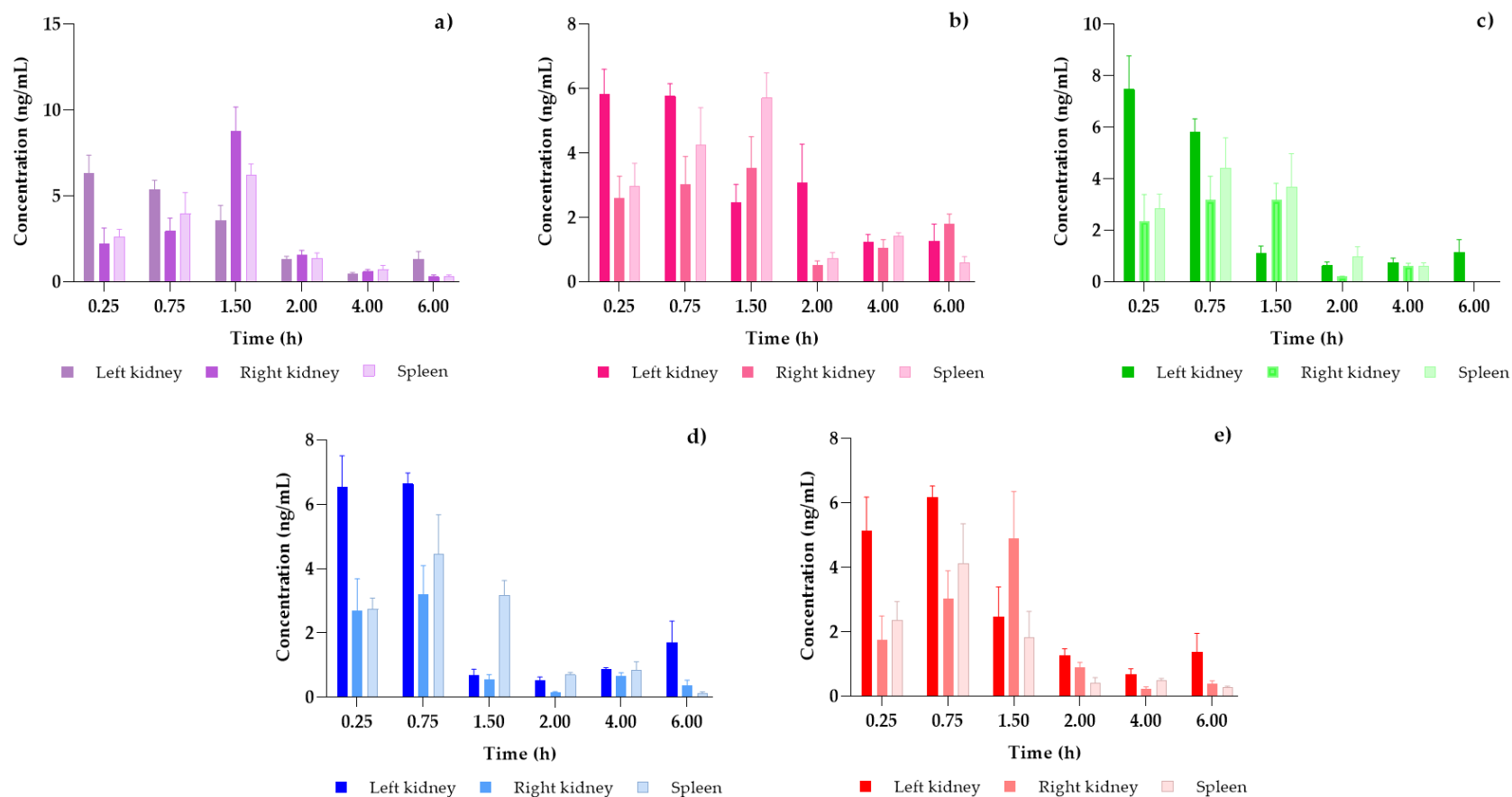


Figure 15. Tissue distribution in kidneys and spleen of 7-O-prenylscopoletin (PE), scoparone (SC), dimethylfraxetin (DF), herniarin (HR), 7-O-prenylumbelliferone (PU) after an oral dose administration of hexanic extract of *T. lucida* in a neuroinflammation LPS-induced model. Values are presented as mean \pm SEM (n = 5).

4.2.5 Vascular permeability assay

To evaluate the neuroprotective potential of the coumarins contained in the fraction derived from the hexane extract of *T. lucida*, the percentage of inhibition of vascular permeability in different organs, mainly in the brain, was determined. With the method of the external standard prepared in formamide, a curve of Evans blue concentration against absorbance was plotted (Figure 16).

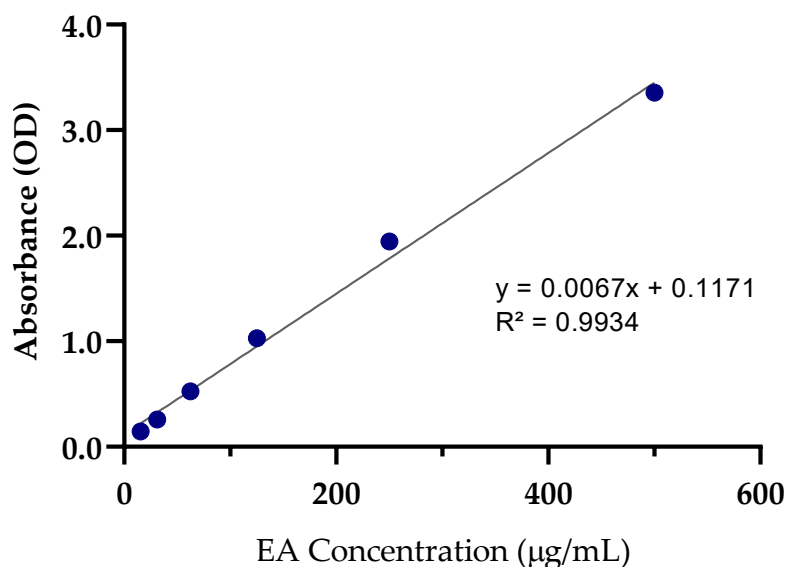


Figure 16. Standard curve for Evans blue dye concentration ($\mu\text{g/mL}$). OD: Optical density at 620 nm.

The administration of 10 mg/kg of the coumarin-rich fraction obtained from *T. lucida* showed an inhibitory effect on vascular permeability in the brain like the basal groups that did not undergo the inflammation process. In addition, the concentration of the quantified Evans blue dye showed significant differences with respect to the groups administered only with the vehicle ($p < 0.01$), as shown in Table 11.

Table 11. Evans blue dye concentrations and relative inhibition in neuroprotection assay.

Treatment group	Quantification time (h)	EB concentration ($\mu\text{g/mL}$)	Inhibition (%)
Basal	0.75	21.86 \pm 4.06**	---
	2.00	20.88 \pm 2.28**	---
	4.00	21.80 \pm 5.31**	---
Vehicle + LPS (2 mg/kg)	0.75	89.26 \pm 8.68	---
	2.00	98.28 \pm 4.27	---
	4.00	120.13 \pm 7.43	---
LPS + Coumarin fraction (10 mg/kg)	0.75	34.37 \pm 4.08**	63.56
	2.00	30.76 \pm 3.31**	68.94
	4.00	28.37 \pm 3.40**	74.64

Data are means \pm SEM (n = 5 per group). ** $p < 0.01$. EB: blue Evans dye; LPS: Lipopolysaccharide.

The amount of EB detected was associated with the fresh weight of the tissues evaluated during the test. Temporal variations of EB concentrations in the organs were plotted (Figure 17). Comparisons of the groups administered with the *T. lucida* fraction against the groups with induced inflammation without treatment, showed a neuroprotective effect, by maintaining EB concentration levels like the basal groups. However, in the kidneys and spleen, concentrations almost doubled in mice with coumarin treatment at 2 and 4 hours after administration.

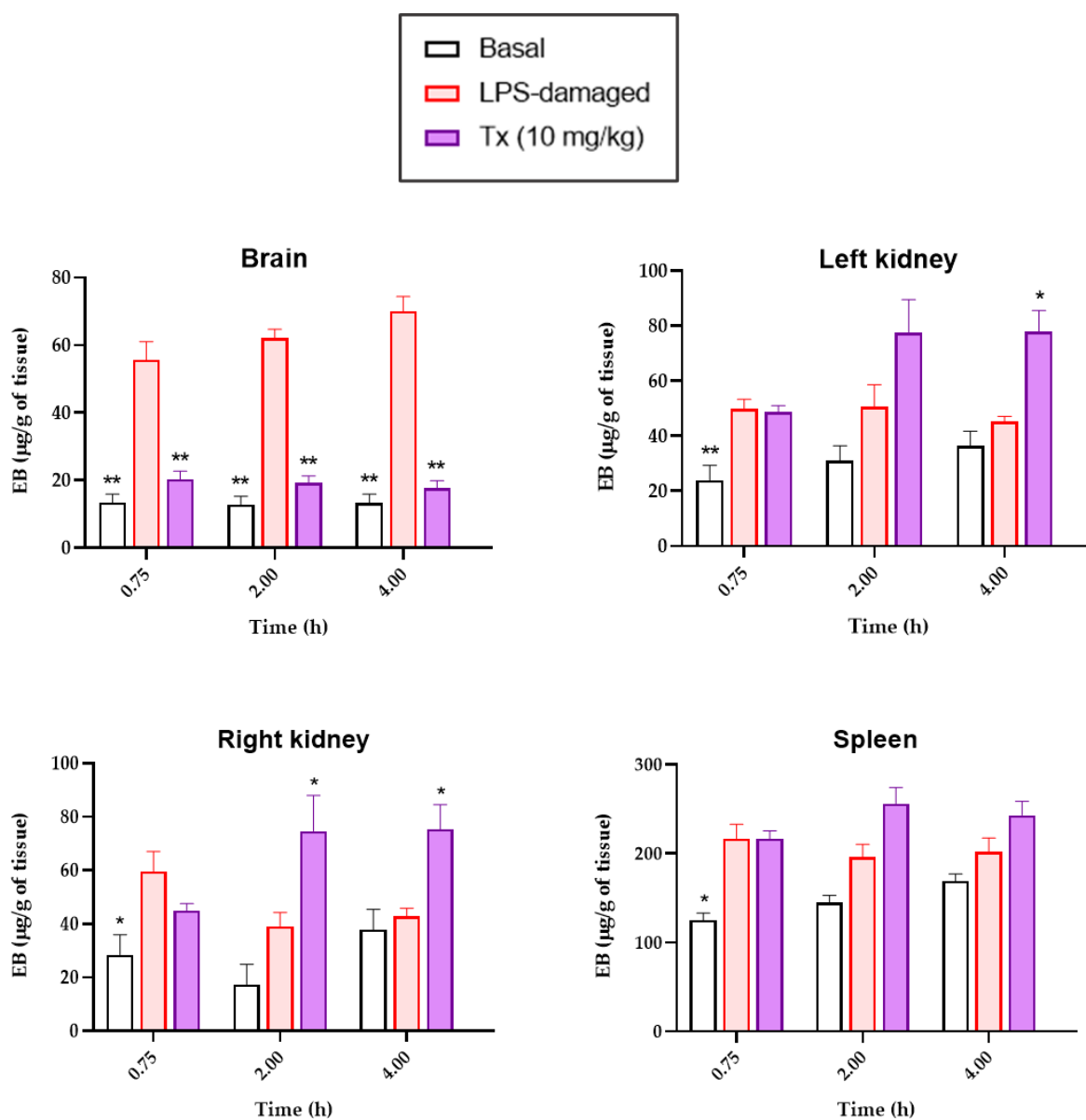


Figure 17. Kinetics of Evans blue dye extravasation observed in several tissues (brain, left and right kidneys, and spleen) after neuroinflammation LPS-induction. Each column represents the mean \pm SEM ($n = 5$, per time. * $p < 0.05$, ** $p < 0.01$ when compared to the vehicle with LPS (ANOVA post hoc Dunnett test).

4.2.6 Cytokine quantification

Cytokines, TNF- α and IL-10, were quantified to evaluate the antineuroinflammatory potential of the active fraction contained in the hexane extract of *T. lucida*. Likewise, the proportion of proinflammatory activity was determined, evaluated by the first cytokine, against IL-10, which was analyzed as the protein linked to its anti-inflammatory effect.

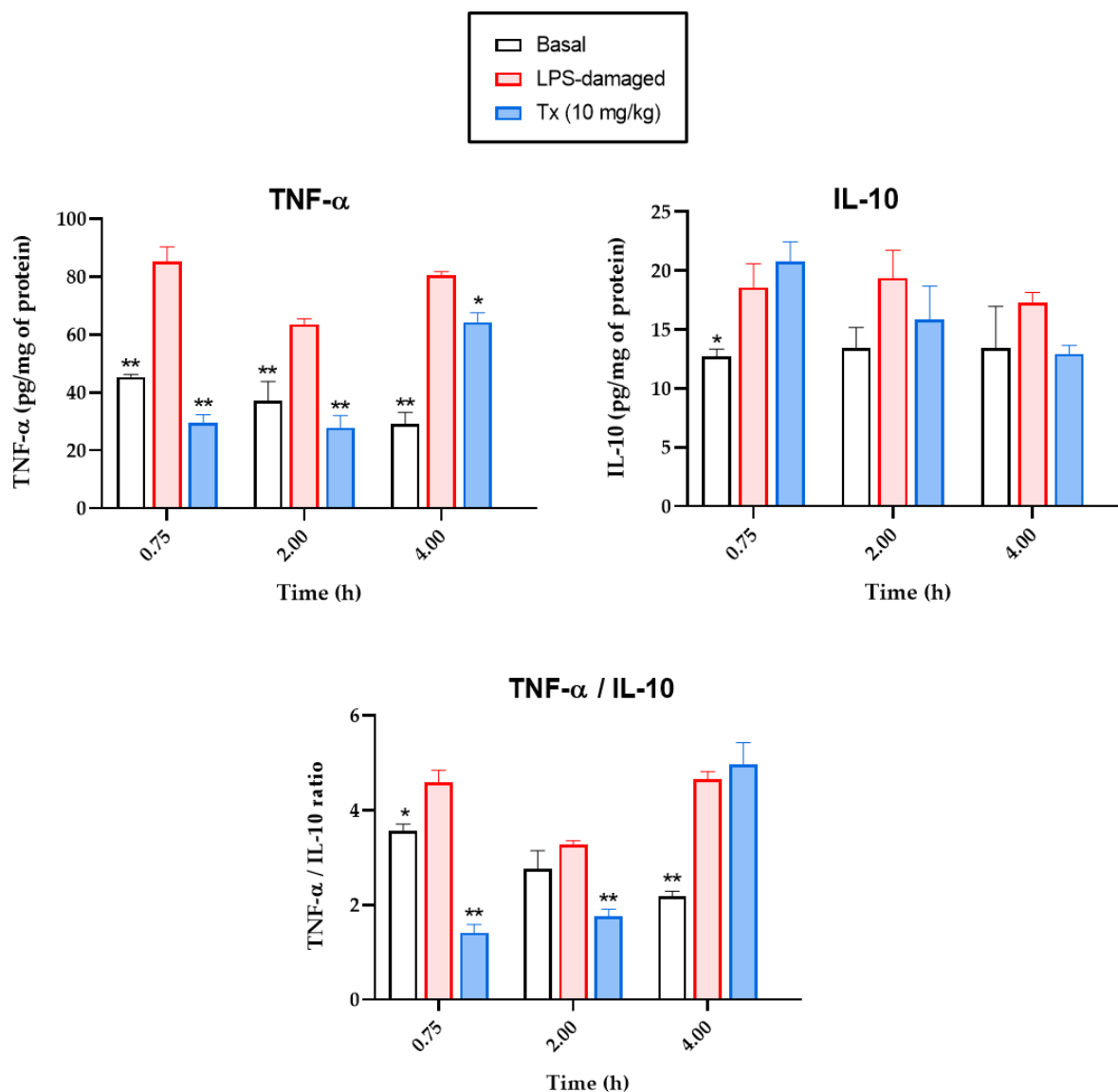


Figure 18. Modulation of the inflammatory response by expression of cytokines TNF- α and IL-10 in brain after LPS-induced neuroinflammation. Each column represents the mean \pm SEM ($n = 5$, per time). * $p < 0.05$, ** $p < 0.01$ when compared to the vehicle with LPS (ANOVA post hoc Dunnett test).

4.3 Discussion

The species of *Tagetes lucida* is rich in content of terpenes, phenolic acids, flavonoids and coumarins, mainly (Aquino et al., 2002; Céspedes et al., 2006; González-Trujano et al., 2019; Guadarrama-Cruz et al., 2008; Monterrosas Brisson et al., 2020; Pérez-Ortega et al., 2016). These constituents offer a wide range of biological activities due to their antidepressant, antibacterial, antinociceptive, antispasmodic, antihypertensive, and especially antioxidant and anti-inflammatory properties (Aquino et al., 2002; Bonilla-Jaime et al., 2015; Estrada-Soto et al., 2021; Guadarrama-Cruz et al., 2012; Hernandez-Leon et al., 2020; Monterrosas Brisson et al., 2020; Pérez-Ortega et al., 2016; Ventura-Martinez et al., 2020). Due to its valuable pharmacological properties, this plant can be used as a potential source of novel herbal medicines to treat conditions related to CNS diseases, such as neurodegenerative diseases, which have related their etiology to neuroinflammation (Amor et al., 2014; Rauf et al., 2022).

In the present work, a fraction rich in coumarins was used: PE, SC, DF, HR, and PU, with previously proven anti-inflammatory activity for each of these components (Monterrosas Brisson et al., 2020). However, one of the main limitations that arise during the development of medicines obtained from natural sources is the poor standardization of bioactive components (Amit Koparde et al., 2019). Therefore, the quantitative composition was determined by chemical screening by HPLC-UV (Figure 12), which showed comparable concentrations of the five coumarins of interest (Table 6).

Using the same bioanalytical quantification method, and after its validation, it was possible to evaluate the temporal concentration profiles in biological samples of plasma, brain, kidneys, and spleen, after an administration of 10 mg/kg of a standardized fraction obtained from the hexanic extract of *Tagetes lucida*. With this, a PK and tissue distribution study was carried out that allowed us to observe, beyond the kinetic behavior of the bioactive molecules, if the coumarins PE, SC, DF, HR and PU reached the target site, brain, and other organs widely related to ADME processes, important in PK evaluations (Chien et al., 2005; Katzung and Vanderah, 2018; Schentag et al., 2001).

The tests were carried out in two study models: healthy mice and mice with LPS-induced neuroinflammation. The LPS damage model is widely used due to the cellular and molecular environment it produces, like diseases such as Alzheimer's or Parkinson's. In addition, the model is relatively easy and produces rapid inflammatory responses at the peripheral level and in the CNS, damaging important brain protections such as the BBB (Batista et al., 2019; Gitler et al., 2017; Jangula and Murphy, 2013; Nava Catorce and Gevorkian, 2016).

Each organ and fluid analyzed in the present study used as biological matrices, both in tissue distribution and PK, show useful information for the future establishment of clinical evaluations for their individual functional and structural capacities. This allowed to observe the time-course behavior of the compounds throughout the components of the animal biological system to determine the adaptations to improve bioavailability when the development of subsequent pharmaceutical forms begins. (Silva Lima and Videira, 2018).

In the specific kinetic profiles of each coumarin it is possible to observe the general ADME process, plotted from the plasma samples (Figure 13). As well as its subsequent distribution to tissue systems, where the bioavailability in each organ at the different evaluated moments can be seen both in healthy mice and in those where an LPS-induced neuroinflammation process was induced (Figure 13 and 14).

The first stage of the process, the absorption, showed positive slopes until reaching the C_{max} of each coumarin, normally within the first hour after the administration of the active fraction of the hexanic extract of *T. lucida*, except for PU, which ended its slopes two to four hours after treatment. The distribution process allowed to compare the presence of coumarins in plasma and for how long they were distributed throughout the organs analyzed. These compounds reached the brain for at least six hours (Figure 14), in accordance with the inhibition of extravasation of blue Evans dye during the times evaluated in the assay (Table 11). Remarkable, SC and DF in LPS-treated mice had a fast distribution as reported in previous studies (Kowalczyk et al., 2022; Yin et al., 2012).

On the other hand, the kidneys and the spleen had tissue distribution concentrations of more than double compared to the target organ, which are linked to the functionality of these organs. The kidneys are mainly responsible for filtering exogenous compounds present in the body, such as anti-inflammatory coumarins, while the spleen is one of the first response organs to inflammatory events. This clarifies the observed recirculation in plasma of all the coumarins at approximately two hours, when the concentration peaks, mainly in the right kidney, occurred at least 30 min before establishing said effect (Katiyar et al., 2012).

In the general scheme of plasma concentrations, it was determined that those mice previously treated with LPS maintained a greater availability of the compounds in plasma compared to healthy mice. This phenomenon is remarkably high in DF and HR (Figure 13c-d), which coincides with what was previously reported, where inflammatory processes increase the concentration/dose ratio of drug exposure (Stanke-Labesque et al., 2020).

Among the pharmacokinetic parameters, it was observed that the response in the damaged mice for C_{max} was greater in each of the coumarins, in addition, these were achieved in shorter times, so that the AUC increased their values, except for SC. As some authors have mentioned, the inflammatory environment can increase the maintenance of exogenous agents such as drugs within the body (Batista et al., 2019). Therefore, in this case the bioavailability of therapeutic agents is increased, this must be considered when designing the pharmaceutical forms in which coumarins will be arranged in future clinical trials to avoid intoxication due to exacerbated exposures, or otherwise that these do not reach adequate concentrations to exert their potential effect (Morgan, 2009).

This is due to the physiological changes caused by the damage process, for example, the increase in vascular exchange between the gastrointestinal tract and the plasma modified the distribution of proteins, increasing the maximum exposure up to three times, as is the case with DF, compared to healthy mice. This is considered a consequence of the decrease in proteins such as albumin and the overproduction of transferrin that are involved in plasma bioavailability (Yang and Lee, 2007).

Following, coumarins present oral clearances (CL/F) up to 32% faster in healthy systems (Tables 9 and 10), which is associated with the type of metabolism that this class of compounds may have, since, as has been described, inflamed systems. Specifically when LPS is administered, those drugs metabolized by the liver greatly decrease their clearance rate, which in turn is determined by the increase in blood flow and the free fraction of compounds that remain in the plasma (Yang and Lee, 2007).

Other organs involved in the process of drug distribution and elimination are the kidneys. These undergo changes in the glomerular filtration rate that affect pharmacokinetic parameters involved in the total exposure of therapeutic agents (Stanke-Labesque et al., 2020). In the present case, the exposure of coumarins increased in a comparative way to other studies, where various drugs were quantified in fluids such as blood serum (Yang and Lee, 2007).

One of the main drawbacks in the design of pharmacological therapies used in general to treat conditions involving the CNS is the poor bioavailability of therapeutic agents in the target organ due to the transfer selectivity of the BBB. Through tissue distribution studies carried out in the brain, kidneys and spleen, it was possible to monitor the distribution capacity of coumarins. Among the organs analyzed, the brain presented the lowest content of compounds (< 5 ng/mL), which, as previously mentioned, may be due to the presence of the BBB. Conversely, in comparison with a study where the distribution of SC in different organs was analyzed, it was reported that it was not possible to quantify this coumarin inside the brain (Yin et al., 2012), where the dose administered to the rats used for this study or the extraction process from the biosamples could be a limitation.

It is known that in addition to the exacerbated presence of pro-inflammatory cytokines such as IL-1 β , IL-6 and TNF- α in plasma when an inflammatory environment is induced with LPS, this agent is also capable of damaging the BBB causing the infiltration of harmful particles that normally would not be able to reach the brain. However, capillary widening and increased permeability under these conditions also offer an advantage in allowing passage of small therapeutic molecules and with it improving the pharmacological treatment (Batista et al., 2019).

This is associated with the results obtained in the quantification of coumarins in both plasma and brain (Figures 13 and 14). In this organ, it was observed that coumarins, with the largest molecular size, such as PE and PU, were able to reach the tissue within the first 15 min after the administration of the active fraction. In addition, the kinetic profiles of HR and DF in plasma and their subsequent distribution in the brain followed very similar processing behaviors throughout the studied times (Nava Catorce and Gevorkian, 2016).

In turn, Figure 15 set out the temporal distribution of coumarins in the kidneys and spleen, in addition to showing the transfer processes between the organs and the blood circulation system, the data obtained will be useful in subsequent PK-PD studies that evaluate the relevance of the pharmacological effects concerning the processes of metabolism and clearance of drugs for their therapeutic monitoring due to the relevance of these organs in the ultimate processes of the pharmacokinetic profile (Moein et al., 2017; Schentag et al., 2001).

The presence of coumarins in the tissues was associated with the neuroprotective effect evaluated in a vascular permeability assay with EB dye, after the induction of inflammation with LPS. This method bases its foundation on the fact that the inflammatory response has three main effects on any system that is part of the body, and they are: vasodilation, increase in blood flow, and increase in vascular permeability (Jangula and Murphy, 2013; Nidavani et al., 2014). Therefore, dyes such as EB, under normal physiological conditions, are unable to cross the BBB due to their selectivity, but when inflammatory agents are administered, they bind to plasma proteins such as albumin and manage to cross the barrier, due to previously established effects. Therefore, vascular permeability is used as a measure of the index of inflammation.

The study of vascular leakage in the different organs evaluated here, showed that EB concentrations increased gradually, between 45 min and 4 hours of the test, in mice that were administered only with LPS, without receiving the anti-inflammatory treatment of coumarins. These results are in agreement with studies where the permeability of the BBB is increased, reaching maximum effects from one hour after the administration of LPS (Jangula and Murphy, 2013; Wang et al., 2019). The anti-inflammatory drugs can

diminish the damage caused to the BBB. Therefore, it was expected that the administration of the coumarins contained in the fraction derived from *T. lucida* would be capable of inhibiting the leaked percentages of EB compared to the administration of LPS alone. This hypothesis was verified as shown in Table 11, where significant differences were obtained in the quantified concentration of BE in the brain, very similar to the normal physiological states expressed in the basal group (Aisen et al., 2003; Jung et al., 2019).

In addition, to relate the PK profile of coumarins with the neuroprotective effect, a kinetic evaluation of the amount of EB in the different tissues was carried out. The fraction exerted a potential increased effect as the evaluation time progressed, having its maximum point at 4 hours, in this point some coumarins reached the final stage of distribution and elimination process, for which it exhibits a late response to plasma concentration and in the brain, as presented in Figures 13 and 14. (Katiyar et al., 2012; Mathur and Hoskins, 2017; Mohs and Greig, 2017).

The inflammatory response derived from the activation of microglia and astrocytes is the main defense mechanism against pathogens and toxic agents in the CNS. This process involves the production of anti- and pro-inflammatory cytokines, depending on the activated phenotype, which also maintains the brain microenvironment homeostasis. However, when the regulation is not carried out, the imbalance causes more damage to neighboring healthy cells (Lobo-Silva et al., 2016; Muhammad, 2020). Therefore, in the present study, the pro- and anti-inflammatory cytokines TNF- α and IL-10, respectively, were evaluated to determine the balance in the brain system. Figure 18 shows a decrease in the concentration of TNF- α up to two hours of analysis, even below the baseline subjects, although with a spike at 4 hours, contrary to IL-10. For its part, the ratio of TNF- α /IL-10 was <2 between 45 min and 2 h, characteristic of normal conditions (Shmarina et al., 2001). Under the short-time analyzes performed in this study, it cannot be determined whether the increase in the proportion of interleukins is due to the fact that the anti-inflammatory effect is diminished or if it represents the polarization of microglia to M1 due to the loss of IL-10 over time, which would subsequently increase the overproduction of proinflammatory agents such as TNF- α (Laffer et al., 2019).

Conclusion and Perspectives

A pharmacokinetic and tissue distribution studies were carried out following an oral administration of the active fraction of *Tagetes lucida* in healthy and damaged mice in a LPS-induced neuroinflammation model by a simultaneous quantification of five coumarins, i.e., PE, SC, HR, DF, and PU, in the plasma, brain, kidneys, and spleen using a sensitive, suitable, and validated HPLC–DAD-UV method. The bioavailability observed in brain tissue and plasma determined that the compounds could reach the target site to exert their potential therapeutic functions in systems damaged by the agents that cause neuroinflammation.

A neuroprotective effect was confirmed by the inhibition of Evans blue dye leakage into the brain when mice received administration of the coumarin-rich fraction in an assay of vascular permeability to the damaged BBB, by intraperitoneal injection of LPS, compared with the mice that were only administered with the vehicle. While the potential anti-neuroinflammatory effect was analyzed with the quantification of pro- and anti-inflammatory cytokines: TNF- α and IL-10, which were able to modulate the inflammatory response in the brain.

The present study has potential applicability for further pharmacokinetic–pharmacodynamic evaluations to determine the correlation between different doses administrations and their therapeutic effects in longer time gaps. The pharmacokinetic and biological preclinical evaluations carried out in this thesis will serve to design pharmaceutical forms capable of exerting a neuroprotective and anti-inflammatory effect that can be tested in future clinical studies, to ensure that they reach the target site without toxic or adverse reactions, such as those presented by most current pharmacological therapies.

Appendix A

Abbreviations

Table 12. Abbreviations.

	Description
AD	Alzheimer's disease
ADME	Absorption, distribution, metabolism, and excretion
A β	β -amyloid
BBB	Blood-brain barrier
CNS	Central Nervous System
DF	Dimethylfraxetin
EB	Evans blue
FDA	Food and Drugs Administration
HPLC-UV	UV-coupled High-Performance Liquid Chromatography
HR	Herniarin
i.p.	intraperitoneal
i.v.	intravascular
IFN- γ	Interferon-Gamma
IL	Interleukin
IMSS	Instituto Mexicano del Seguro Social
IS	Internal standard; Rutin
LLE	Liquid-liquid extraction
LLOQ	Lower limit of quantification
LPS	Lipopolysaccharide
NF- κ B	Nuclear factor kappa B
NO	Nitric oxide
NOM	Official Mexican Standards
NSAIDs	Non-steroidal anti-inflammatory drugs
PaD	Parkinson's disease
PD	Pharmacodynamics
PE	7-O-prenylscopoletin
PK	Pharmacokinetics
PK-PD	Pharmacokinetic-Pharmacodynamic
PPT	Protein precipitation
PU	7-O-prenylumbelliferone
RE	Relative error
RSD	Relative standard deviation
RT	Retention time
SC	Scoparone
SD	Standard deviation
SEM	Standard error of the mean
SPE	Solid phase extraction

TFA	Trifluoroacetic acid
TGF- β	Transforming growth factor-beta
TLR	Toll-like receptor
TNFR	Tumor necrosis factor-alpha
TNFR	Tumor necrosis factor receptor
Tx	Treatment
UV	Ultraviolet
Veh	Vehicle

Appendix B

Variables and Symbols

Table 13. Variables and symbols.

Variable	Description	Units
°C	Celsius degrees	
µg	Micrograms	
µL	Microliters	
µm	Micrometers	
AUC	Area under the concentration time curve	µg·h/mL
CL/F	Oral apparent clearance	(mg/kg)/(µg/ml)/h
C _{max}	Maximum plasma concentration	µg/mL
g	Grams	
h	Hours	
kg	Kilograms	
L	Liters	
mg	Miligrams	
min	Minutes	
mL	Mililiters	
mm	Milimeters	
MRT	Mean residence time	h
n	Número de repeticiones	
nm	Nanometers	
r ²	Coefficient of determination	
rpm	Revolutions per minute	
t _{1/2}	Half life time	h
T _{max}	Time at the C _{max} is observed	h
λ	Wavelength	nm

Bibliography

Ahmad J (2020) *Bioactive Phytochemicals: Drug Discovery to Product Development*. DOI: 10.2174/97898114644851200101.

Aisen PS, Davis KL, Berg JD, et al. (2000) A randomized controlled trial of prednisone in Alzheimer's disease. *Neurology* 54(3). Neurology: 588–593. DOI: 10.1212/wnl.54.3.588.

Aisen PS, Schafer KA, Grundman M, et al. (2003) Effects of Rofecoxib or Naproxen vs Placebo on Alzheimer Disease Progression: A Randomized Controlled Trial. *JAMA* 289(21). JAMA: 2819–2826. DOI: 10.1001/jama.289.21.2819.

Amit Koparde A, Chandrashekar Doijad R and Shripal Magdum C (2019) Natural Products in Drug Discovery. In: *Pharmacognosy - Medicinal Plants*. IntechOpen. DOI: 10.5772/intechopen.82860.

Amor S, Peferoen LAN, Vogel DYS, et al. (2014) Inflammation in neurodegenerative diseases - an update. *Immunology*. Immunology. DOI: 10.1111/imm.12233.

An J, Chen B, Kang X, et al. (2020) Neuroprotective effects of natural compounds on LPS-induced inflammatory responses in microglia. *American Journal of Translational Research*. e-Century Publishing Corporation. Available at: /pmc/articles/PMC7344058/ (accessed 23 October 2022).

Aquino R, Cáceres A, Morelli S, et al. (2002) An extract of *Tagetes lucida* and its phenolic constituents as antioxidants. *Journal of Natural Products* 65(12). American Chemical Society: 1773–1776. DOI: 10.1021/np020018i.

Arbo BD, Schimith LE, Goulart dos Santos M, et al. (2022) Repositioning and development of new treatments for neurodegenerative diseases: Focus on neuroinflammation. *European Journal of Pharmacology* 919. Eur J Pharmacol. DOI:

10.1016/j.ejphar.2022.174800.

Bandeira Reidel RV, Nardoni S, Mancianti F, et al. (2018) Chemical composition and antifungal activity of essential oils from four Asteraceae plants grown in Egypt. *Zeitschrift fur Naturforschung - Section C Journal of Biosciences* 73(7–8). *Z Naturforsch C J Biosci*: 313–318. DOI: 10.1515/znc-2017-0219.

Banks WA, Gray AM, Erickson MA, et al. (2015) Lipopolysaccharide-induced blood-brain barrier disruption: Roles of cyclooxygenase, oxidative stress, neuroinflammation, and elements of the neurovascular unit. *Journal of Neuroinflammation* 12(1). *J Neuroinflammation*. DOI: 10.1186/s12974-015-0434-1.

Batista CRA, Gomes GF, Candelario-Jalil E, et al. (2019) Lipopolysaccharide-induced neuroinflammation as a bridge to understand neurodegeneration. *International Journal of Molecular Sciences*. Multidisciplinary Digital Publishing Institute (MDPI). DOI: 10.3390/ijms20092293.

Bentham P, Gray R, Sellwood E, et al. (2008) Aspirin in Alzheimer's disease (AD2000): a randomised open-label trial. *The Lancet Neurology* 7(1). *Lancet Neurol*: 41–49. DOI: 10.1016/S1474-4422(07)70293-4.

Biblioteca Digital de la Medicina Tradicional Mexicana (2009) Pericón. Available at: <http://www.medicinatradicionalmexicana.unam.mx/apmtm/termino.php?l=3&t=tagetes-lucida> (accessed 23 October 2022).

Bonilla-Jaime H, Guadarrama-Cruz G, Alarcon-Aguilar FJ, et al. (2015) Antidepressant-like activity of *Tagetes lucida* Cav. is mediated by 5-HT_{1A} and 5-HT_{2A} receptors. *Journal of Natural Medicines* 69(4). *J Nat Med*: 463–470. DOI: 10.1007/s11418-015-0909-5.

Bulitta JB and Holford NHG (2014) Noncompartmental Analysis. In: *Methods and Applications of Statistics in Clinical Trials*. John Wiley & Sons, Ltd, pp. 457–482. DOI:

10.1002/9781118596333.ch27.

Burmeister AR and Marriott I (2018) The interleukin-10 family of cytokines and their role in the CNS. *Frontiers in Cellular Neuroscience*. Frontiers Media S.A. DOI: 10.3389/fncel.2018.00458.

Caballero-Gallardo K, Olivero-Verbel J and Stashenko EE (2011) Repellent activity of essential oils and some of their individual constituents against *Tribolium castaneum* herbst. *Journal of Agricultural and Food Chemistry* 59(5). American Chemical Society: 1690–1696. DOI: 10.1021/jf103937p.

Cárdenas PA, Kratz JM, Hernández A, et al. (2017) In vitro intestinal permeability studies, pharmacokinetics and tissue distribution of 6-methylcoumarin after oral and intraperitoneal administration in Wistar rats. *Brazilian Journal of Pharmaceutical Sciences* 53(1). Universidade de São Paulo, Faculdade de Ciências Farmacêuticas: 16081. DOI: 10.1590/s2175-97902017000116081.

Castañeda R, Vilela D, González MC, et al. (2013) SU-8/Pyrex microchip electrophoresis with integrated electrochemical detection for class-selective electrochemical index determination of phenolic compounds in complex samples. *Electrophoresis* 34(14). Electrophoresis: 2129–2135. DOI: 10.1002/elps.201300060.

Céspedes CL, Avila JG, Martínez A, et al. (2006) Antifungal and antibacterial activities of Mexican tarragon (*Tagetes lucida*). *Journal of Agricultural and Food Chemistry* 54(10). J Agric Food Chem: 3521–3527. DOI: 10.1021/jf053071w.

Chien JY, Friedrich S, Heathman MA, et al. (2005) Pharmacokinetics/pharmacodynamics and the stages of drug development: Role of modeling and simulation. *AAPS Journal* 7(3). AAPS J. DOI: 10.1208/aapsj070355.

Chitnis T and Weiner HL (2017) CNS inflammation and neurodegeneration. In: *Journal of Clinical Investigation*, October 2017, pp. 3577–3587. J Clin Invest. DOI:

10.1172/JCI90609.

Cho DY, Ko HM, Kim J, et al. (2016) Scoparone inhibits LPS-simulated inflammatory response by suppressing IRF3 and ERK in BV-2 microglial cells. *Molecules* 21(12). *Molecules*. DOI: 10.3390/molecules21121718.

Christensen JR, Börnsen L, Ratzner R, et al. (2013) Systemic Inflammation in Progressive Multiple Sclerosis Involves Follicular T-Helper, Th17- and Activated B-Cells and Correlates with Progression. *PLoS ONE* 8(3). *PLoS One*. DOI: 10.1371/journal.pone.0057820.

Doménech Berrozpe J, Martínez Lanao J and Pla Delfina JM (1997) *Biofarmacia y Farmacocinética*. Síntesis. Available at: https://books.google.es/books/about/Biofarmacia_y_farmacocinética.html?id=XL45KAAACAAJ&redir_esc=y (accessed 26 October 2022).

Dragojević S, Šunjić V, Bencetić-Mihaljević V, et al. (2011) Determination of aqueous stability and degradation products of series of coumarin dimers. *Journal of Pharmaceutical and Biomedical Analysis* 54(1). *J Pharm Biomed Anal*: 37–47. DOI: 10.1016/j.jpba.2010.08.002.

Egbuna C, Kumar S, Ifemeje JC, et al. (2019) *Phytochemicals as Lead Compounds for New Drug Discovery* (C Egbuna, S Kumar, J Ifemeje, et al.eds). DOI: 10.1016/C2018-0-02367-1.

Estrada-Soto S, González-Trujano ME, Rendón-Vallejo P, et al. (2021) Antihypertensive and vasorelaxant mode of action of the ethanol-soluble extract from *Tagetes lucida* Cav. aerial parts and its main bioactive metabolites. *Journal of Ethnopharmacology* 266. *J Ethnopharmacol*. DOI: 10.1016/j.jep.2020.113399.

FDA (2015) *Analytical Procedures and Methods Validation for Drugs and Biologics. Guidance for Industry*. July. Available at: <https://www.fda.gov/regulatory->

information/search-fda-guidance-documents/analytical-procedures-and-methods-validation-drugs-and-biologics (accessed 29 October 2022).

FDA (2018) *Bioanalytical method validation Guidance for Industry. Biopharmaceutics*. Available at: <https://www.fda.gov/regulatory-information/search-fda-guidance-documents/bioanalytical-method-validation-guidance-industry> (accessed 16 June 2022).

Foster DM (2007) Noncompartmental Versus Compartmental Approaches to Pharmacokinetic Analysis. In: *Principles of Clinical Pharmacology*. Academic Press, pp. 89–105. DOI: 10.1016/B978-012369417-1/50048-1.

Gabrielsson J and Weiner D (2012) Non-compartmental Analysis. In: *Methods in Molecular Biology (Clifton, N.J.)*. Methods Mol Biol, pp. 377–389. DOI: 10.1007/978-1-62703-050-2_16.

Garcia JM, Stillings SA, Leclerc JL, et al. (2017) Role of interleukin-10 in acute brain injuries. *Frontiers in Neurology*. Frontiers Media S.A. DOI: 10.3389/fneur.2017.00244.

Gilhus NE and Deuschl G (2019) Neuroinflammation — a common thread in neurological disorders. *Nature Reviews Neurology* 15(8): 429–430. DOI: 10.1038/s41582-019-0227-8.

Gillespie WR (1991) Noncompartmental Versus Compartmental Modelling in Clinical Pharmacokinetics. *Clinical Pharmacokinetics* 20(4). Clin Pharmacokinet: 253–262. DOI: 10.2165/00003088-199120040-00001.

Gitler AD, Dhillon P and Shorter J (2017) Neurodegenerative disease: Models, mechanisms, and a new hope. *DMM Disease Models and Mechanisms*. Company of Biologists. DOI: 10.1242/dmm.030205.

Goldim MP de S, Della Giustina A and Petronilho F (2019) Using Evans Blue Dye to

Determine Blood-Brain Barrier Integrity in Rodents. *Current Protocols in Immunology* 126(1). Curr Protoc Immunol. DOI: 10.1002/cpim.83.

González-Trujano ME, Gutiérrez-Valentino C, Hernández-Arámburo MY, et al. (2019) Identification of some bioactive metabolites and inhibitory receptors in the antinociceptive activity of *Tagetes lucida* Cav. *Life Sciences* 231. Life Sci. DOI: 10.1016/j.lfs.2019.05.079.

Guadarrama-Cruz G, Alarcon-Aguilar FJ, Lezama-Velasco R, et al. (2008) Antidepressant-like effects of *Tagetes lucida* Cav. in the forced swimming test. *Journal of Ethnopharmacology* 120(2). Elsevier: 277–281. DOI: 10.1016/j.jep.2008.08.013.

Guadarrama-Cruz G, Alarcón Aguilar F, Vega Avila E, et al. (2012) Antidepressant-like effect of *Tagetes lucida* Cav. extract in rats: Involvement of the serotonergic system. *American Journal of Chinese Medicine* 40(4). Am J Chin Med: 753–768. DOI: 10.1142/S0192415X12500565.

Hano C and Tungmunnithum D (2020) Plant Polyphenols, More than Just Simple Natural Antioxidants: Oxidative Stress, Aging and Age-Related Diseases. *Medicines* 7(5). Multidisciplinary Digital Publishing Institute (MDPI): 26. DOI: 10.3390/medicines7050026.

Hernandez-Baltazar D, Nadella R, Bonilla AAB, et al. (2020) Does lipopolysaccharide-based neuroinflammation induce microglia polarization? *Folia Neuropathologica*. Folia Neuropathol. DOI: 10.5114/fn.2020.96755.

Hernandez-Leon A, González-Trujano ME, Narváez-González F, et al. (2020) Role of β -caryophyllene in the antinociceptive and anti-inflammatory effects of *tagetes lucida* Cav. Essential oil. *Molecules* 25(3). Molecules. DOI: 10.3390/molecules25030675.

Hernández T, Canales M, Flores C, et al. (2006) Antimicrobial activity of *Tagetes lucida*.

Pharmaceutical Biology 44(1). Taylor & Francis: 19–22. DOI: 10.1080/13880200500509157.

Indrayanto G, Putra GS and Suhud F (2021) Validation of in-vitro bioassay methods: Application in herbal drug research. In: *Profiles of Drug Substances, Excipients and Related Methodology*. Profiles Drug Subst Excip Relat Methodol, pp. 273–307. DOI: 10.1016/bs.podrm.2020.07.005.

Jangula A and Murphy EJ (2013) Lipopolysaccharide-induced blood brain barrier permeability is enhanced by alpha-synuclein expression. *Neuroscience Letters* 551. NIH Public Access: 23–27. DOI: 10.1016/j.neulet.2013.06.058.

Jeon SW and Kim YK (2018) The role of neuroinflammation and neurovascular dysfunction in major depressive disorder. *Journal of Inflammation Research*. Dove Medical Press Ltd. DOI: 10.2147/JIR.S141033.

Jung YJ, Tweedie D, Scerba MT, et al. (2019) Neuroinflammation as a Factor of Neurodegenerative Disease: Thalidomide Analogs as Treatments. *Frontiers in Cell and Developmental Biology*. Front Cell Dev Biol. DOI: 10.3389/fcell.2019.00313.

Katiyar C, Kanjilal S, Gupta A, et al. (2012) Drug discovery from plant sources: An integrated approach. *AYU (An International Quarterly Journal of Research in Ayurveda)* 33(1). Wolters Kluwer -- Medknow Publications: 10. DOI: 10.4103/0974-8520.100295.

Katzung B and Vanderah T (2018) *Basic and Clinical Pharmacology*. McGraw-Hill Medical. DOI: 10.1213/00000539-198308000-00015.

Kaur N, Chugh H, Sakharkar MK, et al. (2020) Neuroinflammation Mechanisms and Phytotherapeutic Intervention: A Systematic Review. *ACS Chemical Neuroscience* 11(22): 3707–3731. DOI: 10.1021/acscemneuro.0c00427.

Kim HJ, Kang CH, Jayasooriya RGPT, et al. (2016) Hydrangenol inhibits

lipopolysaccharide-induced nitric oxide production in BV2 microglial cells by suppressing the NF- κ B pathway and activating the Nrf2-mediated HO-1 pathway. *International Immunopharmacology* 35. Int Immunopharmacol: 61–69. DOI: 10.1016/j.intimp.2016.03.022.

Kostova I, Bhatia S, Grigorov P, et al. (2012) Coumarins as Antioxidants. *Current Medicinal Chemistry* 18(25). Curr Med Chem: 3929–3951. DOI: 10.2174/092986711803414395.

Kowalczyk J, Budzyńska B, Kurach Ł, et al. (2022) Neuropsychopharmacological profiling of scoparone in mice. *Scientific Reports 2022 12:1* 12(1). Nature Publishing Group: 1–13. DOI: 10.1038/s41598-021-04741-3.

Kwon HS and Koh SH (2020) Neuroinflammation in neurodegenerative disorders: the roles of microglia and astrocytes. *Translational Neurodegeneration*. BioMed Central. DOI: 10.1186/s40035-020-00221-2.

Laffer B, Bauer D, Wasmuth S, et al. (2019) Loss of IL-10 Promotes Differentiation of Microglia to a M1 Phenotype. *Frontiers in Cellular Neuroscience* 13. Frontiers Media S.A.: 430. DOI: 10.3389/fncel.2019.00430.

Liao Z, Wei W, Yang M, et al. (2021) Academic Publication of Neurodegenerative Diseases From a Bibliographic Perspective: A Comparative Scientometric Analysis. *Frontiers in Aging Neuroscience* 13. Frontiers Media S.A.: 661. DOI: 10.3389/fnagi.2021.722944.

Linares E and Bye RA (1987) A study of four medicinal plant complexes of Mexico and adjacent United States. *Journal of Ethnopharmacology* 19(2). Elsevier: 153–183. DOI: 10.1016/0378-8741(87)90039-0.

Linares E, Flores PB and Bye RA (1995) *Selección de Plantas Medicinales de México*. Mexico: Limusa-Noriega.

- Liu J, Liu L, Wang X, et al. (2021) Microglia: A Double-Edged Sword in Intracerebral Hemorrhage From Basic Mechanisms to Clinical Research. *Frontiers in Immunology* 12(May): 1–11. DOI: 10.3389/fimmu.2021.675660.
- Lobo-Silva D, Carriche GM, Castro AG, et al. (2016) Balancing the immune response in the brain: IL-10 and its regulation. *Journal of Neuroinflammation*. BioMed Central. DOI: 10.1186/s12974-016-0763-8.
- Lyman M, Lloyd DG, Ji X, et al. (2014) Neuroinflammation: The role and consequences. *Neuroscience Research*. Elsevier. DOI: 10.1016/j.neures.2013.10.004.
- Mathur S and Hoskins C (2017) Drug development: Lessons from nature. *Biomedical Reports* 6(6). Spandidos Publications: 612–614. DOI: 10.3892/br.2017.909.
- Mendel Nzogang P and Boris Donkeng M (2020) Neuroprotection: The Way of Anti-Inflammatory Agents. In: *Neuroprotection - New Approaches and Prospects*. IntechOpen. DOI: 10.5772/intechopen.90509.
- Miller JH and Das V (2020) Potential for Treatment of Neurodegenerative Diseases with Natural Products or Synthetic Compounds that Stabilize Microtubules. *Current Pharmaceutical Design* 26(35). Curr Pharm Des: 4362–4372. DOI: 10.2174/1381612826666200621171302.
- Mishra A, Bandopadhyay R, Singh PK, et al. (2021) *Neuroinflammation in Neurological Disorders: Pharmacotherapeutic Targets from Bench to Bedside*. Springer US. DOI: 10.1007/s11011-021-00806-4.
- Moein MM, El Beqqali A and Abdel-Rehim M (2017) Bioanalytical method development and validation: Critical concepts and strategies. *Journal of Chromatography B: Analytical Technologies in the Biomedical and Life Sciences* 1043. J Chromatogr B Analyt Technol Biomed Life Sci: 3–11. DOI: 10.1016/j.jchromb.2016.09.028.
- Mohs RC and Greig NH (2017) Drug discovery and development: Role of basic biological

research. *Alzheimer's and Dementia: Translational Research and Clinical Interventions*. Wiley-Blackwell. DOI: 10.1016/j.trci.2017.10.005.

Monterrosas Brisson N, Herrera-Ruiz M, Jiménez Ferrer E, et al. (2020) Anti-inflammatory activity of coumarins isolated from *Tagetes lucida* Cav. *Natural Product Research* 34(22). Nat Prod Res: 3244–3248. DOI: 10.1080/14786419.2018.1553172.

Morgan ET (2009) Impact of infectious and inflammatory disease on cytochrome P450-mediated drug metabolism and pharmacokinetics. *Clinical Pharmacology and Therapeutics*. John Wiley & Sons, Ltd. DOI: 10.1038/clpt.2008.302.

Muhammad M (2020) Tumor Necrosis Factor Alpha: A Major Cytokine of Brain Neuroinflammation. In: *Cytokines*. IntechOpen. DOI: 10.5772/intechopen.85476.

Najmi A, Javed SA, Al Bratty M, et al. (2022) Modern Approaches in the Discovery and Development of Plant-Based Natural Products and Their Analogues as Potential Therapeutic Agents. *Molecules*. Multidisciplinary Digital Publishing Institute. DOI: 10.3390/molecules27020349.

Nava Catorce M and Gevorkian G (2016) LPS-induced Murine Neuroinflammation Model: Main Features and Suitability for Pre-clinical Assessment of Nutraceuticals. *Current Neuropharmacology* 14(2). Bentham Science Publishers: 155–164. DOI: 10.2174/1570159x14666151204122017.

Newman DJ, Cragg GM and Snader KM (2003) Natural products as sources of new drugs over the period 1981-2002. *Journal of Natural Products*. J Nat Prod. DOI: 10.1021/np030096l.

Nidavani RB, Mahalakshmi AM and Shalawadi M (2014) Vascular permeability and Evans blue dye: A physiological and pharmacological approach. *Journal of Applied Pharmaceutical Science* 4(11). Open Science Publishers LLP India.: 106–113. DOI: 10.7324/JAPS.2014.41119.

Nieoullon A (2011) Neurodegenerative diseases and neuroprotection: Current views and prospects. *Journal of Applied Biomedicine*. No longer published by Elsevier. DOI: 10.2478/v10136-011-0013-4.

Noe DA (2020) Parameter Estimation and Reporting in Noncompartmental Analysis of Clinical Pharmacokinetic Data. *Clinical Pharmacology in Drug Development* 9(S1). Clin Pharmacol Drug Dev: S5–S35. DOI: 10.1002/cpdd.810.

Nuzzo D (2021) Role of natural antioxidants on neuroprotection and neuroinflammation. *Antioxidants*. Multidisciplinary Digital Publishing Institute (MDPI). DOI: 10.3390/antiox10040608.

Olajide OA and Sarker SD (2020) *Anti-Inflammatory Natural Products*. 1st ed. Elsevier Inc. DOI: 10.1016/bs.armc.2020.02.002.

PAHO (2021) Burden of Neurological Conditions. Available at: <https://www.paho.org/en/enlace/burden-neurological-conditions> (accessed 4 November 2022).

Parasuraman S (2018) Herbal Drug Discovery: Challenges and Perspectives. *Current Pharmacogenomics and Personalized Medicine* 16(1). Bentham Science Publishers Ltd.: 63–68. DOI: 10.2174/1875692116666180419153313.

Peng X-M, L.V. Damu G and He Zhou C- (2013) Current Developments of Coumarin Compounds in Medicinal Chemistry. *Current Pharmaceutical Design* 19(21). Curr Pharm Des: 3884–3930. DOI: 10.2174/1381612811319210013.

Peng X, Luo Z, He S, et al. (2021) Blood-Brain Barrier Disruption by Lipopolysaccharide and Sepsis-Associated Encephalopathy. *Frontiers in Cellular and Infection Microbiology*. Frontiers Media S.A. DOI: 10.3389/fcimb.2021.768108.

Perdomo-Roldán, Francisco, Mondragón-Pichardo, Juana C (2009) *Tagetes lucida*. Available at: <http://www.conabio.gob.mx/malezasdemexico/asteraceae/tagetes->

lucida/fichas/ficha.htm (accessed 23 October 2022).

Pérez-Ortega G, González-Trujano ME, Ángeles-López GE, et al. (2016) *Tagetes lucida* Cav.: Ethnobotany, phytochemistry and pharmacology of its tranquilizing properties. *Journal of Ethnopharmacology* 181. J Ethnopharmacol: 221–228. DOI: 10.1016/j.jep.2016.01.040.

Petronilho F, Goldman JL and Barichello T (2019) Evans Blue-Albumin as a Marker to Evaluate Blood-Brain Barrier Integrity in Neonatal and Adult Rodents. In: *Neuromethods*. Humana Press Inc., pp. 197–203. DOI: 10.1007/978-1-4939-8946-1_12.

Pringsheim T, Fiest K, Jette N, et al. (2014) Global perspectives: The international incidence and prevalence of neurologic conditions: How common are they? *Neurology*. American Academy of Neurology. DOI: 10.1212/WNL.0000000000000929.

Pruccoli L, Breda C, Teti G, et al. (2021) Esculetin provides neuroprotection against mutant huntingtin-induced toxicity in huntington's disease models. *Pharmaceuticals* 14(10). Pharmaceuticals (Basel). DOI: 10.3390/ph14101044.

Radu M and Chernoff J (2013) An in vivo assay to test blood vessel permeability. *Journal of visualized experiments : JoVE* (73). J Vis Exp. DOI: 10.3791/50062.

Rauf A, Badoni H, Abu-Izneid T, et al. (2022) Neuroinflammatory Markers: Key Indicators in the Pathology of Neurodegenerative Diseases. *Molecules*. Multidisciplinary Digital Publishing Institute (MDPI). DOI: 10.3390/molecules27103194.

Rhie SJ, Jung EY and Shim I (2020) The role of neuroinflammation on pathogenesis of affective disorders. *Journal of Exercise Rehabilitation*. Korean Society of Exercise Rehabilitation. DOI: 10.12965/jer.2040016.008.

Saunders NR, Dziegielewska KM, Møllgård K, et al. (2015) Markers for blood-brain barrier

integrity: How appropriate is Evans blue in the twenty-first century and what are the alternatives? *Frontiers in Neuroscience*. Frontiers Media S.A. DOI: 10.3389/fnins.2015.00385.

Scharf S, Mander A, Ugoni A, et al. (1999) A double-blind, placebo-controlled trial of diclofenac/misoprostol in Alzheimer's disease. *Neurology* 53(1). Neurology: 197–201. DOI: 10.1212/wnl.53.1.197.

Schentag JJ, Gilliland KK and Paladino JA (2001) What have we learned from pharmacokinetic and pharmacodynamic theories? *Clinical Infectious Diseases*. Clin Infect Dis. DOI: 10.1086/319375.

Scudamore O and Ciossek T (2018) Increased oxidative stress exacerbates α -synuclein aggregation in vivo. *Journal of Neuropathology and Experimental Neurology* 77(6). J Neuropathol Exp Neurol: 443–453. DOI: 10.1093/jnen/nly024.

SEMARNAT (2011) NORMA Oficial Mexicana NOM-062-ZOO-1999. *NORMA Oficial Mexicana NOM-062-ZOO-1999*. Mexico: Secretaría de Agricultura, Ganadería, Desarrollo Rural, Pesca y Alimentación. Available at: https://www.gob.mx/cms/uploads/attachment/file/203498/NOM-062-ZOO-1999_220801.pdf (accessed 16 June 2022).

Seo DY, Heo JW, Ko JR, et al. (2019) Exercise and neuroinflammation in health and disease. *International Neurourology Journal*. Korean Continence Society. DOI: 10.5213/inj.1938214.107.

Shabab T, Khanabdali R, Moghadamtousi SZ, et al. (2017) Neuroinflammation pathways: a general review. *International Journal of Neuroscience* 127(7): 624–633. DOI: 10.1080/00207454.2016.1212854.

Shi Y, Liu CH, Roberts AI, et al. (2006) Granulocyte-macrophage colony-stimulating factor (GM-CSF) and T-cell responses: What we do and don't know. In: *Cell*

Research, February 2006, pp. 126–133. *Cell Res*. DOI: 10.1038/sj.cr.7310017.

Shmarina G V., Pukhalsky AL, Kokarovtseva SN, et al. (2001) Tumor necrosis factor- α /interleukin-10 balance in normal and cystic fibrosis children. *Mediators of Inflammation* 10(4). *Mediators Inflamm*: 191–197. DOI: 10.1080/09629350123387.

Siddiqui MR, AlOthman ZA and Rahman N (2017) Analytical techniques in pharmaceutical analysis: A review. *Arabian Journal of Chemistry*. Elsevier. DOI: 10.1016/j.arabjc.2013.04.016.

Silva Lima B and Videira MA (2018) Toxicology and Biodistribution: The Clinical Value of Animal Biodistribution Studies. *Molecular Therapy - Methods and Clinical Development*. American Society of Gene & Cell Therapy. DOI: 10.1016/j.omtm.2018.01.003.

Singh SS, Rai SN, Birla H, et al. (2018) Effect of chlorogenic acid supplementation in MPTP-intoxicated mouse. *Frontiers in Pharmacology* 9(AUG). *Front Pharmacol*. DOI: 10.3389/fphar.2018.00757.

Singh SS, Rai SN, Birla H, et al. (2020) NF- κ B-Mediated Neuroinflammation in Parkinson's Disease and Potential Therapeutic Effect of Polyphenols. *Neurotoxicity Research*. *Neurotox Res*. DOI: 10.1007/s12640-019-00147-2.

SSA (2012) NOM-072-SSA1-2012, Etiquetado de medicamentos y de remedios herbolarios. Available at: https://www.dof.gob.mx/nota_detalle.php?codigo=5278341&fecha=21/11/2012#gsc.tab=0 (accessed 23 October 2022).

Stanke-Labesque F, Gautier-Veyret E, Chhun S, et al. (2020) Inflammation is a major regulator of drug metabolizing enzymes and transporters: Consequences for the personalization of drug treatment. *Pharmacology and Therapeutics*. Elsevier. DOI: 10.1016/j.pharmthera.2020.107627.

- Subhramanyam CS, Wang C, Hu Q, et al. (2019) Microglia-mediated neuroinflammation in neurodegenerative diseases. *Seminars in Cell and Developmental Biology*. Semin Cell Dev Biol. DOI: 10.1016/j.semcdb.2019.05.004.
- Thomford NE, Senthebane DA, Rowe A, et al. (2018) Natural products for drug discovery in the 21st century: Innovations for novel drug discovery. *International Journal of Molecular Sciences*. Int J Mol Sci. DOI: 10.3390/ijms19061578.
- Tijare LK, Rangari NT and Mahajan UN (2016) A review on bioanalytical method development and validation. *Asian Journal of Pharmaceutical and Clinical Research*. Innovare Academics Sciences Pvt. Ltd. DOI: 10.22159/ajpcr.2016.v9s3.14321.
- Tripanichkul W and Jaroensuppaperch EO (2012) Curcumin protects nigrostriatal dopaminergic neurons and reduces glial activation in 6-hydroxydopamine hemiparkinsonian mice model. *International Journal of Neuroscience* 122(5): 263–270. DOI: 10.3109/00207454.2011.648760.
- Ventura-Martinez R, Angeles-Lopez GE, Gonzalez-Trujano ME, et al. (2020) Study of Antispasmodic and Antidiarrheal Activities of *Tagetes lucida* (Mexican Tarragon) in Experimental Models and Its Mechanism of Action. *Evidence-based Complementary and Alternative Medicine* 2020. Hindawi Limited. DOI: 10.1155/2020/7140642.
- Vera SS, Zambrano DF, Méndez-Sánchez SC, et al. (2014) Essential oils with insecticidal activity against larvae of *Aedes aegypti* (Diptera: Culicidae). *Parasitology Research* 113(7). Parasitol Res: 2647–2654. DOI: 10.1007/s00436-014-3917-6.
- Waller D, Sampson AP and Hitchings A (2021) Pharmacokinetics. In: *Medical Pharmacology & Therapeutics*.
- Wang Q, Deng Y, Huang L, et al. (2019) Hypertonic saline downregulates endothelial cell-derived VEGF expression and reduces blood-brain barrier permeability induced by cerebral ischaemia via the VEGFR2/eNOS pathway. *International Journal of*

Molecular Medicine 44(3). *Int J Mol Med*: 1078–1090. DOI: 10.3892/ijmm.2019.4262.

Wiciński M, Wódkiewicz E, Słupski M, et al. (2018) Neuroprotective Activity of Sitagliptin via Reduction of Neuroinflammation beyond the Incretin Effect: Focus on Alzheimer's Disease. *BioMed Research International*. *Biomed Res Int*. DOI: 10.1155/2018/6091014.

Yang K-H and Lee M-G (2007) Effects of Lipopolysaccharide on Pharmacokinetics of Drugs. *Toxicological Research* 23(4). Korean Society of Toxicology & Korea Environmental Mutagen Society: 289–299. DOI: 10.5487/tr.2007.23.4.289.

Yang X, Xu S, Qian Y, et al. (2017) Resveratrol regulates microglia M1/M2 polarization via PGC-1 α in conditions of neuroinflammatory injury. *Brain, Behavior, and Immunity* 64. *Brain Behav Immun*: 162–172. DOI: 10.1016/j.bbi.2017.03.003.

Yin Q, Sun H, Zhang A, et al. (2012) Pharmacokinetics and tissue distribution study of scoparone in rats by ultraperformance liquid-chromatography with tandem high-definition mass spectrometry. *Fitoterapia* 83(4). Elsevier: 795–800. DOI: 10.1016/J.FITOTE.2012.03.010.

Zeng KW, Yu Q, Liao LX, et al. (2015) Anti-neuroinflammatory effect of MC13, a novel coumarin compound from condiment murraya, through inhibiting lipopolysaccharide-induced TRAF6-TAK1-NF- κ B, P38/ERK MAPKS and Jak2-Stat1/Stat3 pathways. *Journal of Cellular Biochemistry* 116(7). *J Cell Biochem*: 1286–1299. DOI: 10.1002/jcb.25084.

Zhang Y, Huo M, Zhou J, et al. (2010) PKSolver: An add-in program for pharmacokinetic and pharmacodynamic data analysis in Microsoft Excel. *Computer Methods and Programs in Biomedicine* 99(3). *Comput Methods Programs Biomed*: 306–314. DOI: 10.1016/j.cmpb.2010.01.007.

Zhao G, Peng C, Du W, et al. (2013) Pharmacokinetic study of eight coumarins of Radix

Angelicae Dahuricae in rats by gas chromatography-mass spectrometry. *Fitoterapia* 89(1). Elsevier: 250–256. DOI: 10.1016/j.fitote.2013.06.007.

Zhao M, Ding W, Wang S, et al. (2016) Simultaneous determination of nine coumarins in rat plasma by HPLC-MS/MS for pharmacokinetics studies following oral administration of Fraxini Cortex extract. *Journal of Chromatography B: Analytical Technologies in the Biomedical and Life Sciences* 1025. Elsevier: 25–32. DOI: 10.1016/j.jchromb.2016.04.042.

Published papers



Article

Pharmacokinetics and Tissue Distribution of Coumarins from *Tagetes lucida* in an LPS-Induced Neuroinflammation Model

Anislada Santibáñez ^{1,2}, Maribel Herrera-Ruiz ¹, Manasés González-Cortazar ¹, Pilar Nicasio-Torres ¹, Ashutosh Sharma ^{2,*} and Enrique Jiménez-Ferrer ^{1,*}

¹ Centro de Investigación Biomédica del Sur, Instituto Mexicano del Seguro Social, Argentina No. 1 Col Centro, Xochitepec 62790, Mexico

² School of Engineering and Sciences, Tecnológico de Monterrey, Av. Epigmenio González No. 500, San Pablo, Queretaro 76130, Mexico

* Correspondence: asharma@tec.mx (A.S.); enriqueferrer_mx@yahoo.com (E.J.-F.)

Abstract: *Tagetes lucida* has been widely used as a folk remedy in illnesses associated with the central nervous system and inflammatory ailments. Among the chemical compounds that stand out in the plant against these conditions are coumarins, such as 7-*O*-prenylscopoletin (PE), scoparone (SC), dimethylfraxetin (DF), herniarin (HR), and 7-*O*-prenylumbelliferone (PU), considered potential anti-neuroinflammatory compounds. Therefore, the relationship between the therapeutic effect and the dose can be evaluated through pharmacokinetic–pharmacodynamic (PK–PD) studies under a model of neuroinflammation induced by lipopolysaccharide (LPS). Nonetheless, accomplishing those studies requires an accurate and robust analytical method for the detection of these compounds in different biological matrices of interest. Due to the above, in the present study, a bioanalytical method was established by HPLC–DAD–UV for the simultaneous quantification of the coumarins present in the hexane extract of *T. lucida*, which was able to determine the temporal concentration profiles of each of the coumarins in the plasma, brain, kidney, and spleen samples of healthy and damaged mice. Coumarins showed an increase in plasma concentrations of up to three times in the neuroinflammation model, compared to healthy mice, so it was possible to quantify the therapeutic agents in the main target organ, the brain. The ability of compounds to cross the blood–brain barrier is an advantage in the treatment of diseases associated with neuroinflammation processes that can be studied in future PK–PD evaluations.

Keywords: HPLC–UV; coumarins; *Tagetes lucida*; pharmacokinetics



Citation: Santibáñez, A.; Herrera-Ruiz, M.; González-Cortazar, M.; Nicasio-Torres, P.; Sharma, A.; Jiménez-Ferrer, E. Pharmacokinetics and Tissue Distribution of Coumarins from *Tagetes lucida* in an LPS-Induced Neuroinflammation Model. *Plants* **2022**, *11*, 2805. <https://doi.org/10.3390/plants11212805>

Academic Editor: Corina Danciu

Received: 30 September 2022

Accepted: 19 October 2022

Published: 22 October 2022

Publisher's Note: MDPI stays neutral with regard to jurisdictional claims in published maps and institutional affiliations.



Copyright: © 2022 by the authors. Licensee MDPI, Basel, Switzerland. This article is an open access article distributed under the terms and conditions of the Creative Commons Attribution (CC BY) license (<https://creativecommons.org/licenses/by/4.0/>).

1. Introduction

Tagetes lucida Cav. of the Asteraceae family is a herb widely distributed in Mexico, well-known as “pericón”, “hierba anís”, “yauhtli”, or Mexican mint marigold [1]. Along with the use of *T. lucida*, as a ceremonial plant in some states of central Mexico, in traditional medicine, the leaves and flowers infusions are used as a folk remedy for gastrointestinal, respiratory, and inflammatory ailments, as well as an important appliance in illnesses associated with the central nervous system (CNS), such as “susto” and “nervios” (nervous sickness) [2].

Pharmacological activities have been evaluated with the essential oil and extracts of different polarities obtained from *T. lucida*. These effects have been related to the chemical content of the plant, where the phenolic compounds, such as coumarins, stand out [1,3–6]. Recent studies have proposed that 7-*O*-prenylscopoletin (PE), scoparone (SC), dimethylfraxetin (DF), herniarin (HR), and 7-*O*-prenylumbelliferone (PU), are the main coumarins characterized within the hexane, acetone, and aqueous extracts. Anti-inflammatory [5] anxiolytic [1], antidepressant [7], and vasorelaxant [6] activities have been reported for these compounds, which provides a reference for studies in more specific complaint states, such as neuroinflammation.

Neuroinflammation is a response to alterations in neuronal structure and function within the CNS caused by various peripheral inflammatory stimuli [8]. Neuroinflammatory long-state has been pointed out for its harmful effects on the development of neurodegenerative diseases [9]. Due to the complex scheme of the establishment and progression of the damage caused by neuroinflammation, combinations of therapeutic agents have been proposed in search of a treatment capable of stopping or reversing neuronal damage [10].

Due to its reproducibility, mice damaged with lipopolysaccharide (LPS) are one of the neuroinflammation models most widely used for the evaluation of anti-inflammatory phytochemicals over CNS [11]. This model could allow for a connection between pharmacokinetic-pharmacodynamic (PK-PD) studies for the anti-neuroinflammatory coumarins potential. Nonetheless, accomplishing those studies requires an accurate and robust analytical method for the detection of these types of compounds in different biological matrices.

Several studies of *T. lucida* have been focused mainly on pharmacological activities and phytochemical isolation and identification [12,13]. Additionally, high-performance liquid chromatography–diode array detection (HPLC–DAD) coupled with ultraviolet (UV) has been commonly used in the identification of coumarins from *T. lucida* extracts [1,3,5,14]. Nonetheless, a validated analytical method has not been designed to determine chemical composition diversity among the active extracts that can modify the pharmacological potency in live organisms by the interaction of these compounds. Anyway, the pharmacokinetic studies of these coumarins are null practically, and any study has evaluated the time-course concentration of these compounds with a potential neuroprotective effect.

In the present study it was established and validated, based on FDA guidelines [15], a sensitive and cost-effective bioanalytical method by HPLC–DAD–UV to quantify five coumarins with potential neuroprotector effects, PE, SC, DF, HR, and PU, from hexanic extract of *T. lucida* in some of the main biological matrices used for in vivo preclinical studies: plasma, brain, kidney, and spleen. This quantification method allowed us to carry out a tissue distribution evaluation and a preliminary pharmacokinetic study that are fundamental requirements in monitoring therapeutic agents for the future establishment of PK–PD correlations in a neuroinflammatory state induced by LPS.

2. Results and Discussion

2.1. Optimization of Chromatographic Conditions

To our knowledge, an analytical method useful for the identification and quantification of the bioactive compounds obtained from the hexane extract of *T. lucida* has not been developed [1,3–5,7,14]. Therefore, the five coumarins, PE, SC, DF, HR, and PU, and the internal standard were injected under the liquid chromatographic system conditions to determine their retention time (RT), along with their UV spectra, shown in Figure 1. The system allowed for a suitable separation of the compounds from each for their further analysis in the validation process. Considering the UV spectrum of the analyzed compounds, maximum absorption wavelengths between 320 and 350 nm were observed. For this reason, a $\lambda = 330$ nm was used to identify and quantify all compounds in a single reading.

2.2. Sample Preparation

The optimal recovery of the interest compounds disseminated in these biological matrices is a critical step, since the presence of endogenous interferents must be avoided as much as possible. Liquid–liquid extraction (LLE) accompanied by previous protein precipitation (PP) is widely used, due to it guarantee regarding the elimination of interferences, as a result of the protein solubility decrease by the addition of organic solvents, such as methanol and acetonitrile, as well as its speed and feasibility, allowing for a better availability of the bioactive compounds present in the matrices [16].

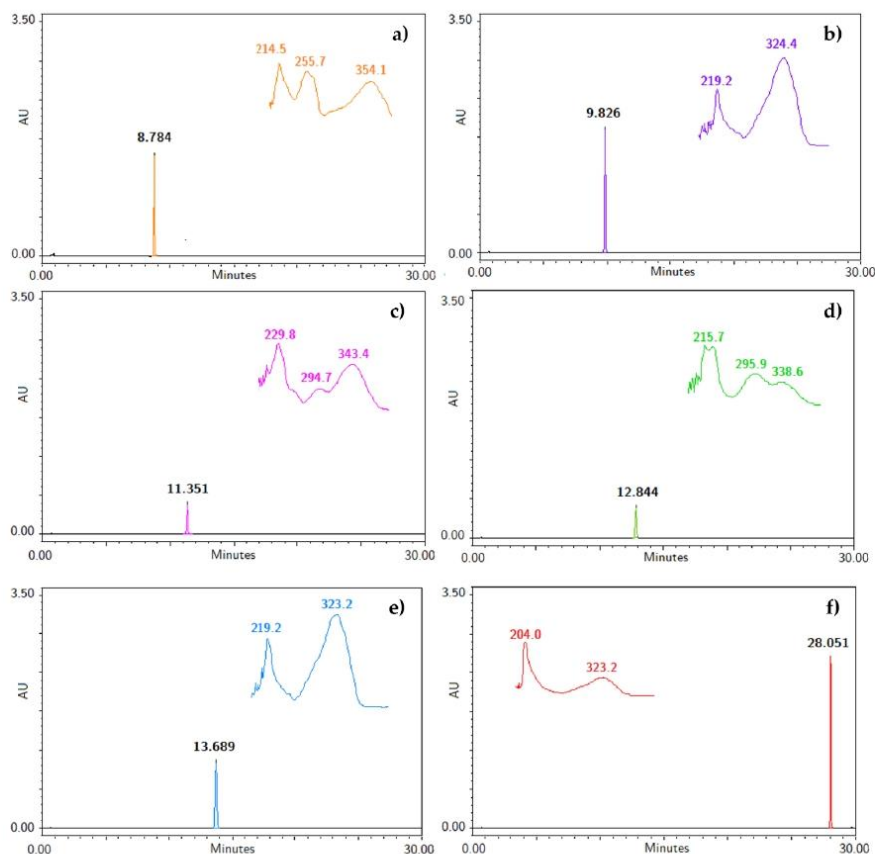


Figure 1. Chromatograms with retention time (RT) and specific UV spectra of (a) IS, (b) PE, (c) SC, (d) DF, (e) HR, and (f) PU at a concentration of 200 µg/mL.

In the present study, the PP was evaluated by adding methanol or acetonitrile to the plasma or tissue suspension. The PP with acetonitrile improved the sensitivity of the recovery method, although the recoveries were lower than the acceptance criteria established in the matrices evaluated. Then, a LLE step with dichloromethane was included, which guaranteed recovery above 85% of coumarins and IS in all cases of matrices. Finally, the supernatants of the centrifuged samples were evaporated and reconstituted in 100 µL of methanol to increase the coumarin concentration.

2.3. Method Validation

The validation of the bioanalytical method by HPLC–UV was completed, according to the recommendations established by the FDA guidance [15] for chromatographic assays.

2.3.1. Specificity

The specificity was evaluated by comparing the chromatograms of blank matrices and blank matrices enriched with the analytes at the corresponding LLOQ concentrations, and plasma and tissue samples collected 15 min after oral administration of the bioactive fraction of *T. lucida* in the pharmacokinetic study (Figure 2). The analyzed samples did not

show any interference in the matrices for the detection of PE (9.8 min), SC (11.4 min), DF (12.8 min), HR (13.7 min), PU (28.0 min), and IS (8.8 min).

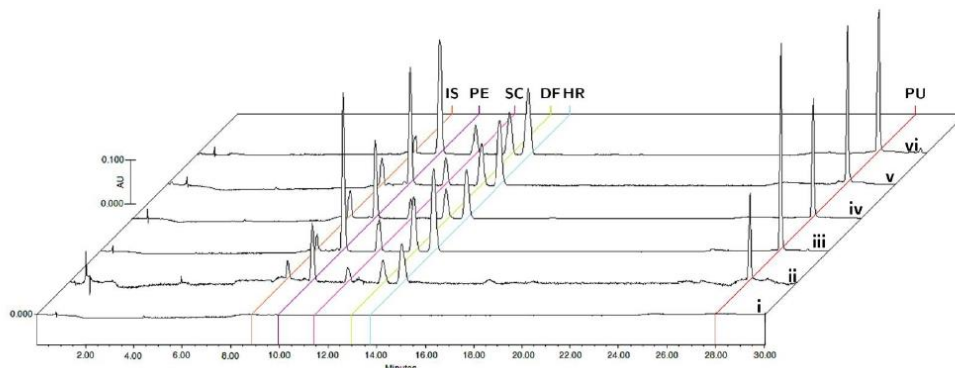


Figure 2. Representative chromatograms of (i) blank matrix, (ii) blank matrix spiked with LLOQ concentration, and processed samples collected at 15 min after oral administration of standardized hexane extract spiked with IS in plasma (iii), brain (iv), kidneys (v), and spleen (vi).

2.3.2. Linearity and Selectivity

The calibration curves were constructed from the ratio of the peak areas of the analytes and the IS. The curves were linear in all the biological matrices in a concentration range between 0.156–40 $\mu\text{g}/\text{mL}$ for each coumarin and 1.5 $\mu\text{g}/\text{mL}$ for IS. The equations that describe the linear regression models, the coefficients of determination (r^2), and the specific LLOQs for each compound in the matrices are shown in Table 1. In the case of LLOQs, a single minimum concentration was established for all coumarins that correspond to 156 ng/mL, which meets the precision and accuracy acceptance criteria established above.

Table 1. Linearity equations of calibration curves and LLOQ determined for coumarins in plasma and tissue matrices.

Matrix	Analytes	Linearity Equation	r^2	LLOQ ($\mu\text{g}/\text{mL}$)
Plasma	PE	$y = 0.2278x + 0.0246$	0.9996	0.18
	SC	$y = 0.0743x - 0.0126$	0.9987	0.05
	DF	$y = 0.1260x - 0.0322$	0.9965	0.15
	HR	$y = 0.2082x + 0.0294$	0.9997	0.17
	PU	$y = 0.2705x + 0.0916$	0.9976	0.10
Brain	PE	$y = 0.1607x + 0.0046$	0.9995	0.13
	SC	$y = 0.0510x - 0.0094$	0.9991	0.10
	DF	$y = 0.0841x - 0.0037$	0.9997	0.08
	HR	$y = 0.1455x - 0.0043$	0.9969	0.10
	PU	$y = 0.1886x + 0.0275$	0.9997	0.02
Kidney	PE	$y = 0.2394x + 0.024$	0.9998	0.07
	SC	$y = 0.0746x - 0.0054$	0.9995	0.18
	DF	$y = 0.1273x - 0.0119$	0.9994	0.03
	HR	$y = 0.2104x - 0.0376$	0.9986	0.16
	PU	$y = 0.2794x - 0.0397$	0.9993	0.02
Spleen	PE	$y = 0.3918x + 0.0278$	0.9996	0.12
	SC	$y = 0.1238x - 0.0284$	0.9986	0.02
	DF	$y = 0.2090x - 0.0218$	0.9991	0.05
	HR	$y = 0.3603x + 0.0271$	0.9989	0.11
	PU	$y = 0.4728x - 0.1095$	0.9989	0.02

PE = 7-O-prenylscopoletin, SC = scoparone, DF = dimethylfraxetin, HR = herniarin, and PU = 7-O-prenylumbelliferone.

2.3.3. Precision and Accuracy

The precision and accuracy estimated at the intra- and inter-day levels were evaluated in the five biological matrices by analyte mixed with the concentrations established for the low, medium, and high levels of the QC samples. The precision values for these levels were less than 11.05%, while the accuracy represented by %RE ranged from −14.01 to 8.66, varying between each matrix and analyte evaluated. All precision and accuracy values meet the criteria established by the FDA [15] and are summarized in Table 2.

Table 2. Data of accuracy and precision determined for coumarins in plasma and tissue matrices.

Nominal Concentrations (µg/mL)		30.0				3.0				0.3			
Matrix	Analytes	Repeatability		Reproducibility		Repeatability		Reproducibility		Repeatability		Reproducibility	
		RE (%)	RSD (%)	RE (%)	RSD (%)	RE (%)	RSD (%)	RE (%)	RSD (%)	RE (%)	RSD (%)	RE (%)	RSD (%)
Plasma	PE	1.30	1.73	1.05	1.49	1.44	1.79	1.71	1.34	8.66	1.49	4.59	4.83
	SC	−5.28	2.41	−4.94	1.73	−9.61	3.74	−8.25	3.04	−6.67	3.55	−12.71	6.69
	DF	−11.95	1.45	−7.80	5.19	−7.85	1.08	−5.39	2.93	−14.01	6.30	−10.64	5.7
	HR	−6.69	1.51	−2.56	4.74	1.31	1.03	1.84	1.02	−2.18	2.83	0.06	3.07
	PU	1.96	1.66	1.94	1.27	−0.17	0.90	0.06	0.75	−5.66	2.11	−4.36	2.02
Brain	PE	0.99	4.14	−0.12	3.10	5.34	1.58	2.96	2.76	2.09	1.28	2.37	1.94
	SC	−0.64	1.82	−1.81	2.19	3.97	0.61	1.96	2.39	−6.41	5.35	−7.98	5.41
	DF	1.97	3.71	1.54	2.46	7.81	2.78	3.17	7.07	−4.03	2.36	−2.68	3.77
	HR	1.77	3.74	1.17	3.47	−1.79	3.70	−5.53	5.10	2.78	1.35	3.69	1.62
	PU	3.47	1.98	1.49	2.75	4.32	0.92	−0.98	6.28	−5.11	6.81	−7.60	5.42
Kidney	PE	−3.59	2.30	−2.08	2.35	0.94	0.23	0.51	1.06	−2.02	1.21	−1.46	1.06
	SC	−0.65	2.03	−0.90	1.45	2.39	1.04	1.35	1.51	0.07	1.27	0.20	0.86
	DF	−0.27	1.23	−0.20	0.90	−2.18	6.29	−1.81	4.08	−0.07	3.08	−1.08	4.33
	HR	3.58	3.12	2.10	2.99	−4.14	2.43	−0.26	5.07	−6.52	3.33	−7.12	2.66
	PU	−0.21	2.02	−0.15	1.90	−4.41	6.51	−1.66	5.24	−5.93	6.14	−4.70	5.71
Spleen	PE	1.64	1.30	1.90	3.04	−10.29	6.93	−4.80	8.00	−4.52	2.50	−8.01	9.87
	SC	−0.43	7.32	−2.54	11.05	−12.42	3.32	−11.73	6.25	−6.69	8.82	−7.46	8.03
	DF	−9.08	7.89	−10.04	5.33	−4.93	10.71	−5.10	8.77	−3.77	9.44	−4.16	7.76
	HR	2.34	2.65	1.47	2.95	−3.52	9.67	−2.20	6.82	−2.38	5.45	−5.44	6.58
	PU	−7.17	4.30	−6.18	3.39	−10.72	2.70	−8.36	7.00	−8.99	2.94	−4.00	6.55

PE = 7-O-prenylscopoletin, SC = scoparone, DF = dimethylfraxetin, HR = herniarin, and PU = 7-O-prenylumbelliferone.

2.3.4. Recovery and Matrix Effect

Plasma and tissue matrices, spiked after the extraction process with QC levels, were compared to the previously spiked samples to determine the extraction recovery of both coumarin and IS. The lowest extraction value was 87.15% for PE in plasma (Table 3). Likewise, the matrix effect was evaluated with values between 85.09% and 107.77%, with RSD < 12.6%, for the different coumarins, while for the IS varied up to 7.59%, as shown in Table 3.

2.3.5. Stability

The stability of the compounds obtained from each enriched matrices at the QC concentrations was evaluated under different conditions that covered the processing, handling, and storage phases that could be developed throughout the study. In all cases, the RE values showed that there were no significant losses of the analytes under short-term (autosampler) and long-term storage conditions, as well as in the freeze-thaw cycles of the samples, and data are summarized in Table S1.

Table 3. Data of extraction recovery and matrix effects determined for coumarins in plasma and tissue matrices.

Spiked Concentrations (µg/mL)		30.0				3.0				0.3			
Matrix	Analytes	Extraction Recovery		Matrix Effect		Extraction Recovery		Matrix Effect		Extraction Recovery		Matrix Effect	
		RE (%)	RSD (%)	RE (%)	RSD (%)	RE (%)	RSD (%)	RE (%)	RSD (%)	RE (%)	RSD (%)	RE (%)	RSD (%)
Plasma	PE	99.04	7.11	94.60	7.78	87.15	8.25	89.72	9.55	88.00	10.41	86.27	10.43
	SC	98.30	2.38	98.55	7.53	91.67	8.16	92.52	9.53	94.13	5.78	89.59	9.33
	DF	102.04	3.91	101.23	5.45	100.88	10.35	94.83	11.26	97.58	7.33	102.99	4.70
	HR	99.67	6.21	94.79	6.08	87.83	7.20	92.93	8.53	93.82	3.83	99.70	6.13
	PU	102.17	8.05	94.66	7.11	94.77	1.27	85.09	3.10	101.67	9.42	108.91	10.23
	IS	99.42	4.66	99.61	7.59	94.22	2.43	92.24	2.38	99.71	3.77	100.59	3.66
Brain	PE	91.64	4.80	106.08	6.48	88.01	0.54	102.28	2.64	92.19	1.21	98.72	3.11
	SC	99.44	1.23	104.99	7.68	94.65	1.06	100.94	4.21	89.70	6.03	94.89	4.67
	DF	90.13	1.60	107.26	5.22	96.44	5.16	105.50	7.29	93.08	3.45	94.55	5.75
	HR	91.81	3.22	105.11	4.90	94.27	3.10	104.20	5.42	112.29	1.54	100.92	3.04
	PU	93.49	5.98	107.77	7.35	99.56	3.95	101.16	9.57	95.23	5.72	96.32	9.37
	IS	95.11	2.75	95.32	6.31	98.97	2.28	99.01	2.81	99.84	2.65	94.71	3.90
Kidney	PE	97.95	2.29	96.77	2.67	99.28	0.93	96.08	6.18	91.30	1.16	100.34	4.79
	SC	99.99	2.80	98.86	1.70	105.72	0.97	95.55	5.96	94.28	9.05	100.39	12.60
	DF	99.40	2.30	97.20	2.81	104.84	4.78	98.51	7.05	87.24	2.72	96.97	9.83
	HR	103.06	6.55	100.89	4.06	91.38	2.42	95.68	6.09	90.39	1.25	99.26	5.03
	PU	100.87	8.68	98.52	5.28	103.27	5.16	97.70	10.57	93.11	3.89	97.25	6.83
	IS	101.26	1.25	101.28	1.63	103.72	3.20	103.89	5.66	99.94	2.75	109.67	4.86
Spleen	PE	98.33	11.85	99.87	6.05	100.55	1.93	100.36	2.92	90.36	1.02	100.04	4.43
	SC	100.16	3.04	101.09	5.38	109.71	1.28	99.54	1.78	88.30	7.77	103.43	9.26
	DF	100.77	6.28	101.70	5.41	104.20	2.71	98.98	5.98	92.01	6.31	105.13	7.23
	HR	100.99	10.13	101.12	6.77	92.58	2.45	98.66	3.54	88.74	1.56	101.12	3.64
	PU	99.31	14.67	98.83	3.34	105.05	4.03	102.63	6.70	91.89	4.61	99.32	4.65
	IS	98.87	3.19	98.96	4.87	99.98	0.94	100.00	1.73	99.02	2.74	97.02	2.78

PE = 7-O-prenylscopoletin, SC = scoparone, DF = dimethylfraxetin, HR = herniarin, and PU = 7-O-prenylumbelliferone.

2.4. Pharmacokinetic and Tissue Distribution Study

The optimized HPLC-validated method for the quantification of coumarins present in the hexane extract of *T. lucida* was used to evaluate the concentration profiles over time in the plasma, brain, kidney, and spleen biological matrices after an oral administration of 10 mg/kg of the extract.

Within PK and tissue distribution studies in animal models, whether healthy or diseased, it is important to look at the functional and structural capacities of each organ or system studied to obtain the most relevant information for the subsequent pharmacological studies or their later translation to humans. Therefore, in this study, each of these biological matrices offered a tool for the analysis of the dynamic behavior of compounds within the system [17].

Plasma presented a general scheme of the administration, distribution, metabolism, and excretion (ADME) processes and the bioavailability of the coumarins found in the hexane extract of *T. lucida* after its administration in both healthy mice and those subjected to LPS-induced neuroinflammation. Once the absorption process began, it was possible to determine if these compounds reached the target organ that corresponds to the brain and for how long they remained. In parallel, the elimination stage was compared with the amounts present in the kidneys to establish an association between excretion and systemic circulation. Finally, the presence of potential therapeutic agents in the spleen, one of the

organs involved in the initial response to inflammatory processes, may clarify the results for subsequent pharmacodynamic studies, such as the evaluation of the presence of anti- and pro-inflammatory markers and its temporal relationship with coumarin concentrations, giving way to essential PK–PD studies in the development of new pharmacological therapies. The concentration mean time curves in the plasma of PE, SC, DF, HR, and PU from healthy and LPS-induced neuroinflammation mice were plotted in Figure 3.

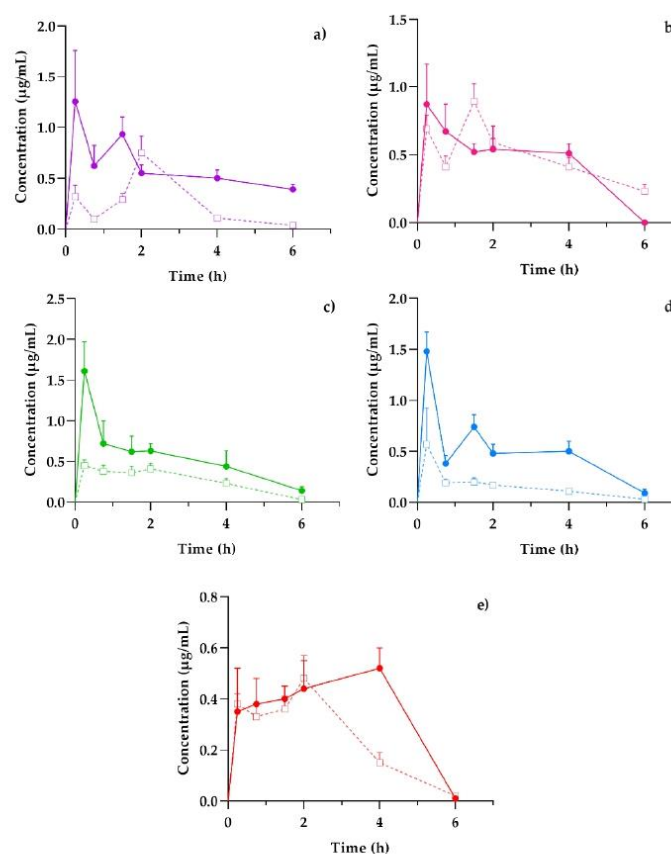


Figure 3. Concentration–time profiles of coumarins: (a) PE, (b) SC, (c) DF, (d) HR, and (e) PU after a 10 mg/kg oral dose administration of hexanic extract of *Tagetes lucida* in healthy (–□–) and LPS-damaged (–●–) ICR mice. The results are presented as mean \pm SEM ($n = 5$).

The behavior of the concentration variations over time between healthy and damaged subjects was similar in each of the coumarins. However, the graphic representation suggests that, in those mice that were previously administered with LPS, the amount of drug available in the plasma was three-fold higher than the value obtained in healthy subjects, as is the case of DF (Figure 3c) and HR (Figure 3d). Other studies have reported the impact of inflammation on pharmacokinetic variations, especially for plasma drug exposure by increasing the concentration/dose ratio [18].

Among the pharmacokinetic characteristics in the LPS-treated mice, the SC (Figure 3b) and DF (Figure 3c) highlight their fast distribution and subsequent elimination, consistent with that reported in previous studies [19,20]. The remaining coumarins show processes where the concentrations increase repeatedly or continuously, as is the case of PU (Figure 3e),

which reaches a concentration peak up to 4 h after the administration of the *T. lucida* extract. This response should be considered for the design of the pharmaceutical forms used in further clinical studies, since its varied absorption may modify the effectiveness of some of the components.

From these temporal profiles, the preliminary pharmacokinetic parameters shown in Table 4 were calculated for both conditions.

Table 4. Pharmacokinetic parameters of coumarins estimated by non-compartmental analysis in plasma after oral administration of hexanic extract of *Tagetes lucida* in healthy and LPS-damaged ICR mice.

Parameter	Unit	PE		SC		DF		HR		PU	
		Healthy	LPS	Healthy	LPS	Healthy	LPS	Healthy	LPS	Healthy	LPS
C_{max}	µg/mL	0.93 ± 0.29	1.77 ± 0.31	0.97 ± 0.10	1.28 ± 0.11	0.58 ± 0.02	1.82 ± 0.27	0.62 ± 0.34	1.48 ± 0.19	0.56 ± 0.05	0.69 ± 0.07
T_{max}	h	1.55 ± 0.34	0.85 ± 0.28	1.25 ± 0.25	0.70 ± 0.34	1.20 ± 0.31	0.60 ± 0.24	0.95 ± 0.35	0.25 ± 0.00	1.55 ± 0.23	1.05 ± 0.31
$t_{1/2}$	h	1.86 ± 0.55	4.48 ± 1.31	2.88 ± 0.83	0.65 ± 0.06	0.98 ± 0.27	1.50 ± 0.37	1.66 ± 0.46	1.49 ± 0.35	0.92 ± 0.06	0.95 ± 0.10
AUC_{0-t}	µg·h/mL	1.56 ± 0.35	3.52 ± 0.10	2.87 ± 0.09	2.77 ± 0.21	1.64 ± 0.17	3.25 ± 0.31	0.92 ± 0.12	2.95 ± 0.28	1.49 ± 0.11	2.22 ± 0.26
$AUC_{0-∞}$	µg·h/mL	1.70 ± 0.31	6.37 ± 1.20	4.03 ± 0.63	2.78 ± 0.21	1.71 ± 0.19	3.61 ± 0.40	1.03 ± 0.14	3.21 ± 0.38	1.52 ± 0.12	2.24 ± 0.26
MRT	h	3.04 ± 0.45	6.96 ± 1.92	4.68 ± 1.16	2.26 ± 0.17	2.35 ± 0.33	2.72 ± 0.30	2.77 ± 0.35	2.77 ± 0.25	2.15 ± 0.11	2.68 ± 0.14
Cl/F	*	65.83 ± 10.18	17.38 ± 2.25	26.64 ± 3.00	36.32 ± 2.68	62.45 ± 9.38	28.81 ± 2.51	103.7 ± 13.0	32.50 ± 2.91	67.37 ± 5.33	46.95 ± 5.03

Values represent mean ± SEM ($n = 5$). PE = 7-*O*-prenylscopoletin, SC = scoparone, DF = dimethylfraxetin, HR = hemiarin, and PU = 7-*O*-prenylumbelliferone. * (mg/kg)/(µg/mL)/h.

Mean C_{max} response in each coumarin was greater in mice damaged with LPS, and it was obtained with a shorter T_{max} , so it was expected that the general exposure of each compound could be diversified among the animals. Except for SC, the AUC values showed a greater maintenance presence of therapeutic agents in plasma over time when the inflammatory agent was present, so theoretically, a system affected by an acute inflammation environment can increase the bioavailability of the therapeutic compounds in the bloodstream; then, it is important to consider adequate doses in pharmaceutical design to avoid intoxications or increased adverse effects, due to excess exposures [21].

ADME processes are known to be modified by the presence of inflammatory factors, such as pretreatment with agents, such as LPS [22]. Normally during the process of inflammation, absorption in the gastrointestinal tract can be modified by the presence of diarrhea as a result of the damage, thus modifying the distribution of therapeutic agents by changes in acute-phase plasma protein binding in response to inflammation. For instance, with the decrease in protein syntheses, such as albumin, and the increase in transferrin [23]. This may be related to the increase in the C_{max} of each of the coumarins in the damaged animals of up to three times more, as is the case with DF.

Additionally, it has been reported that the alterations in the hepatic and intestinal metabolism of drugs depend on factors such as blood flow rate, the free fraction of the drug in plasma, and the clearance rate defined by each compound. In pharmacokinetic studies of drugs metabolized mainly by the liver, the clearance rate is significantly slowed when individuals are subjected to LPS-mediated inflammatory processes [23]. The foregoing coincides with what is expressed in the observed values of oral clearance (Cl/F) in Table 4, where practically all the compounds studied presented a faster clearance in healthy systems (up to 31.4% increase), apart from SC, which maintained clearance rates close to each other.

Another of the main organs associated with drug clearance are the kidneys. When these are exposed to inflammatory states, renal excretion mediated by the glomerular filtration rate, as well as the plasma flow rate, shows a change in the pharmacokinetic profiles [18]. In our case, the net exposure of coumarins, detailed by AUC, increased and, in the case of SC, they remained comparable because of a slower excretion. The comparative results also showed an increase in serum concentration [23], compatible with the increase in plasma concentrations of the compounds observed in the present study.

Due to the profiles and pharmacokinetic parameters obtained, it was important to determine the distribution capacity of coumarins in the tissues. Figure 4 shows the distribution of the compounds in the brain, the main target organ, under conditions of systemic inflammation, compared to mice without damage. In turn, Figure S1 set out the temporal distribution of coumarins in the kidneys and spleen, in addition to showing the

transfer processes between the organs and the blood circulation system, the data obtained will be useful in subsequent PK–PD studies that evaluate the relevance of the pharmacological effects, concerning the processes of metabolism and clearance of drugs, for their therapeutic monitoring.

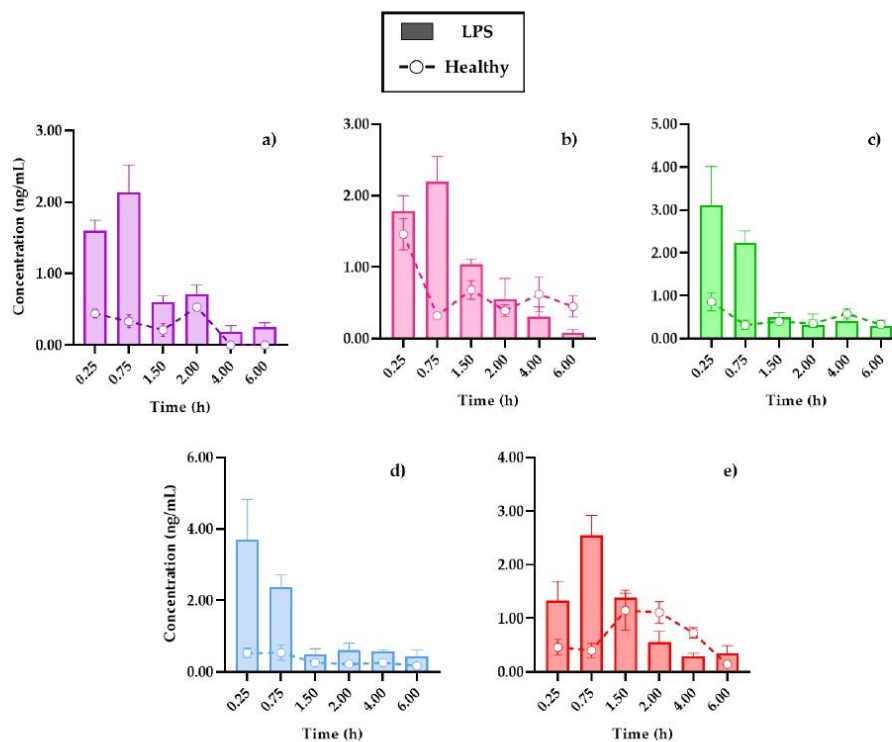


Figure 4. Distribution in the brain of (a) 7-O-prenylscopoletin (PE), (b) scoparone (SC), (c) dimethylfraxetin (DF), (d) herniarin (HR), (e) 7-O-prenylumbelliferone (PU) after an oral dose administration of hexanic extract of *Tagetes lucida* in healthy and LPS-administrated mice. Values are presented as mean \pm SEM ($n = 5$).

In all cases, the brain was the organ with the lowest content of coumarins, below 5 ng/mL of the compounds in tissue, and this could be due to low penetration caused by the presence of the blood–brain barrier. Conversely, in comparison with a study where the distribution of SC in different organs was analyzed, it was reported that it was not possible to quantify this coumarin inside the brain [19], where the dose administered to the rats used for this study or the extraction process from the biosamples could be a limitation.

The review carried out by Batista et al. (2019) detailed how the brain is affected in the LPS-induced systemic inflammation model, mentioning that, in addition to the presence of cytokines, such as interleukins IL-1 β , IL-6, and TNF- α in plasma, there is evidence that LPS damages the blood–brain barrier, which allows for the infiltration of small therapeutic molecules, thus improving the pharmacological treatment [22].

The cooperation of the coumarins bioavailability in plasma (Figure 3) with the kinetic profiles in the brain (Figure 4) shows that the highest concentration in the tissue is reached 15 min after the initial absorption process of PE, SC, and PU coumarins. Moreover, HR and DF maintain similar behaviors in the plasma and brain, although in much lower

concentrations for the latter. Factors such as the size of the molecules, as well as the highest in plasma, compared to the other compounds, influence this behavior.

In the distribution brain profile, an increase of the compounds up to three times more in the damaged mice is observed in the first 90 min, after this time, some coumarins, such as SC (Figure 4b) and PU (Figure 4e), maintain levels of higher tissue concentrations in control mice. It is possible that the neuroinflammation process by i.p. LPS administration caused damage to the blood–brain barrier, allowing for the permeability of these compounds, as previously described, which is an advantage in the treatment of diseases associated with neuroinflammation processes [11].

3. Materials and Methods

3.1. Reagents and Materials

Coumarins 7-*O*-prenylscopoletin (PE), scoparone (SC), dimethylfraxetin (DF), herniarin (HR), and 7-*O*-prenylumbelliferone (PU) were isolated and purified in the laboratory from a hexanic extract of *Tagetes lucida* (Figure 5). Each compound was identified by ¹H- and ¹³C-NMR analyses, which were compared with those described in previous studies [5]. The internal standard rutin (IS, purity ≥ 98%), trifluoroacetic acid (TFA), and lipopolysaccharide (LPS) were purchased from Sigma-Aldrich (St. Louis, MO, USA); acetonitrile, methanol, and water solvents HPLC-grade from Tecsiquim (Mexico, Mexico), and reagent-grade hexane was purchased from Merck (Darmstadt, Germany).

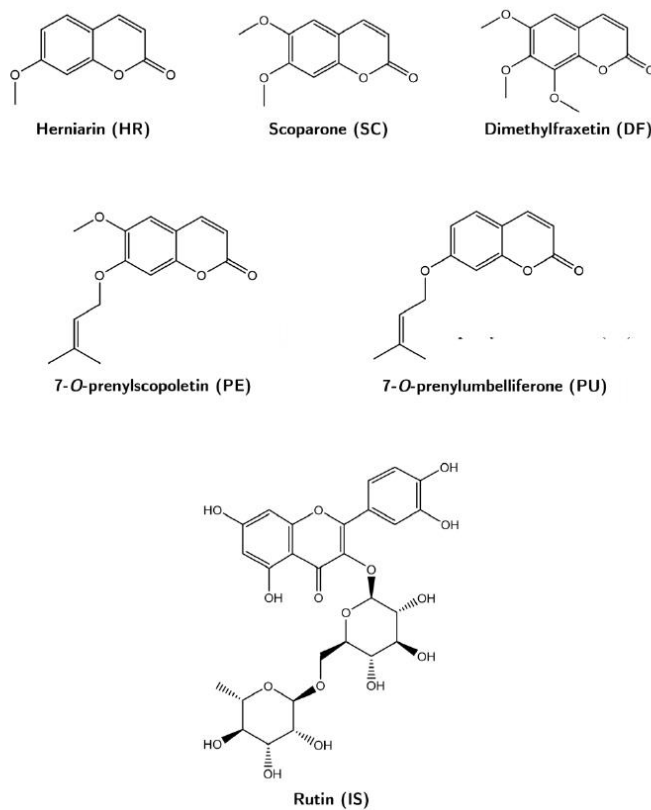


Figure 5. Chemical structures of the coumarins 7-*O*-prenylscopoletin (PE), scoparone (SC), dimethylfraxetin (DF), herniarin (HR), and 7-*O*-prenylumbelliferone (PU), and of the rutin (IS).

3.2. Hexanic Extract Preparation

From a collection of *T. lucida* carried out in Xochitepec, Morelos, Mexico, the aerial parts of previously identified specimen material (Voucher No. 2081) [3] were dried on wire mesh beds at room temperature. The dry plant material was pulverized in a mill, until a particle size of 4–6 mm was obtained. Subsequently, 200 g of plant material was macerated three times in hexane for 24 h, each time the solvent was removed under reduced pressure. The standardization of the extract, in the content of coumarins, was determined by HPLC using the external standard method, calculating the following concentrations in mg/g of extract: 20.81 (PE), 14.64 (SC), 13.18 (DF), 19.79 (HR), and 20.35 (PU).

3.3. Animals

Male ICR mice (30 ± 5 g) were provided by the animal facility of XXI Century Medical Center, IMSS (CDMX, Mexico). The animals were kept at room temperature (22 ± 4 °C) with 12-h light-dark cycles (07:00 to 19:00 h). Access to food and water was allowed *ad libitum*, until 12 h before starting the experiment.

The studies were carried out following the Official Mexican Standard NOM-062-ZOO-1999: Technical Specifications for the Production, Care, and Use of Laboratory Animals [24]. This project was approved by the Local Committee for Research in Health and Ethics of the Mexican Institute of Social Security (IMSS) on 16 August 2021, with the registration number R 2021-1702-009.

3.4. Samples Collection

Blood samples were obtained from the retro-orbital sinus of mice and collected in heparinized tubes. Plasma was separated by centrifugation at 3500 rpm for 5 min and stored in new Eppendorf tubes at -70 °C, until further processing.

After blood sampling, the mice were sacrificed in a chamber with chloroform by an overdose of anesthesia. The brain, kidney, and spleen were quickly removed and rinsed with saline solution, fresh weight was recorded, and immediately placed on ice. Subsequently, the organs were freeze-dried, grounded, and weighted. The lyophilized organs were individually suspended in methanol in a 1:1 volume: dry weight ratio for 24 h, then sonicated for 5 min and centrifuged at 14,000 rpm for 7 min. The supernatants were recovered in clean tubes and stored at -70 °C until their use.

3.5. Preparation of Working Solutions, Calibration Curves, and Quality Control (QC) Samples

Individual stock solutions of PE, SC, DF, HR, PU, and rutin (IS) were prepared separately in methanol (1 mg/mL) and stored at -4 °C until use. From the stocks, a working solution in methanol was prepared at a concentration of 200 µg/mL of each coumarin. Blank plasma or organs supernatant samples (80 µL) were spiked with 20 µL of serial dilutions of working solution to obtain calibration curves ranging between 0.156, 0.312, 0.625, 1.25, 2.5, 5, 10, 20, and 40 µg/mL of each coumarin. Quality control (QC) samples were prepared at three levels of 0.3 (low), 3 (medium), and 30 (high) µg/mL for each coumarin.

3.6. Plasma and Tissue Samples Processing

One hundred microliters of plasma and organs samples, spiked with calibration and QC concentration or samples from the pharmacokinetic study, were mixed with 300 µL of acetonitrile containing the IS at 10 µg/mL for protein precipitation, and vortexed for 3 min. Then, 200 µL of dichloromethane were added, for liquid–liquid extraction of the bioactive compounds, and vortexed for 5 min. The mixture was centrifuged at 14,000 rpm for 10 min, and the extracted organic layers were placed in new tubes, until completely dry at room temperature. For quantitative analysis, samples were resuspended in 100 µL of methanol, transferred to sampling vials, and injected into the chromatographic system, described below.

3.7. HPLC–DAD–UV Handling Conditions

Biological and standard samples analysis was carried out by a high-performance liquid chromatography Waters 2695 series. The Waters 2995 series HPLC separation module consisted of a quaternary pump, degasser, autosampler, and thermostatted column. Additionally, it was connected to a photodiode array UV–VIS detector, Waters 2996 series. A Supelco Discovery® C18 column (250 × 4.6 mm, 5 μm, Merck) was used for chromatographic separation and method validation. The injection volume of all described samples was 10 μL, using a mobile phase flow set at 0.9 mL/min, consisting of a 0.5% trifluoroacetic acid aqueous solution (A) and acetonitrile (B). The final run time of the samples was established at 30 min, with a gradient solution as follows: 0–2 min, 100–95% (A); 2–4 min, 95–70% (A); 4–21 min, 70–50% (A); 21–24 min, 50–20% (A); 24–27 min, 20–0% (A); and 27–30 min, 0–100% (A). The readings were carried out at a wavelength (λ) of 330 nm and processed with the Empower Pro 3.0 software (Waters, MA, USA).

3.8. Validation of HPLC–DAD–UV Quantification Method

The validation of the HPLC quantification method of the coumarins present in the *T. lucida* hexanic extract was carried out under the FDA Bioanalytical Method Validation: Guidance for Industry [15].

3.8.1. Specificity, Linearity, and Sensitivity

Specificity was ensured by evaluating that there were no endogenous interferents in the working matrix corresponding to blank biological matrices (plasma and tissues) from six mice. Linearity was determined by linear regression of the calibration curves, based on the ratio of the area under the curve (AUC) of the analyte peak against the same IS signal. Sensitivity was defined as the lowest concentration that can be determined, according to the signal/noise (S/N) ≥ 5 of the analyte peaks, obtained by the lower limit of quantification (LLOQ). The evaluation of the LLOQ must meet the acceptance criteria of accuracy and precision, which are evaluated with relative standard deviation (RSD) ≤ 20%.

3.8.2. Extraction Recovery and Matrix Effects

Recovery was analyzed in the concentrations of the QC samples by comparing the peak areas of samples extracted under the normal procedure with the post-extraction spiked samples at the same concentration levels ($n = 5$). On the other hand, the effect of the matrix on the analytical evaluation of the coumarins was obtained by comparing five samples extracted from plasma and each organ against five samples prepared directly in the mobile phase. The matched concentrations corresponded to the three QC points, including the LLOQ established before. The effect of the matrix was calculated by means of the coefficients of the AUC of samples extracted from the matrices and those prepared in the system, with respect to the response signal of the IS for each coumarin. The nominal concentration obtained in the processed matrices must range between ±15%, evaluated by relative error (RE) and ≤15% for RSD.

3.8.3. Precision and Accuracy

Intra- and inter-day precision and accuracy were determined by evaluating six replicates of QC samples, prepared independently from three different sets. The acceptance criteria corresponded to RSD ≤ 15% and RE ± 15%, according to the nominal concentration.

3.8.4. Stability

The stability of the analytes in plasma, brain, kidneys, and spleen was evaluated by the analyzed concentrations of QC subjected to three different conditions. Short-term stability was determined by analysis of samples processed in the autosampler vials at 24 h at room temperature. Long-term stability was tested on samples stored at −70 °C for 30 days. Freeze-thaw stability was determined after three cycles (−4 °C to 25 °C) on three consecutive days.

3.9. LPS-Induced Neuroinflammation and Pharmacokinetic Study

A pharmacokinetic study was carried out in sixty mice, divided in six subgroups, according to sample collection times. An acute inflammation process by the intraperitoneal (i.p.) administration of LPS at 2 mg/kg was induced in half of the mice per group, while the other half received an i.p. injection of saline solution. Ten min after the damage was induced, the mice were administered with an oral dose of 10 mg/kg of the bioactive fraction dissolved in a 1% Tween-20 aqueous solution. Blood and tissue samples were obtained and processed at 0, 0.25, 0.75, 1.5, 2, 4, and 6 h post-dosing, as indicated in the “Samples collection” and “Plasma and tissue samples processing” sections.

3.10. Pharmacokinetic and Tissue Distribution Analysis

Pharmacokinetic parameters of PE, SC, DF, HR, and PU in plasma were calculated by PKSolver software [25]. The maximum plasma concentration (C_{max}), time to reach the maximal concentration (T_{max}), half-life time ($t_{1/2}$), area under the concentration–time curve to 6 h (AUC_{0-6}) and infinity ($AUC_{0-\infty}$), mean residence time (MRT), and the observed oral clearance (Cl/F) were obtained using a non-compartmental model, expressed as mean \pm SEM.

To evaluate the distribution in the tissues, bioactive coumarins were quantified in the lyophilized organs, and concentrations were adjusted to the volumes of liquid obtained by the difference between the dry and fresh weights of each tissue to simulate a distribution approximation of the compounds by tissue system.

4. Conclusions

A sensitive, suitable, and validated HPLC–DAD–UV method for the simultaneous quantification of five coumarins, i.e., PE, SC, HR, DF, and PU, in the plasma, brain, kidneys, and spleen was developed and successfully applied in preclinical pharmacokinetic and tissue distribution studies, following an oral administration of hexanic extract of *Tagetes lucida* in healthy and damaged mice by an LPS-induced neuroinflammation model. The bioavailability observed in brain tissue and plasma determined that the compounds could reach the target site to exert their potential therapeutic functions in systems damaged by the agents that cause neuroinflammation. The present study has potential applicability for further pharmacokinetic–pharmacodynamic evaluations to determine the correlation between different dose administrations and their therapeutic effects on central nervous system ailments.

Supplementary Materials: The following supporting information can be downloaded at: <https://www.mdpi.com/article/10.3390/plants11212805/s1>, Table S1: Stability test of PE, ES, DF, HR, and PU in plasma and tissue matrices. Figure S1: Tissue distribution in kidneys and spleen of 7-O-prenylscopoletin (PE), scoparone (SC), dimethylfraxetin (DF), herniarin (HR), 7-O-prenylumbelliferone (PU) after an oral dose administration of hexanic extract of *Tagetes lucida*. Values are presented as mean \pm SEM ($n = 5$).

Author Contributions: Conceptualization, A.S. (Anislada Santibáñez) and E.J.-F.; formal analysis, A.S. (Anislada Santibáñez); investigation, A.S. (Anislada Santibáñez) and E.J.-F.; methodology, A.S. (Anislada Santibáñez), M.H.-R., M.G.-C., and E.J.-F.; resources, M.H.-R., M.G.-C., P.N.-T., A.S. (Ashutosh Sharma), and E.J.-F.; project administration, E.J.-F.; software, A.S. (Anislada Santibáñez); supervision, E.J.-F. and A.S. (Ashutosh Sharma); validation, A.S. (Anislada Santibáñez); writing—original draft preparation, A.S. (Anislada Santibáñez); writing—review and editing, A.S. (Ashutosh Sharma), E.J.-F., M.H.-R., M.G.-C., P.N.-T., and A.S. (Anislada Santibáñez). All authors have read and agreed to the published version of the manuscript.

Funding: This research received no external funding.

Institutional Review Board Statement: The animal study protocol was approved by the Institutional Ethics Committee of Instituto Mexicano del Seguro Social (protocol code R-2021-17022-009 on 21 August 2021).

Informed Consent Statement: Not applicable.

Data Availability Statement: The data presented in the study are available in the article and its Supplementary Materials.

Acknowledgments: This work was supported by CONACYT Mexico grant (825903). We thank the Centro de Investigación Biomédica del Sur-IMSS.

Conflicts of Interest: The authors declare no conflict of interest.

References

1. Pérez-Ortega, G.; González-Trujano, M.E.; Ángeles-López, G.E.; Brindis, F.; Vibrans, H.; Reyes-Chilpa, R. *Tagetes lucida* Cav.: Ethnobotany, phytochemistry, and pharmacology of its tranquilizing properties. *J. Ethnopharmacol.* **2016**, *181*, 221–228. [[CrossRef](#)]
2. Linares, E.; Bye, R.A. A study of four medicinal plant complexes of Mexico and adjacent United States. *J. Ethnopharmacol.* **1987**, *19*, 153–183. [[CrossRef](#)]
3. Porras Dávila, S.L.; González Cortazar, M.; Jiménez Ferrer, E.; Román Ramos, R.; Bello Peralta, C.; Martínez Hernández, B.; Zamilpa, A.; Herrera Ruiz, M. Isolation, chemical characterization, and anti-inflammatory activity of coumarins, flavonoids, and terpenes from *Tagetes lucida*. *Nat. Prod. Res.* **2022**, *36*, 4745–4750. [[CrossRef](#)]
4. González-Trujano, M.E.; Gutiérrez-Valentino, C.; Hernández-Arámburo, M.Y.; Díaz-Reval, M.I.; Pellicer, F. Identification of some bioactive metabolites and inhibitory receptors in the antinociceptive activity of *Tagetes lucida* Cav. *Life Sci.* **2019**, *231*, 116523. [[CrossRef](#)]
5. Monterrosas Brisson, N.; Herrera Ruiz, M.; Jiménez Ferrer, E.; Bahena Pérez, R.; Avilés Flores, M.; Fuentes Mata, M.; Martínez Duncker, I.; González Cortazar, M. Anti-inflammatory activity of coumarins isolated from *Tagetes lucida* Cav. *Nat. Prod. Res.* **2020**, *34*, 3244–3248. [[CrossRef](#)]
6. Estrada-Soto, S.; González-Trujano, M.E.; Rendón-Vallejo, P.; Arias-Durán, L.; Ávila-Villarreal, G.; Villalobos-Molina, R. Anti-hypertensive and vasorelaxant mode of action of the ethanol-soluble extract from *Tagetes lucida* Cav. aerial parts and its main bioactive metabolites. *J. Ethnopharmacol.* **2021**, *266*, 113399. [[CrossRef](#)] [[PubMed](#)]
7. Bonilla-Jaime, H.; Guadarrama-Cruz, G.; Alarcon-Aguilar, F.J.; Limón-Morales, O.; Vazquez-Palacios, G. Antidepressant-like activity of *Tagetes lucida* Cav. is mediated by 5-HT_{1A} and 5-HT_{2A} receptors. *J. Nat. Med.* **2015**, *69*, 463–470. [[CrossRef](#)] [[PubMed](#)]
8. DiSabato, D.J.; Quan, N.; Godbout, J.P. Neuroinflammation: The devil is in the details. *J. Neurochem.* **2016**, *139*, 136–153. [[CrossRef](#)] [[PubMed](#)]
9. Kempuraj, D.; Thangavel, R.; Natteru, P.A.; Selvakumar, G.P.; Saeed, D.; Zahoor, H.; Zaheer, S.; Iyer, S.S.; Zaheer, A. Neuroinflammation Induces Neurodegeneration. *J. Neurol. Neurosurg. Spine* **2016**, *1*, 1003. [[PubMed](#)]
10. Lyman, M.; Lloyd, D.G.; Ji, X.; Vizcaychipi, M.P.; Ma, D. Neuroinflammation: The role and consequences. *Neurosci. Res.* **2014**, *79*, 1–12. [[CrossRef](#)] [[PubMed](#)]
11. Nava Catorce, M.; Gevorkian, G. LPS-induced Murine Neuroinflammation Model: Main Features and Suitability for Pre-clinical Assessment of Nutraceuticals. *Curr. Neuropharmacol.* **2016**, *14*, 155–164. [[CrossRef](#)] [[PubMed](#)]
12. Salehi, B.; Valussi, M.; Flaviana Bezerra Morais-Braga, M.; Nalyda Pereira Carneiro, J.; Lincoln Alves Borges Leal, A.; Douglas Melo Coutinho, H.; Vitalini, S.; Kregiel, D.; Antolak, H.; Sharifi-Rad, M.; et al. *Tagetes* spp. Essential oils and other extracts: Chemical characterization and biological activity. *Molecules* **2018**, *23*, 2847. [[CrossRef](#)]
13. Castañeda, R.; Cáceres, A.; Velásquez, D.; Rodríguez, C.; Morales, D.; Castillo, A. Medicinal plants used in traditional Mayan medicine for the treatment of central nervous system disorders: An overview. *J. Ethnopharmacol.* **2022**, *283*, 114746. [[CrossRef](#)] [[PubMed](#)]
14. Céspedes, C.L.; Avila, J.G.; Martínez, A.; Serrato, B.; Calderón-Mugica, J.C.; Salgado-Garciglia, R. Antifungal and antibacterial activities of Mexican tarragon (*Tagetes lucida*). *J. Agric. Food Chem.* **2006**, *54*, 3521–3527. [[CrossRef](#)] [[PubMed](#)]
15. FDA. Bioanalytical method validation Guidance for Industry. *Biopharmaceutics* **2018**, *66*, 1–41.
16. Heredia-Díaz, Y.I.; Machado-García, R.I.; Marllelyn Mendoza, L.; Docente Clínico Quirúrgico Ginecobstétrico, H.; Bruno Zayas, J. Desproteinización de Muestras de Suero y Plasma Para el Estudio Analítico de Carbamazepina. *Rev. Cuba. de Química* **2016**, *28*, 870–889.
17. Silva Lima, B.; Videira, M.A. Toxicology and Biodistribution: The Clinical Value of Animal Biodistribution Studies. *Mol. Ther.-Methods Clin. Dev.* **2018**, *8*, 183–197. [[CrossRef](#)]
18. Stanke-Labesque, F.; Gautier-Veyret, E.; Chhun, S.; Guilhaumou, R. Inflammation is a major regulator of drug metabolizing enzymes and transporters: Consequences for the personalization of drug treatment. *Pharmacol. Ther.* **2020**, *215*, 107627. [[CrossRef](#)] [[PubMed](#)]
19. Yin, Q.; Sun, H.; Zhang, A.; Wang, X. Pharmacokinetics and tissue distribution study of scopolamine in rats by ultraperformance liquid-chromatography with tandem high-definition mass spectrometry. *Fitoterapia* **2012**, *83*, 795–800. [[CrossRef](#)] [[PubMed](#)]
20. Kowalczyk, J.; Budzyńska, B.; Kurach, L.; Pellegata, D.; El Sayed, N.S.; Gertsch, J.; Skalicka-Woźniak, K. Neuropsychopharmacological profiling of scopolamine in mice. *Sci. Rep.* **2022**, *12*, 822. [[CrossRef](#)] [[PubMed](#)]
21. Morgan, E.T. Impact of infectious and inflammatory disease on cytochrome P450-mediated drug metabolism and pharmacokinetics. *Clin. Pharmacol. Ther.* **2009**, *85*, 434–438. [[CrossRef](#)] [[PubMed](#)]

22. Batista, C.R.A.; Gomes, G.F.; Candelario-Jalil, E.; Fiebich, B.L.; de Oliveira, A.C.P. Lipopolysaccharide-induced neuroinflammation as a bridge to understand neurodegeneration. *Int. J. Mol. Sci.* **2019**, *20*, 2293. [[CrossRef](#)] [[PubMed](#)]
23. Yang, K.-H.; Lee, M.-G. Effects of Lipopolysaccharide on Pharmacokinetics of Drugs. *Toxicol. Res.* **2007**, *23*, 289–299. [[CrossRef](#)]
24. SEMARNAT. *NORMA Oficial Mexicana NOM-062-ZOO-1999*; Secretaría de Agricultura, Ganadería, Desarrollo Rural, Pesca y Alimentación: Ciudad de México, Mexico, 2011; Volume 42, p. 2.
25. Zhang, Y.; Huo, M.; Zhou, J.; Xie, S. PKSolver: An add-in program for pharmacokinetic and pharmacodynamic data analysis in Microsoft Excel. *Comput. Methods Programs Biomed.* **2010**, *99*, 306–314. [[CrossRef](#)] [[PubMed](#)]

Curriculum Vitae

Anislada Santibáñez was born in Morelos, Mexico, on December 5, 1991. She obtained a degree in Biotechnology Engineering from the *Universidad Politécnica del Estado de Morelos (UPEMOR)* in 2014. Later, she did her first graduate studies at the *Universidad Autónoma del Estado de Morelos (UAEM)*, where he received a Master of Pharmacy degree with an honorable mention in May 2019, for the pharmacokinetic study carried out to treat cerebrovascular disease.

In the same year, she was accepted into the Ph.D. program in Biotechnology by the Tecnológico de Monterrey, Campus Querétaro, which is nearing completion under the direction of Dr. Ashutosh Sharma and Dr. Enrique Jiménez-Ferrer. As part of the development of her doctoral research, in 2021, she was awarded as a winner in the virtual poster session by the Phytochemical Society of North America (PSNA) in the Graduate student category. Recently, she published her first scientific article “Pharmacokinetics and Tissue Distribution of Coumarins from *Tagetes lucida* in an LPS-Induced Neuroinflammation Model” as part of the special issue *Biological and Chemical Activity of Metabolites of Medicinal Plants* of the journal *Plants*.

This document was typed in using Microsoft Word by Guadalupe Anislada Santibáñez
García.